INFORMATION TO USERS

This manuscript has been reproduced from the microfilm master. UMI films the text directly from the original or copy submitted. Thus, some thesis and dissertation copies are in typewriter face, while others may be from any type of computer printer.

The quality of this reproduction is dependent upon the quality of the copy submitted. Broken or indistinct print, colored or poor quality illustrations and photographs, print bleedthrough, substandard margins, and improper alignment can adversely affect reproduction.

In the unlikely event that the author did not send UMI a complete manuscript and there are missing pages, these will be noted. Also, if unauthorized copyright material had to be removed, a note will indicate the deletion.

Oversize materials (e.g., maps, drawings, charts) are reproduced by sectioning the original, beginning at the upper left-hand corner and continuing from left to right in equal sections with small overlaps. Each original is also photographed in one exposure and is included in reduced form at the back of the book.

Photographs included in the original manuscript have been reproduced xerographically in this copy. Higher quality 6" x 9" black and white photographic prints are available for any photographs or illustrations appearing in this copy for an additional charge. Contact UMI directly to order.

UMI

A Bell & Howell Information Company
300 North Zeeb Road, Ann Arbor, MI 48106-1346 USA
313/761-4700 800/521-0600

STUDY OF CYCLIC ALFA-FACTOR ANALOGS OF THE YEAST *SACCHAROMYCES CEREVISIAE*

by

Wei Yang

A dissertation submitted to the Graduate Faculty in Chemistry in partial fulfillment of the requirements for the degree of Doctor of Philosophy, The City University of New York

1995

This manuscript has been read and accepted for the Graduate Faculty in Chemistry in satisfaction of the dissertation requirement for the degree of Doctor of Philosophy.

7/7/95
Date

Fred Naider
Chair of Examining Committee
Dr. Fred Naider

7/13/95
Date

Executive Officer

Ruth E. Stark
Dr. Ruth Stark

Dr. Nan Lon Yang

Robert Bittman
Dr. Robert Bittman

Supervisory Committee

THE CITY UNIVERSITY OF NEW YORK

ABSTRACT

STUDY OF CYCLIC ALFA-FACTOR ANALOGS OF THE YEAST *SACCHAROMYCES CEREVISIAE*

By

Wei Yang

Adviser: Professor Fred Naider

Previous biophysical studies on the α-factor mating pheromone (WHWLQLKP-GQPMY) of *Saccharomyces cerevisiae* suggested that this peptide adopted a type II β-turn in DMSO, water or in the presence of lipid vesicles (Jelicks et al., 1988; Jelicks et al., 1989). The results of studies on linear and cyclic α-factor analogs by Gounarides et al. (1993; 1994) indicated a type II β-turn spanning residues 7 and 10 in active analogs such as [*D*-Ala^{9}]α-factor or cyclo^{7,10}[Cys^{7,10}, *D*-Ala^{9}, Nle^{12}]α-factor but not in the less active analogs such as [*L*-Ala^{9}]α-factor or cyclo^{7,10}[Cys^{7,10}, *L*-Ala^{9}, Nle^{12}]α-factor. To further understand the conformational properties of the central region in α-factor, we synthesized eight cyclic analogs and their corresponding linear homologs. The cyclic analogs contained a lactam ring formed from the side chains of residues 7 and 10, and the size of the ring was systematically varied from 14 to 18 atoms. All peptides were synthesized using the solid phase method and purified to high homogeneity (over 99% pure as judged by acetonitrile/water/trifluoro-acetic acid gradients on reversed-phase HPLC). The chemical structures of the analogs were

characterized by FABMS, amino acid analysis and NMR spectroscopy. The biological activities of the cyclic analogs varied from 10% to less than 0.1% of that of [Nle^{12}]α-factor against strain RC629 (*sst1*) of *S. cerevisiae*. Except for the Orn^{7}-containing cyclic peptides (**C32** and **C31**), analogs with Glu in position 10 were more active than the homologs with Asp at this position. The bioactivity results suggested that the γ-carbonyl group of residue 10 is a critical determinant of the biological activity.

The conformations of the cyclic α-factor analogs were examined in a water/methanol (1:1, v/v) solvent mixture. For comparison CD spectra of the linear analogs were acquired in the same solvent. All linear analogs showed similar unstructured CD spectra. In contrast, the CD spectra of the cyclic analogs appeared quite different from each other. Except for **C12** and **C(4)2**, a positive band below 200 nm and a minimum between ~200 and 215 nm were observed in the CD spectra of the cyclic analogs. Such spectral features were not observed in the CD spectra of the linear homologs. CD studies on model cyclic tetrapeptides (Tetra **42** and Tetra **32**) and examination of solutions containing both the linear tridecapeptide (**L32**) and Tetra **32** suggested that the constrained region from residues 7 to 10 in the cyclic analog (**C32**) retained the same conformation as the model cyclic tetrapeptide.

Two cyclic α-factor analogs, **C42** and **C32**, were analyzed by NMR techniques. NOE, NH dδ/dT and $^{3}J_{\alpha NH}$ coupling constants suggested that in DMSO solution **C32** adopts a type II β-turn spanning residues 7-10 with some distortion, and **C42** exists as mixture of a type II β-turn centered around the Pro^{8}-Gly^{9} sequence and a γ-turn around Pro^{8}. The Corey-Pauling-Koltun (CPK) model building based on the NOE constraints and amide proton temperature dependence revealed the

importance of spatial orientation of the Glu^{10} γ-carbonyl from a conformational point of view. This observation is in agreement with the results of our bioactivity analysis.

This thesis is dedicated to my parents,

Zi-Gao Yang and Ju-Ying Xu

ACKNOWLEDGMENTS

First and foremost, I would like to acknowledge Professor Fred Naider, my mentor during my graduate years in CSI, for his continuous support, constructive guidance, and stimulating criticism. I would like to thank Dr. Naider especially for the great patience and the many hours spent painstakingly revising this dissertation. Dr. Naider taught me a lot about science, and about life itself. I will always remember the experience of getting our paper published.

I would like to express my gratitude to the members of my dissertation committee, Professor Ruth Stark, Professor Nan Lon Yang, Professor Robert Bittman, for their encouragement and valuable suggestions, and for serving on my committee. Dr. Stark, in particular, provided much advice during my tenure at CUNY. As a female professional I respect her as my role model.

I also thank all of my colleagues in the Naider group, in particular, Dr. Michael Tallon, for his encouragement and generous assistance during my early days in the group, and for training me in the field of NMR. I would like to thank Dr. Chu-Biao Xue, who gave me assistance in the peptide synthesis. I thank Dr. John Gounarides for his good advice in the NMR study. I thank Dr. Michael Breslav, who synthesized **L42** during my pregnancy, thereby, aiding us to publish the paper in *Biochemistry*.

I would like to thank Professor Jeffrey M. Becker and the members in his group for their biological results. I am grateful to Dr. Ming-Ming Gao who offered to run two 2D NMR experiments on **C32** free of charge.

In addition I would like to thank Professor Tom Strekas who letting me carry out the CD experiments on his Jasco J-500 spectropolarimeter, the CUNY facility located at Queens college. Thanks also go to Dr. Michael Blumenstein for the NMR facility located at Hunter college.

Finally, I would like to express my deepest thanks to my long time suffering husband, Dongwei Cai: this thesis should also be dedicated to you for your unconditional love and support throughout the years.

TABLE OF CONTENTS

List of Tables

List of Figures

List of Abbreviations

Å	Ångström
Ac	acetyl
Boc	*tert*-butoxycarbonyl
BOP	benzotriazol-1-yloxy-tris(dimethylamino)-phosphonium hexafluorophosphate
2-BrZ	2-bromobenzyloxycarbonyl
CD	circular dichroism
COSY	two-dimensional correlated spectroscopy
$d_{\alpha N(i, i+1)}$	internuclear distance between the αCH of i residue and the NH of i+1 residue
$d_{\beta N(i, i+1)}$	internuclear distance between the βCH of i residue and the NH of i+1 residue
Dbr	*L*-2,4-diaminobutyric acid
DCC	*N,N'*-dicyclohexylcarbodiimide
Dhp	3,4-dehydro-*L*-proline
DIEA	*N,N*-diisopropylethylamine
DIPC	*N,N'*-diisopropylcarbodiimide
DMAP	4-(*N*-dimethyamino)-pyridine
DMF	*N, N*-dimethylformamide
DMS	dimethyl sulfide
DMSO	dimethyl sulfoxide
Dpr	*L*-2,3-diaminopropionic acid
DQF COSY	double-quantum filtered correlated spectroscopy
Fmoc	9-fluorenylmethyloxycarbonyl

FABMS	fast atom bombardment mass spectrometry
HF	hydrogen fluoride
^{1}H NMR	proton nuclear magnetic resonance spectroscopy
HOBt	1-hydroxybenzotriazole
HPLC	high-performance liquid chromatography
Hz	Hertz (cycles per second)
$^3J_{N\alpha}$	spin-spin coupling constant between NH and αCH
MeOH	methanol
Nle	norleucine
NOE	nuclear Overhauser effect
NOESY	two-dimensional nuclear Overhauser spectroscopy
OBzl	benzyl ester
OFm	9-fluorenylmethyl
PAM	phenylacetamidomethyl
Ph	phenyl
Relayed COSY	two-dimensional relayed coherence transfer spectroscopy
ROESY	two-dimensional rotating-frame nuclear Overhauser effect spectroscopy
TFA	trifluoroacetic acid
TLC	thin-layer chromatography
t_m	mixing time
TOCSY	total correlated spectroscopy
TRNOE	transferred NOE
VCD	vibrational circular dichroism spectroscopy

CHAPTER 1

Introduction

The two different haploid cell types (**a** cells and α cells) of *Saccharomyces cerevisiae* (baker's yeast) are able to mate with each other to form diploids (**a**/α cells). The mating process between the two haploid cells has provided an incisive means to investigate the biochemical basis of intercellular signaling and intracellular signal transduction because the conjugation is triggered by mutual exchange of diffusible peptide pheromones that act through cell surface G-protein-coupled receptors (Sprague and Thorner, 1993).

The signal transduction pathway in *Saccharomyces cerevisiae* is similar to the pathways in other eukaryotic cells, including those manifested by the rhodopsins (Godchaux and Zimmerman, 1979), by the β_2-adrenergic receptors (Sibley et al., 1987), and by the nicotinic acetylcholine receptors (Moscona-Amir et al., 1986). The common structural/topological organization shared by the yeast receptors and by the larger family of seven transmembrane-segment receptors (Dohlman et al., 1991; Rose, 1989) reflects a common functional organization, as revealed by mutational analysis (Sprague and Thorner, 1993; Konopka et al., 1988; Reneke et al., 1988). This suggests that there is a fundamental relationship between the signal transduction process in the simple yeast cells and the cells of higher level eukaryotic systems. Therefore, insights gained from studying the interaction between the two haploid cells should have a more universal impact on the understanding of the interactions between cells in other higher eukaryotic organisms. Given the ease with which this organism is grown in the laboratory and subjected to molecular biological manipulation, *S. cerevisiae* provides an

excellent model to study the mode of action of peptide hormones and their receptors.

The events of mating in *S. cerevisiae* are initiated by the mating pheromones, α-factor or a-factor, that are produced by each haploid cell type. The peptide pheromones start their action by binding to their receptors on the surface of the reciprocal cells (Sprague et al., 1983). These receptors have been found to be integral membrane proteins (Reneke et al., 1988; Clark et al., 1988). Due to the fact that it is very difficult to isolate and study these large membrane proteins, efforts have been devoted to the study of the peptide hormones and, more recently to selective recombinant DNA analyses of the receptors (Sen and Marsh, 1994; Clark et al., 1994). One major goal of these investigations is to determine the biologically active conformation of the mating pheromone. In particular, extensive studies have been focused on the α-factor, one of the peptide pheromones in *S. cerevisiae*. Study of the relationship between structure and activity on α-factor has suggested that a type II β-turn involving Pro^{8}-Gly^{9} may be an important feature of the biologically active conformation of α-factor (Naider and Becker, 1986). NMR study indicated that a type II β-turn is an important spectral feature among the active analogs (Jelicks et al., 1988). Furthermore, a cyclic analog, cyclo^{7,10}[Nle^{12}]α-factor, was found to retain one tenth to one twentieth the activity of the native pheromone (Xue et al., 1989). In an extension of these studies, the goal of my research is to carry out a detailed conformational analysis of the presumed turn region, that is, the region between Lys^{7} and Gln^{10} of α-factor.

CHAPTER 2

Background

I. Mating Process of *Saccharomyces cerevisiae*

The yeast *S. cerevisiae* has two haploid cell types, designated as **a** cells and α cells (Thorner, 1980). Both haploid cells can asexually reproduce through the process of budding. As an alternative to vegetative (mitotic) proliferation, these two haploid cells can conjugate to form diploids (**a**/α cells). The dipoid cells cannot conjugate with either of the haploid cells or with other **a**/α cells, but have the capability to undergo meiosis and sporulation (Sprague et al., 1983; Herskowitz, 1988).

The mating process is initiated through the reciprocal exchange of diffusible peptide pheromones. α-Cells secrete a tridecapeptide α-factor, Trp-His-Trp-Leu-Gln-Leu-Lys-Pro-Gly-Gln-Pro-Met-Tyr, which targets its receptor on the surface of **a**-cells (Stotzler et al., 1976; Betz et al., 1981); whereas **a**-cells secrete a dodecapeptide **a**-factor, Tyr-Ile-Ile-Lys-Gly-Val-Pro-Trp-Asp-Pro-Ala-Cys (S-farnesyl)-$COOCH_3$, which targets its receptor on the surface of α-cells (Anderegg et al., 1988). Both receptors are coupled to the same heterotrimeric guanine nucleotide-binding protein ("G-protein") (Blumer and Thorner, 1990). In the absence of a pheromone/receptor interaction, the G-protein is in an inactive state. When the pheromone binds, the receptor presumably undergoes a conformational change that, in turn, activates the G-protein. The activation of G-protein leads to the dissociation of its $G\alpha$ subunit from $G\beta\gamma$. The $G\beta\gamma$ so released then interacts with a down stream target(s) to propagate the signal from the plasma membrane

FIGURE 1: The mating process of *S. cerevisiae* (data from Sprague and Thorner, 1993)

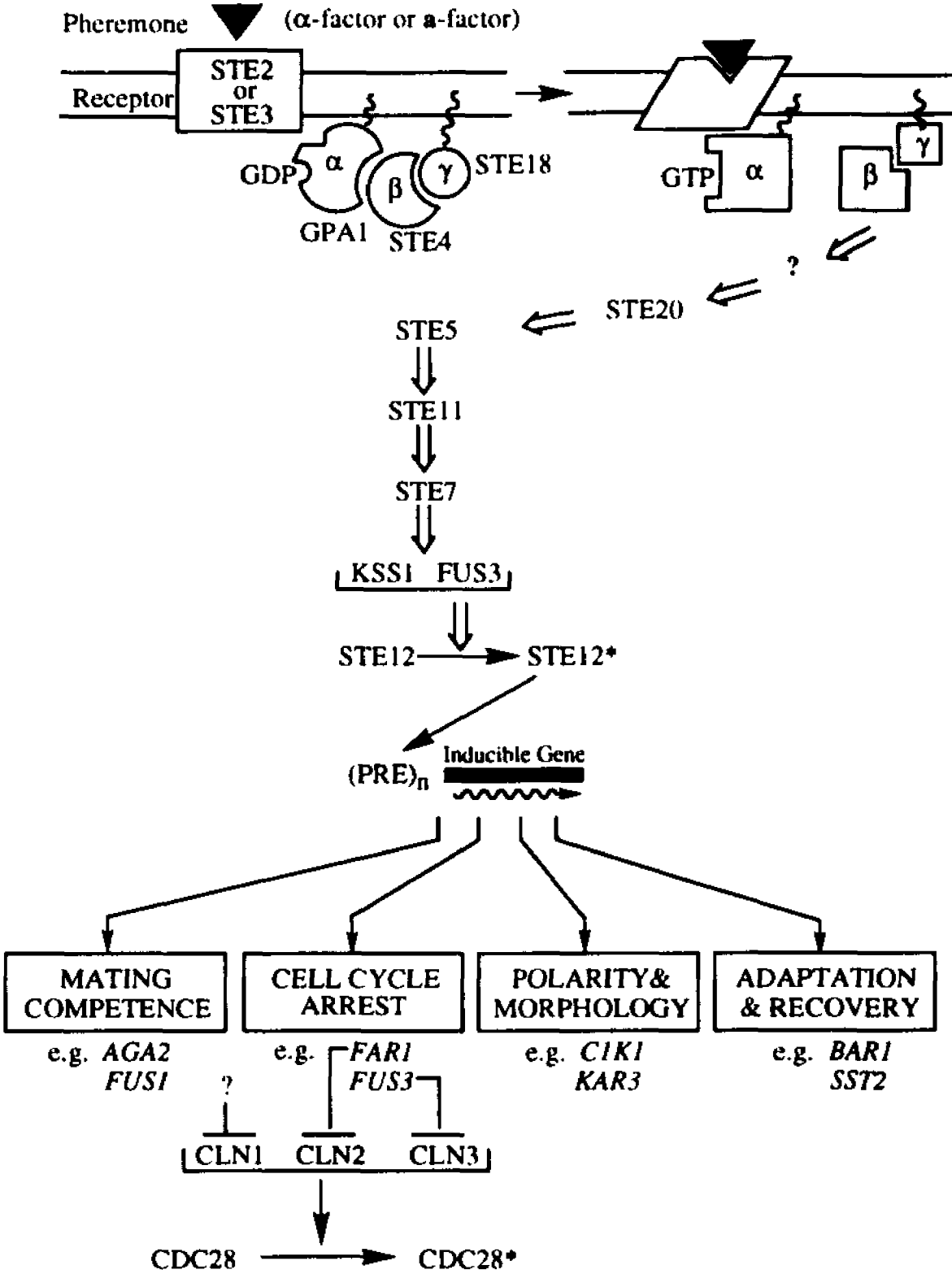
Pheremone
(α-factor or a-factor)
Receptor
STE2 or STE3
GDP
α
β
γ
STE18
GPA1
STE4
GTP
α
β
γ
?
STE20
STE5
STE11
STE7
KSS1 FUS3
STE12
STE12*
(PRE)n
Inducible Gene
MATING COMPETENCE
CELL CYCLE ARREST
POLARITY& MORPHOLOGY
ADAPTATION & RECOVERY
e.g. AGA2 FUS1
e.g. FAR1 FUS3
e.g. CIK1 KAR3
e.g. BAR1 SST2
?
CLN1
CLN2
CLN3
CDC28
CDC28*

to the nucleus and triggers a series of events which causes various physiological responses (Figure 1) (Duntze et al., 1970; Sprague and Thorner, 1993).

II. The Secretory Pathway of α-Factor

The mature extracellular α-factor is generated from larger precursors that are encoded by two genes, MFα1 and MFα2 (Kurjan and Herskowitz, 1982; Singh et al., 1983). Both precursors have an *N*-terminal hydrophobic leader, a hydrophilic domain and a *C*-terminal segment consisting of repeats of the α-factor sequence which are separated by "spacer" sequences (Sprague and Thorner, 1993). The hydrophobic leader of each precursor directs the precursor to enter the endoplasmic reticulum where the signal sequence is removed by a signal peptidase (Waters et al., 1988) and where three Asn-linked mannose-rich core oligosaccharides are added to the hydrophilic domain (Julius et al., 1984). The core oligosaccharides are extended by additional outer chain oligosaccharides when the precursors pass through the Golgi cisternae (Julius et al., 1984; Franzusoff et al., 1991). The precursor is then cleaved by the KEX2 endoprotease on the carboxyl side of the pair of basic residues (-Lys-Arg-) in each spacer, and the pairs of basic residues are removed by the KEX1 exoprotease. Finally, the dipeptide spacers at the N-terminus of each pro-α-factor unit are removed by dipeptidyl aminopeptidase A (STE 13), and the mature α-factor is secreted (Figure 2) (Wickner and Leibowitz, 1976; Julius et al., 1983; Dmochowska et al., 1987; Wagner and Wolf, 1987; Bussey, 1988; Sprague and Thorner, 1993).

FIGURE 2: The secretory pathway of α-factor (data from Sprague and Thorner, 1993)

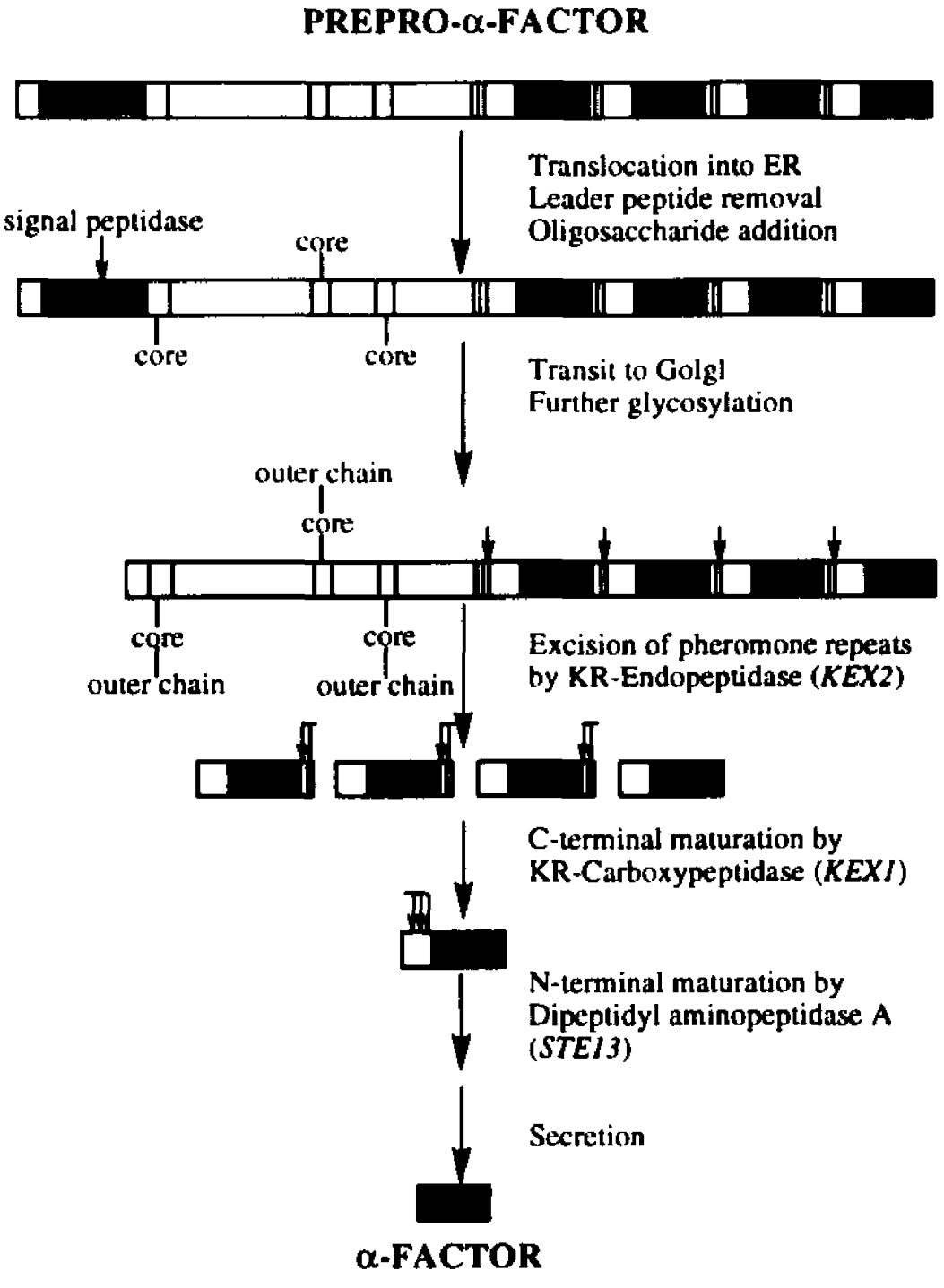
PREPRO-α-FACTOR
Translocation into ER
Leader peptide removal
Oligosaccharide addition
signal peptidase
core
core
core
Transit to Golgl
Further glycosylation
outer chain
core
core
core
outer chain
outer chain
Excision of pheromone repeats
by KR-Endopeptidase (KEX2)
C-terminal maturation by
KR-Carboxypeptidase (KEX1)
N-terminal maturation by
Dipeptidyl aminopeptidase A
(STE13)
Secretion
α-FACTOR

III. The Structure of α-Factor Receptor

The α-factor receptor is encoded by the STE2 gene (MacKay and Manney, 1974; Hartwell, 1980; Hagen et al., 1986). The nucleotide sequence of STE2 encodes an integral membrane protein (Ste2p) which is member of a large family of receptor proteins that includes the rhodopsins and the β-adrenergic receptors (Burkholder and Hartwell 1985; Nakayama and Miyajima, 1985; Hagen et al., 1986). Biochemical analysis demonstrates that this gene product is indeed an integral protein, and that the Ste2p protein is *N*-glycosylated (Reneke et al., 1988). As deduced from hydropathy analysis, this receptor contains seven highly hydrophobic, potentially α-helical, membrane-spanning segments within the *N*-terminal region followed by a hydrophilic, presumably cytoplasmic *C*-terminal domain (Blumer et al., 1988; Blumer and Thorner, 1990). The deduced topology of Ste2p is consistent with studies of post-translational modification of the receptor (Blumer and Thorner, 1990) and with *in vivo* topological analysis using gene fusions (Cartwright and Tipper, 1991). Two of the transmembrane fragments of α-factor receptor have been synthesized and a CD study confirmed their α-helical structure (Reddy et al., 1994). By using chimeric receptors, it was shown that two noncontiguous domains that include putative extracellular loops 1 and 3 and associated transmembrane segments, but exclude the extracellular NH_2 terminus and loop 2, appear to contribute to α-factor receptor ligand specificity (Sen and Marsh, 1994). The *C*-terminal sequences of the α-factor receptor regulate receptor number and adaptation to pheromone, but are not essential for pheromone binding or signaling (Konopka et al., 1988; Kurjan et al., 1991). Two extracellular loop peptides and an intracellular carboxyl loop peptides were synthesized. A CD study of these peptides indicated that the latter one was partially helical in TFE whereas the others were either disordered or aggregated

in this solvent (Tallon, 1992; Reddy et al., 1994). Results from mutagenesis of the third cytoplasmic loop of Ste2p suggest that it is a multifunctional domain that controls pathway activation and/or desensitization, and influences the processes of receptor activation, ligand discrimination and internalization (Stefan and Blumer, 1993; Clark et al., 1994).

IV. Physiological Responses to the α-Factor

The presence of α-factor can: (1) reversibly arrest the growth of **a** cells in the early G1 period of the cell cycle by blocking the initiation of nuclear DNA synthesis; (2) increase agglutinability to the opposite cell-type, which aids in the cell fusion process; (3) cause changes in the biosynthesis of cell-wall components; (4) cause changes in the morphology of the **a** cells (shmooing). All these responses can be used in bioassay for detection of the pheromones. For example, one can observe the accumulation of unbudded cells in a population of **a**-cells using light microscope; one can measure the size of the growth arrest halo on a lawn of responsive **a** cells; or one can score the number of prolonged **a** cells (shmoos) under the microscope (Thorner, 1981).

V. Structure-Activity Studies of α-Factor

Study of structure-activity relationships involves the following approaches: (1) amino acid substitutions; (2) blockage of amino groups or carboxy groups at the chain ends or in the side chains; (3) truncation of the α-factor peptide chain; (4) elongation of the peptide chain; (5) peptide fragmentation. All of these types of

studies have been conducted on the α-factor. Most structure-activity studies on α-factor come from the laboratories of Dr. Masui in Japan and that of Dr. Naider and Dr. Becker. The structure-activity studies from these laboratories were based on three types of analogs; those of α-factor, of desTrp^{1}α-factor and of [Nle^{12}]α-factor. In order to properly analyze these results, one has to note the difference and similarity between the parent peptides used in each investigation. DesTrp^{1}α-factor was used as a parent peptide based on the suggestion that desTrp^{1}α-factor has equal activity to α-factor in the cell-shape or "shmoo" assay (Stotzler et al., 1976; Masui et al., 1977; Ciejek et al., 1977). However, using the same type of strain 2180-1A, Shengbagamurthi et al., (1983) reported that the synthetic tridecapeptide (homogeneity over 98%) was 16 times more potent than the synthetic dodecapeptide (desTrp^{1}α-factor, homogeneity over 98%). [Nle^{12}]α-factor was used as a parent peptide because [Nle^{12}]α-factor was found to have the same activity as α-factor in both the halo assay and the shmoo assay, and to have no difference in binding affinity compared to the α-factor (Raths et al., 1988) against *S. cerevisiae* strains 4202-15-3 (MATa cryl bar1-1 ade2-1 his4-580 lys2 trp1 tyr1 SUP4-3) or 4202-1-2(MATa cry1 bar1-1 ade2-1 his4-580 lys2 trp1 SUP4-3). Since Nle is isosteric with Met and is much less prone to oxidation and alkylation, its incorporation results in significant improvement when used in place of Met during the analog synthesis.

Finally, there is a significant disagreement between the results from Masui's laboratory and our laboratory. The Japanese group reported that the minimum amount of α-factor needed to induce morphological changes in 2180-1A a cells was 6 x 10^{-12} g/mL. In contrast, our group found that 5 x 10^{-8} g/mL α-factor was required to cause morphological changes in this strain. The biological activity of the homogeneous preparation of α-factor (Duntze et al., 1973) or

synthetic α-factor (Ciejek et al., 1977; Samokhin et al., 1979) was closer to the scale of 5×10^{-8} g/mL. Obviously one has to be cautious when comparing the results from different sources. Some of the results were consistent. For example, both labs found that the configuration at position 2 is very important and that the hydrophobicity is important at position 3. Yet some of the results were inconsistent with each other. For example, [Phe^3]α-factor was reported to retain one twenty-third activity of α-factor (Masui et al., 1979); however desTrp^1[Phe^3] was found to be devoid of activity (Naider and Becker, 1986). Nevertheless, in the following sections it is assumed that the results from both laboratories provide complementary information. No attempt is made to normalize the SAR results and conclusions will be made based on comparison to the parent peptide used at the time.

5.1 Effects of Amino Acid Substitutions

It appears that the hydrophobicity and aromatic moiety are important in position 1. Replacement of Trp with Phe in position 1 as in [Phe^1]α-factor only resulted in a 12-fold loss in activity whereas substitution of the more hydrophilic Tyr, as in [Tyr^1]α-factor, resulted in a 2500-fold loss in activity (Masui et al., 1979). A further increase of hydrophobicity in this position as in [di-iodo-Tyr^1, Nle^{12}]α-factor resulted in an analog having equal activity of [Nle^{12}]α-factor (Breslav et al., personal communication). Replacement of Trp^1 with an alicyclic Leu or a positively charged Lys resulted in a 500-fold or a 50,000,000-fold loss in activity, respectively (Masui et al., 1979). Substitution of Bpa (both hydrophobic and aromatic) in position 1 results in a pheromone with one third of the activity of [Nle^{12}]α-factor (Jiang et al., 1994).

The His in position 2 was studied quite thoroughly and was found to be extremely important for activity. Substitution of this residue by basic (Lys), hydrophobic (Phe, Leu) amino acids resulted in at least a 40,000-fold loss in activity (Masui et al., 1979). The *L* configuration in position 2 also was critical. Replacement of the enantiomeric residue (*D*-His) lead to a 50,000,000-fold loss of activity. The importance of the *L* configuration in position 2 was also observed in [Nle^{12}]α-factor analogs. For example, [β-*L*-thienylAla^{2}, Nle^{12}]α-factor had one hundredth activity and [1-*L*-MeHis^{2}, Nle^{12}]α-factor had one-tenth activity of [Nle^{12}]α-factor; in contrast both [β-*D*-thienylAla^{2}, Nle^{12}]α-factor and [1-*D*-MeHis^{2}, Nle^{12}]α-factor had less than one-thousandth activity of the [Nle^{12}]α-factor. Further study of this residue showed that a nucleophilic 3-nitrogen of the imidazole side chain may be especially important. Deletion of this nitrogen, as in [Phe^{2}]α-factor (Masui et al., 1979) and [β-thienylAla^{2}, Nle^{12}]α-factor, resulted in a marked drop in activity, whereas retention of this nitrogen, as in [1-*L*-MeHis^{2}, Nle^{12}]α-factor and [3-*L*-PydAla^{2}, Nle^{12}]α-factor, lead to analogs with relatively high activity (Levin et al., 1993). The hydrophobicity of Trp in position 3 appears important. Analogs with hydrophobic amino acids in this position exhibited only a 3-38 fold loss in activity as in analogs [Ala^{3}]α-factor, [Phe^{3}]α-factor, [Leu^{3}]α-factor, desTrp^{1}[Cha^{3}, Nle^{12}]α-factor and [Bpa^{3}, Arg^{7}]α-factor (Masui et al., 1979; Jiang et al., 1994). In contrast, replacement of Trp^{3} with more hydrophilic amino acids (such as Tyr, Lys, Gly and Asp) resulted 133-86000 fold loss in activity (Masui et al., 1979).

It appears that a bulky hydrophobic side chain is required for high activity in position 6. As the size of the side chain of residue 6 was increased from a methyl to a butyl group, as in desTrp^{1}[Cha^{3}, Ala^{6}]α-factor, desTrp^{1}[Cha^{3}, Val^{6}]α-factor and desTrp^{1}[Cha^{3}, Nle^{6}]α-factor the activity increased from twenty-thousandth

to equal activity compared with that of desTrp^1[Cha^3]α-factor (Baffi et al., 1985). Changing the chirality from *L* to *D* in position 6 resulted in a 2500-fold loss in activity (Masui et al., 1979). For position 7, it seems that the proper chirality was critical. Change of chirality, as in [*D*-Lys^7]α-factor, resulted in 18000-fold loss in activity (Masui et al., 1979). Furthermore, blocking of the protonatable amine or reducing the length of the Lys side chain as in desTrp^1[Cha^3, ε-Ac-Lys^7]α-factor, and desTrp^1[Cha^3, Orn^7]α-factor resulted in a 10-30 fold loss in activity. Replacement of Lys^7 with Arg lead to an analog with equal activity to α-factor (Samokhin et al., 1979). Removal of the protonatable ε-amino group by substitution of Nle in position 7 (desTrp^1[Cha^3, Nle^7]α-factor) only reduced the activity by 27-fold (Baffi et al., 1984). It was also shown that α-factor can tolerate a large group at the side chain of residue 7; analogs such as desTrp^1[Cha^3, ε-butanoyl-Lys^7]α-factor, desTrp^1[Cha^3, ε-octanoyl-Lys^7]α-factor, desTrp^1[Cha^3, ε-lauryl-Lys^7]α-factor and desTrp^1[Cha^3, ε-biotinyl-Lys^7]α-factor have one third to one twenty-fourth the activity of that of desTrp^1[Cha^3]α-factor (Shenbagamurthi et al., 1983; Naider and Becker, 1986). Obviously, a protonatable amino group in the side chain of residue 7 is not essential for activity. In addition the peptide can tolerate a large group at that position, which is very useful for making a tagged α-factor analog.

Placement of Gly in position 8 and position 11 resulted 2500-3330 fold loss in activity (Masui et al., 1979), but replacement of Dhp (Dhp = 3,4-dehydro-*L*-Pro) in both position 8 and 11 had no effect on activity (Raths et al., 1988). Placement of *D*-Ala in position 9 not only retained activity but also retained the binding ability to the receptor (Naider and Becker, 1986; Raths et al., 1988; Gounarides et al., 1993). The substitutional study of residue 9 gave very

important information related to the conformation of α-factor, which will be discussed further in Section 6.1 (this chapter).

A nucleophilic sulfur atom was not required at position 12. Replacement of oxidized Met (Stotzler et al., 1976) or an isosteric residue (Nle) (Raths et al., 1988) in this position resulted in analogs with the same potency as α-factor against strain 4202-15-3. In contrast, Masui et al., (1979) reported that substitution of Met^{12} by Nle lowered the activity to one-thirtieth of the α-factor against strain 2180-1A. The Tyr in position 13 was found to be very important. Substitution of Phe or *D*-Tyr in this position resulted in a 2500-5000 fold loss in activity (Masui et al., 1979). Deletion of Tyr in this position as in desTyr^{13}α-factor (Masui et al., 1977) or desTyr^{13}[Nle^{12}]α-factor (Eriotou-Bargiota et al., 1992) leads to virtually inactive or much less active analogs, respectively.

5.2 Effects of the Blockage of the Terminal groups

Reports in the literature suggest that both a free amino group at the *N*-terminus and a free carboxyl group at the *C*-terminus are important for activities. Blockage of the amino group, as in *N*-acetylated α-factor (Lipke, 1976), fluorescein isothiocyanate (FITC)-α-factor (Thorner, 1981), benzoyl-desTrp^{1}α-factor (Masui et al., 1979) and [(I-HPP)Trp^{1}, Bpa^{3}, Arg^{7}, Nle^{12}]-α-factor (Jiang et al., 1994) resulted in analogs having no activity or little activity. However, an analog without a free amine group, desTrp^{1}[α-Dns-His^{2}, Cha^{3}]α-factor, was found to exhibit significant activity which was explained on the basis of the similarity of the protonatable groups such as $N(CH_3)_2$ and NH_2 in the *N*-terminus (Jiang et al., 1994). The blockage of the terminal carboxy group resulted in either 1000-fold lower or inactive analogs. Examples are [Tyr^{13}-OR]α-factor (Thorner, 1990) and

[Tyr^{13}-NH_2]α-factor (Masui et al., 1979), and [Tyr^{13}-PEG]α-factor (Shenbagamurthi et al., 1983).

5.3 Effects of the Truncation and Elongation of the Peptide Chain

The results from the study of the truncated α-factor are interesting. In part, the results were consistent with the ones from the study of amino acid substitution which showed that His in position 2 and Tyr in position 13 were very important. Removal of Trp in position 1 (desTrp^{1}α-factor) only reduced the activity 16-fold (Shengbagamurthi et al., 1983). However, analogs lacking His in position 2 or Tyr in position 13 had little or virtually no activity as in desTyr^{13}[Nle^{12}]α-factor, desTrp^1, desHis^{2}α-factor, desMet^{12},desTyr^{13}α-factor or desTyr^{13}α-factor (Masui et al., 1977; Eriotou-Bargiota et al., 1992). Interestingly, detailed analyses showed that an *N*-terminal truncated pheromone (desTrp^1, desHis^2[Nle^{12}]α-factor) acted as an antagonist by competing with both the binding and activity of the native pheromone, and a carboxyl terminal truncated pheromone (desMet^{12}, desTyr^{13}α-factor) acted as a synergist by causing a marked increase in activity of α-factor (Eriotou-Bargiota et al., 1992).

Although removal of two residues at either terminal of α-factor resulted in a dramatic decrease in activity, additional residues on the *N*-terminal appears to be tolerated by the α-factor receptor. The addition of Ala, Glu-Ala, or Ala-Glu-Ala to the *N*-terminal resulted in only a slight loss of activity whereas an addition of Glu-Ala-Glu-Ala lead to an analog with 10-fold less activity (Tallon et al., 1987).

5.4 Effects of the Fragmentation of the Peptide Chain

Besides the truncated α-factor analogs discussed above, none of the fragments containing the partial sequences of the native α-factor are active (Masui et al., 1977). The finding of virtually inactive desTrp^{1}, desGln^{10}, desPro^{11}, desMet^{12}, desTyr^{13}α-factor, desTrp^{1}, desPro^{11}, desMet^{12}, desTyr^{13}α-factor (Masui et al., 1977), desTrp^{1}, desMet^{12}, desTyr^{13}α-factor (Masui et al., 1977; Eriotou-Bargiota et al., 1992) was consistent with the results form the study of amino acid substitution or truncated α-factor. It was significant that the fragments with sequences of Trp-His-Trp-Leu-Gln-Leu and Lys-Pro-Gly-Gln-Pro-Met-Tyr had no activity since a-cells of *S. cerevisiae* contain a surface-associated peptidase which hydrolyzes α-factor by cleavage of the Leu^{6}-Lys^{7} peptide bond. The inactivity of the fragments suggests that intact α-factor is responsible for all biological responses tested and that degradation of α-factor allows a-cells to recover from the cellular control promulgated by the pheromone (Tanaka and Kita, 1978; Ciejek and Thorner, 1979; Naider and Becker, 1986).

VI. Conformational Analysis

6.1 Conformational Study of α-Factor

The conformation of α-factor has been studied by utilizing CD spectroscopy (Higashijima et al., 1983; Naider and Becker, 1986). The CD spectrum of α-factor in Tris buffer at pH 7.2 suggested a random-coiled structure (Naider and Becker, 1986). In the presence of lipid or small unilamellar vesicles, changes observed in the CD profile near 220 nm suggested a more ordered structure which is

associable with both α-helical and β structures (Higashijima et al., 1983). Due to the inherent flexibility associated with a small linear peptide like α-factor, the secondary structure of the molecule is not well defined and the information from CD study is of limited value.

The conformation of α-factor in solution and in the presence of lipid has been the subject of a number of NMR studies. Higashijima et al., (1979) proposed a structure for α-factor in aqueous solution which included two β-turns spanning residues 7-10 and 10-13. This structure was based on the temperature coefficients and the pH dependencies of αNHs, and $^{3}J_{\alpha NH}$ coupling constants. Based on the examination of the Gd(III) induced relaxation effects on α-factor, the same research group confirmed the β-turn structures and suggested a helical structure at the *N*-terminus of α-factor (Higashijima et al., 1984). Because a conformational change was observed by Higashijima et al., (1983) on changing from an aqueous solution to the presence of lipid, Wakamatsu et al., (1986) studied the conformation of α-factor in perdeuterated phospholipid using TRNOE, and concluded: (I) the *N*-terminal nine residues (Trp^{1}-Gly^{9}) are tightly bound to the bilayer, while the *C*-terminal four residues (Gln^{10}-Tyr^{13}) are left free in aqueous phase; (II) a compact helical structure is present for residues 1-5, and the residues Gln^{6}-Gly^{9} form an extended conformation. It has to be emphasized that the above results are based on a 1D NMR study. Therefore, no direct internuclear distance information was available from such experiments.

The conformation of α-factor in DMSO-d_6, water and in the presence of lipid was examined using 2D NMR techniques (Jelicks et al., 1988; Jelicks et al., 1989; Naider et al., 1989). Using the 2D NOE results, these authors indicated that in both aqueous and organic solution α-factor is a flexible molecule and exhibits

features indicative of a transient type II β-turn spanning residues 7-10; the β-turn is stabilized on interaction of the peptide with the lipid vesicles. It should be noted that the finding of a type II β-turn by NMR is consistent with conclusions from structure-activity investigations. As indicated above (Section 5.1 in this chapter) replacement of Gly by *D*-Ala in position 9 not only retained the activity but also retained the binding ability to the receptor. For example, the des Trp^1[Cha^3, *D*-Ala^9]α-factor had an activity almost equal to that of des Trp^1[Cha^3]α-factor and [*D*-Ala^9]α-factor had an activity comparable to that of the native pheromone. In contrast, the des Trp^1[Cha^3, *L*-Ala^9]α-factor was at least 200-fold less active than the corresponding *D*-homolog and the [*L*-Ala^9]α-factor was 10-fold less active than the [*D*-Ala^9]α-factor (Naider and Becker, 1986; Raths et al., 1988; Gounarides et al., 1993). The influence of the chirality of residue 9 suggests that the conformation of the Pro-Xxx dipeptide may play an important role in the activity of α-factor. The Pro-Gly sequences are often found in β-turns and were predicted to prefer a type II β-turn (Venkatachalam, 1968). In addition, it is known that the Pro-*D*-Ala sequence favors a type II β-turn and the Pro-*L*-Ala sequence favors a type I β-turn (Venkatachalam, 1968; Aubry et al., 1985; Rose et al., 1985). Therefore, results both from structure-activity studies and from NMR studies supported the existence of a type II β-turn in the central portion of α-factor.

6.2 Conformational Study of Linear α-Factor Analogs

Jelicks et al., (1988) studied several analogs in DMSO-d$_6$ using ^{1}H NMR techniques and found that there was a type II β-turn in the active analogs (such as desTrp^1[Cha^3, *D*-Ala^9]α-factor and desTrp^1[Cha^3, *D*-Leu^9]α-factor). This result was based on the strong Pro^8$_{\alpha CH}$-Ala^9$_{NH}$ cross-peak and relatively weak

$Ala^{9}\alpha CH$-$Gln^{10}NH$ cross-peak. The absence of these cross-peaks led to the conclusion that the β-turn is not present in inactive analogs, such as desTrp^{1}[Cha^{3}, *L*-Ala^{9}]α-factor and desTrp^{1}[Cha^{3}, *L*-Leu^{9}]α-factor in DMSO-d_6.

The conformations of [Xxx^{9}] α-factor in solution and in the presence of lipid were examined by Gounarides et al., (1993). It was found that [*D*-Ala^{9}]α-factor adopted a type II β-turn in DMSO-d_6, water, and in the presence of lipid. This conclusion was based on the relative intensity of the cross-peaks, such as $Pro^{8}\alpha CH$-$Ala^{9}NH$, $Ala^{9}\alpha CH$-$Gln^{10}NH$, $Ala^{9}NH$-$Gln^{10}NH$, and the low amide temperature coefficient of residue 10. Using the same approach, the authors did not find any evidence for a type II β-turn for [*L*-Ala^{9}]α-factor which is 10-fold less active than [*D*-Ala^{9}]α-factor.

6.3 Conformational Study of Cyclic α-Factor Analogs

The results from the conformational study of α-factor and its linear analogs lead to the conclusion that α-factor might be bent when it binds to its receptor. If this were the case, a cyclization of the peptide chain should help to reduce the entropy of the free pheromone and, therefore, its binding to the receptor would be favorable compared to the linear native pheromone. Several cyclic α-factor analogs were synthesized (Xue et al., 1989; Xue et al., personal communication). It was shown that cyclo^{7,10}[Nle^{12}]α-factor retained one-tenth to one-twentieth of the activity of α-factor, whereas cyclo^{7,10}[Cys^{7,10}, Xxx^{9}, Nle^{12}]α-factor (Xxx = Gly, *D*-Ala) retained one-fifth to one-twentieth of the activity of the native pheromone. Cyclo^{7,10}[Cys^{7,10}, *L*-Ala^{9}, Nle^{12}]α-factor was less active. Cyclo^{7,10}[Cys^{7,10}, APA^{8,9}, Nle^{12}]α-factor was neither an agonist nor antagonist (Xue et al., personal communication).

The conformation of cyclo^{7,10}[Cys^{7,10}, X^{9}, Nle^{12}]α-factor analogs in DMSO-d6/water was studied by vibrational circular dichroism (VCD) (Barlow A., personal communication) and 2D NMR techniques (Gounarides et al., 1994). Using NMR techniques the authors found that cyclo^{7,10}[Cys^{7,10}, Gly^{9}, Nle^{12}]α-factor, cyclo^{7,10}[Cys^{7,10}, *D*-Ala^{9}, Nle^{12}]α-factor and cyclo^{7,10}[Cys^{7,10}, *D*-Val^{9}, Nle^{12}]α-factor adopt a type II β-turn in DMSO-d6/water (80:20, v/v). The most active analog among these peptides, cyclo^{7,10}[Cys^{7,10}, *D*-Ala^{9}, Nle^{12}]α-factor can also adopt a type II β-turn in aqueous solution. The less active analog, cyclo^{7,10}[Cys^{7,10}, *L*-Ala^{9}, Nle^{12}]α-factor adopts a type I β-turn in DMSO-d6/water (80:20, v/v) and a type I/III β-turn in aqueous solution. From the VCD spectra, the authors were able to conclude that both cyclo^{7,10}[Cys^{7,10}, *D*-Ala^{9}, Nle^{12}]α-factor and cyclo^{7,10}[Cys^{7,10}, *L*-Ala^{9}, Nle^{12}]α-factor exhibit features indicative of a β-sheet conformation. Cyclo^{7,10}[Cys^{7}, (5-amino pentanoic acid)^{8,9}, Cys^{10}, Nle^{12}]α-factor cannot form a β-turn involving residues 7 through 10. Comparison of the VCD spectra of the analogs (cyclo^{7,10}[Cys^{7,10}, *D*-Ala^{9}, Nle^{12}]α-factor and cyclo^{7,10}[Cys^{7,10}, *L*-Ala^{9}, Nle^{12}]α-factor) with the one for cyclo^{7,10}[Cys^{7}, (5-amino pentanoic acid)^{8,9}, Cys^{10}, Nle^{12}]α-factor allowed the authors to conclude that this β-sheet like feature in the VCD spectrum was due to loosely associated *C*- and *N*-terminal chains.

CHAPTER 3

Objectives and Strategy

As mentioned earlier, NMR studies on the α-factor suggested there is a β-turn spanning through position 7-10 (Higashijima et al., 1979; Jelicks et al., 1988). Linear analogs of α-factor with *D*-amino acid residues at position 9 were found to be much more active than the homologs with the *L*-amino acid residues. In addition, NMR study of those α-factor analogs showed evidence of a type II β-turn in the active analogs but not in the inactive ones (Jelicks et al., 1988; Gounarides et al., 1993). Combining these results with theoretical studies (Venkatachalam, 1968) and the experimental results from model compounds (Aubry et al., 1985) indicated that a type II β-turn in the central region of α-factor may be an important feature of the biologically active conformation. The above conclusions prompted us to carry out a detail conformational analysis on the central region of the α-factor.

NMR investigations have proved to be a very useful technique to study the solution conformation of proteins. In most studies, NOE intensities are converted into rather coarse distance constraints with wide bounds, typically large NOEs, 1.8-2.7 Å; medium NOEs, 2.0-3.3 Å; small NOEs, 2.4-5.0 Å; and very small NOEs, 2.8-6.0 Å (Clore et al., 1990). The coarse distance constraints are used successfully in the protein structure determination because the macromolecule contains the regular secondary structures and/or stable tertiary structure which gives the characteristic medium- and long-range NOEs (Borgias and James, 1988). However, small biologically active peptides are not blessed because their inherent flexibility leads to conformational averaging. The result is often challenged by

the relevance of the solution structures to the structure in the biologically active state. To surmount this problem, conformationally constrained peptides have been used to limit the conformational freedom of the peptide. These peptides have been synthesized by covalently cyclizing the peptide backbone or the side chains by a disulfide or an amide bond (Hruby et al., 1990). This helps to alleviate the conformational averaging problem associated with short linear peptides like α-factor which usually have a vast number of low energy conformations in solution. Furthermore, the constrained peptides are more amenable to conformational analysis in solution by modern NMR spectroscopic techniques, and it is possible to correlate the conformational information to the biologically active conformation of the peptide (Jiao et al., 1993). From another point of view, in the case of α-factor, if this peptide were bent when bound to its receptor, as suggested by the previous studies, the conformationally constrained analog would be expected to have a lower entropy (S_1') in the unbound-state compared with the linear native pheromone (S_1). Therefore, the absolute value of $\Delta S'$ ($\Delta S' = S_2 - S_1'$; where S_2 is the entropy of the peptide in the bound-state) would be smaller than that of ΔS ($\Delta S = S_2 - S_1$). As S_2 is smaller than S_1 or S_1', the term ΔS is negative and according to the equation $\Delta G = \Delta H - T\Delta S$, $\Delta G'$ ($= \Delta H - T\Delta S'$) would be smaller than ΔG. This means that the cyclic molecule would require less free energy to achieve the receptor-bound conformation. Thus, it should be possible in principle to produce an analog with a higher binding constant and perhaps a higher potency than the linear native pheromone.

The goal of my dissertation is to assess the relationship between the conformation of the central region of α-factor and the biological activity of the pheromone. To accomplish this goal we developed the following strategy: (I) Systematically synthesize a series of cyclic analogs by incorporation of amino acids with

different side chain length in positions 7 and 10. The resulting peptides will have lactam rings containing 18 to 14 atoms in the central region. The chemical structures of these peptides are shown in Figure 3. (II) The biological activities and binding affinities of these analogs will be scanned. (III) The solution conformations of several of the analogs will be studied by spectroscopic techniques such as NMR and CD.

FIGURE 3: Structures of the cyclic and linear analogs of α-factor

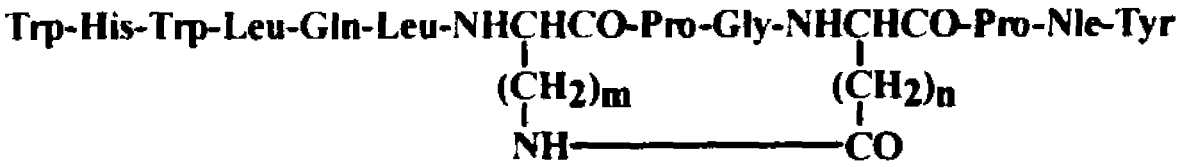

C(4)2: m = 4; n = 2
C32: m = 3; n = 2
C22: m = 2; n = 2
C12: m = 1; n = 2

C41: m = 4; n = 1
C31: m = 3; n = 1
C21: m = 2; n = 1
C11: m = 1; n = 1

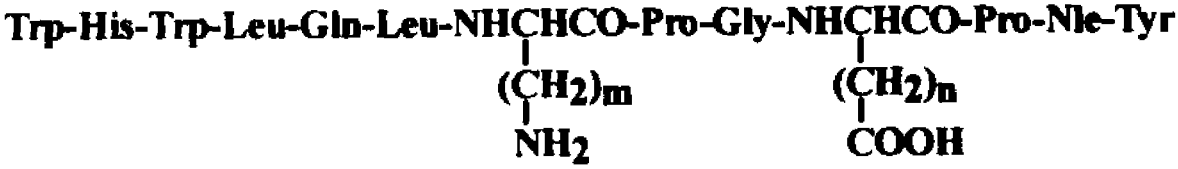

L(4)2: m = 4; n = 2
L32: m = 3; n = 2
L22: m = 2; n = 2
L12: m = 1; n = 2

L41: m = 4; n = 1
L31: m = 3; n = 1
L21: m = 2; n = 1
L11: m = 1; n = 1

CHAPTER 4

Syntheses of Peptides

I. Materials and Methods

All amino acid derivatives were purchased from BaChem Inc. (Torrance, CA) except for N^{α}-t-butyloxycarbonyl-O^{γ}-9-fluorenylmethyl-*L*-glutamic acid (**1a**), N^{α}-t-butyloxycarbonyl-O^{β}-9-fluorenylmethyl-*L*-aspartic acid (**2a**), N^{α}-t-butyloxycarbonyl-N^{δ}-9-fluorenylmethoxycarbonyl-*L*-ornithine (**3a**), N^{α}-t-butyloxycarbonyl-N^{γ}-9-fluorenylmethoxycarbonyl-*L*-diaminobutyric acid (**4a**) and N^{α}-t-butyloxycarbonyl-N^{β}-9-fluorenylmethoxycarbonyl-*L*-diaminopropionic acid (**5a**). All solvents were supplied from Fisher Scientific (Pittsburgh, PA). Solvents for high performance liquid chromatography (HPLC) were HPLC grade and other solvents were A.C.S. reagent grade. The following chemicals: 4-(*N*,*N*-dimethylamino)-pyridine (DMAP), pyridine, 9-fluorenylmethanol, *N*-(9-fluorenylmethoxy-carbonyloxyl)succinimide, 9-fluorenylmethyl chloroformate, bis[trifluoroacetoxy]phenyliodine, benzotriazol-1-yl-oxy-tris(dimethylamino)-phosphonium hexafluorophosphate (BOP reagent), DIEA, DCC, DIPC and CH_2Cl_2 were purchased from Aldrich Chemical Co. (Milwaukee, WI) and used without purification. Aminomethyl resin and 4-methyl-benzhydrylamine resin were purchased from Peninsula Laboratories and BaChem, Inc., respectively. Anhydrous hydrogen fluoride (HF) was supplied by Matheson.

Thin-layer chromatography (TLC) was performed using glass plates obtained from E. I. Merck which were precoated with a 0.25-mm-thick layer of Kieselgel 60F-254. Spots were visualized by UV light (254 nm) and/or by ninhydrin (0.5 g

of ninhydrin in 100 mL of acetone) followed by staining in a sulfuric acid vapor chamber and a brief heating. Optical rotations were obtained on a Jasco Dip-370 digital polarimeter at 589 nm. The reported [α] values were the average of six determinations.

HPLC was performed on a Waters Model 501 system and a 3.9 mm x 300 mm stainless steel column packed with μBONDAPAK C_{18} for analytical work or on a Waters Model 510 system with a stainless steel μBONDAPAK C_{18} column (19 mm x 150mm or 19 mm x 300 mm) for preparative work. The detector was a Waters Model 490 ultraviolet detector which monitored absorbance at 220 nm for analytical HPLC or a Waters Model 481 ultraviolet detector which monitored absorbance at 279 nm for preparative HPLC.

Amino acid analysis was carried out at the Wistar Institute, and FABMS was measured at the University of Tennessee Mass Spectrometry Center. ^1H NMR spectra were acquired on a Bruker 200-MHz spectrometer equipped with Aspect 2000 NMR software. NMR data are reported as follows: chemical shift in parts per million downfield from tetramethylsilane (δ = 0.00) and/or using the residual solvent as an internal standard, multiplicity (s = singlet, d = doublet, t = triplet, dd = doublet of doublet, dt = doublet of triplet, m = multiplet, br = broad).

II. Synthesis of the Amino Acid Derivatives

2.1 Synthesis of N^{α}-t-butyloxycarbonyl-O^{γ}-9-fluorenylmethyl-*L*-glutamic acid (**1a**)

Synthesis of N^{α}-t-butyloxycarbonyl-O^{γ}-9-fluorenylmethyl-*L*-glutamic acid (**1a**) followed the procedures of Bolin et al., (1989). N^{α}-*t*-Butyloxycarbonyl-O^{α}-benzyl-*L*-glutamate (13.53 g, 40 mmol) and 9-fluorenylmethanol (7.58 g, 38 mmol) were dissolved in 200 mL CH_2Cl_2. The stirred solution was chilled in an ice bath and to it was added 4-(*N,N*-dimethylamino)-pyridine (DMAP) (47.5 mg, 0.38 mmol). *N,N'*-dicyclohexylcarbodiimide (DCC) (8.27 g, 40 mmol) was added in portions over 10 minutes and the resulting mixture was stirred with cooling for 4 hours. Precipitated *N,N'*-dicyclohexylurea (as a white solid) was removed by filtration and the filtrate was diluted with 150 mL CH_2Cl_2. The solution was extracted with 2 x 100 mL 10% citric acid, 2 x 100 mL H_2O, 2 x 100 mL 2.5% $NaHCO_3$, and 2 x 100 mL H_2O, dried over $MgSO_4$ (anhydrous), filtered, and concentrated to a mixture of white solid and yellowish oil. Recrystallization from methanol/ether/pet. ether yielded 16.60 g (yield 84.8%) of N^{α}-*t*-butyloxycarbonyl-O^{α}-benzyl-O^{γ}-9-fluorenylmethyl-*L*-glutamate (**1b**). NMR ($CDCl_3$) δ 1.43 (s, 9H), 1.97 (m, 1H), 2.19 (m, 1H), 2.46 (m, 2H), 4.20 (t, 1H), 4.39 (m, 1H), 4.40 (d, 2H), 5.12 (m, 1H), 5.18 (s, 2H), 7.36 (s, 5H), 7.46 - 7.26 (m, 9H), 7.59 (d, 2H), 7.78 (d, 2H). This compound was used directly to prepare **1a**.

N^{α}-*t*-Butyloxycarbonyl-O^{α}-benzyl-O^{γ}-9-fluorenylmethyl-*L*-glutamate (**1b**) (5.00 g, 9.69 mmol) was hydrogenated in 180 mL methanol containing about 4 g 10% Pd/C catalyst for 1.5 hours at room temperature at 20 - 30 psi. The methanol solution was filtered and concentrated to an oily residue. The residue was

redissolved in 150 mL ether and extracted with 100 mL 5% citric acid. The aqueous layer was back-extracted with 2 x 50 mL ether. The combined ether layers were dried over $MgSO_4$ (anhydrous), filtered, and concentrated to a white foam (4.54 g). Recrystallization from ether/pet. ether in a refrigerator overnight yielded 3.24 g of **1a** (yield 78%); mp 128 - 129 °C (lit. 130 - 131°C) (Bolin et al., 1989); NMR ($CDCl_3$) δ 1.44 (s, 9H), 2.16 (m, 1H), 2.27 (m, 1H), 2.58 (m, 2H), 4.22 (t, 1H), 4.35 (m, 1H), 4.40 (d, 2H), 5.19 (br d, 1H), 6.49 (br, 1H), 7.48 - 7.24 (m, 4H), 7.60 (d, 2H), 7.78 (d, 2H). $[\alpha]_D^{25}$: +6.0°(*c* 1.1, EtOAc) (lit. +9.33°, *c* 1, EtOAc) (Bolin et al., 1989). HPLC (CH_3CN/H_2O/0.025% TFA) proved the purity was over 99% (k' = 2.24; linear gradient from 40% CH_3CN - 60% CH_3CN over 30 min). TLC CH_2Cl_2/MeOH/HOAc (10:1:0.5, v/v/v) showed only one spot under the detection of UV and ninhydrin (R_f 0.59).

2.2 Synthesis of N^{α}-t-butyloxycarbonyl-O^{β}-9-fluorenylmethyl-*L*-aspartic acid (**2a**)

Synthesis of N^{α}-*t*-butyloxycarbonyl-O^{β}-9-fluorenylmethyl-*L*-aspartic acid (**2a**) followed the procedures of Bolin et al., (1989). *N*-*t*-Butyloxycarbonyl-O^{α}-benzyl-*L*-aspartate (12.90 g, 40 mmol) and 9-fluorenylmethanol (7.58 g, 38 mmol) were dissolved in 200 mL CH_2Cl_2. The stirred solution was chilled in an ice bath and to it was added DMAP (47.5 mg, 0.38 mmol). DCC (8.27 g, 40 mmol) was added in portions over 10 minutes, and the resulting mixture was stirred with cooling for 4 hours. Precipitated *N,N'*-dicyclohexylurea (as a white solid) was removed by filtration and the filtrate was diluted with 200 mL CH_2Cl_2. The solution was extracted with 2 x 50 mL 10% citric acid, 2 x 50 mL H_2O, 2 x 50 mL 2.5% $NaHCO_3$, and 2 x 50 mL H_2O, dried with $MgSO_4$ (anhydrous) overnight, filtered, and concentrated to a yellowish oil. Recrystallization from

methanol/ether/pet. ether yielded white yield 14.75 g (yield 77.5%) of N^{α}-*t*-butyloxycarbonyl-O^{α}-benzyl-O^{γ}-9-fluorenylmethyl-*L*-aspartate (**2b**) as a white solid; mp 75 - 76 °C (lit. 74 - 76 °C) (Bolin et al., 1989); NMR ($CDCl_3$) δ 1.44 (s, 9H), 2.91 (dd, 1H), 3.12 (dd, 1H), 4.14 (t, 1H), 4.35 (d, 2H), 4.62 (m, 1H), 5.12 (s, 2H), 5.47 (br d, 1H), 7.30 (s, 5H), 7.50 - 7.24 (m, 4H), 7.57 (d, 2H), 7.79 (d, 2H); $[\alpha]_D$: -8.9° (*c* 1.1, MeOH) (lit. -11.67°, *c* 1, MeOH) (Bolin et al., 1989). TLC CH_2Cl_2/MeOH/HOAc (10:1:0.5, v/v/v) showed only one spot under the detection of UV and ninhydrin (Rf 0.78).

N^{α}-*t*-Butyloxycarbonyl-O^{α}-benzyl-O^{γ}-9-fluorenylmethyl-*L*-aspartate (**2b**) (7.00 g, 13.97 mmol) was hydrogenated in 110 mL methanol containing 390 mg 10% Pd/C catalyst for 35 minutes at room temperature at 10 - 29 psi. The methanol solution was filtered and concentrated to white foam (3.75 g). The residue was redissolved in 150 mL ether and extracted with 100 mL 5% citric acid. The aqueous layer was back-extracted with 2 x 50 mL ether. The combined ether layers were dried over $MgSO_4$ (anhydrous), filtered, and concentrated to a white foam. The crude material was recrystallized from ether/methanol (a few drops) in a refrigerator overnight to 4.90 g of **2a** (yield 86%); mp 139 - 140 °C (lit. 141 - 142 °C) (Bolin et al., 1989). NMR ($CDCl_3$) δ 1.47 (s, 9H), 2.91 (dd, 1H), 3.14 (dd, 1H), 4.21 (t, 1H), 4.42 (m, 2H), 4.62 (m, 1H), 5.49 (d, 1H), 6.95 (br, 1H), 7.48 - 7.27 (m, 4H), 7.58 (d, 2H), 7.78 (d, 2H). $[\alpha]_D^{25}$: +3.3° (*c* 1.0, MeOH) (lit. +5.52°, *c* 1, MeOH) (Bolin et al., 1989). HPLC (CH_3CN/H_2O/0.025% TFA) proved the purity was over 99% (k' = 9.04; linear gradient from 30% CH_3CN - 90% CH_3CN over 30 min). TLC CH_2Cl_2/MeOH/HOAc (10:1:0.5, v/v/v) showed only one spot under the detection of UV and ninhydrin (Rf 0.45).

2.3 Synthesis of N^{α}-*t*-butyloxycarbonyl-N^{δ}-9-fluorenylmethoxycarbonyl-*L*-ornithine (3a)

N^{α}-*t*-Butyloxycarbonyl-N^{δ}-9-fluorenylmethoxycarbonyl-*L*-ornithine (3a) was prepared following the procedures of Bodanszky and Bodanszky (1984). N^{α}-*t*-butyloxycarbonyl-*L*-ornithine (1.77 g, 7.6 mmol) was dissolved in 10% Na_2CO_3 (20 mL, 19 mmol). To it was added dioxane (11.4 mL), and the mixture was stirred in an ice-bath. *N*-(9-Fluorenylmethoxycarbonyloxyl)succinimide (2.56 g, 7.6 mmol) was added in small portions. The solution was stirred in an ice-water bath for 4.5 hours. TLC showed the reaction was almost complete. The reaction mixture was diluted with H_2O (25 mL) and extracted with ether (2 x 100 mL). The aqueous solution was cooled in an ice-water bath and acidified under vigorous stirring with concentrated HCl to pH 2 (gel formed at pH 7), and diluted with H_2O. The mixture was stored in the refrigerator overnight. The white solid was filtered and washed with H_2O three times and dried in a vacuum for 2 hours. The crude product was recrystallized from methanol/ether/cyclohexane in the refrigerator overnight to yield 3a (3.12 g, yield 90%); mp 150.5 - 151.5 °C (lit. 150 - 152 °C) (BaChem, Inc.) ; NMR (DMSO-d_6) δ 1.39 (s, 9H), 1.48 (m, 2H), 1.57 (m, 1H), 1.70 (m, 1H), 2.97 (m, 2H), 3.83 (m, 1H), 4.22 (m, 1H), 4.28 (d, 2H), 7.08 (br d, 1H), 7.50 - 7.20 (m, 4H), 7.69 (d, 2H), 7.90 (d, 1H). $[\alpha]_D^{25}$: +8.5°(*c* 1.0, $CHCl_3$)(lit. +8.3°, *c* 1.0, $CHCl_3$) (BaChem Inc., King of Prussia, PA). HPLC (CH_3CN/H_2O/0.025% TFA) proved the purity was over 99% (k' = 7.19; linear gradient from 20% CH_3CN - 80% CH_3CN over 30 min). TLC CH_2Cl_2/MeOH/HOAc (10:1:0.5, v/v/v) showed only one spot under the detection of UV (R_f 0.54).

2.4 Synthesis of N^{α}-*t*-butyloxycarbonyl-N^{γ}-9-fluorenylmethoxycarbonyl-*L*-diaminobutyric acid (4a)

N^{α}-*t*-Butyloxycarbonyl-*L*-diaminobutyric acid **4b** was synthesized by following the procedures described by Waki et al. (1981). Bis[trifluoroacetoxy]-phenyliodine (10.00 g, 23.3 mmol) was dissolved in 60 mL DMF/H_2O (1:1, v/v). To it was added *N*-*t*-butyloxycarbonyl-*L*-glutamine (3.80 g, 15.5 mmol) at room temperature. After 15 minutes, pyridine (2.48 mL, 31.0 mmol) was added, and stirring was continued for 3.5 hours. The solvents were evaporated in vacuum overnight. The residue was dissolved in 150 mL water. The solution was washed extensively with ether (10 x 100 mL) and evaporated in a vacuum overnight to a yellowish oil **4b** (7.31 g).

The crude N^{α}-*t*-butyloxycarbonyl-*L*-diaminobutyric acid **4b** (7.31 g, 15.5 mmol) was dissolved in 10% Na_2CO_3 (100 mL). To it was added dioxane (30 mL). The mixture was stirred in an ice-water bath. *N*-(9-Fluorenylmethoxy-carbonyloxyl)succinimide (5.23 g, 15.5 mmol) was added in small portions. The solution was stirred in an ice-water bath for 4.5 hours. The reaction mixture was diluted with H_2O (250 mL), and extracted with ether (3 x 100 mL). The aqueous solution was cooled in an ice-water bath and acidified under vigorous stirring with concentrated HCl to pH 2. The mixture was stored in a refrigerator overnight. The white solid was filtered and washed with H_2O three times and dried in a vacuum for 2 hours to yield the crude product (6.59 g). The crude product was recrystallized from ethyl acetate/ether/cyclohexane in a refrigerator overnight to yield **4a** (4.28 g, yield 63%); mp sublimes at 155 - 165 °C (lit. sublimes at 85 - 95°C) (Stanfield et al., 1990); NMR (DMSO-d_6) δ 1.49 (s, 9H), 1.69 (m, 1H), 1.84 (m, 1H), 3.05 (m, 2H), 3.91 (m, 1H), 4.35 -4.15 (m, 3H), 7.15 (br. d,

1H), 7.48 - 7.25 (m, 4H), 7.70 (d, 2H), 7.89 (d, 2H). $[\alpha]_D^{25}$ -1.8° (*c* 1.1, $CHCl_3$) (lit. -3.63°, *c* 1.0 $CHCl_3$) (Stanfield et al., 1990). HPLC (CH_3CN/H_2O/0.025% TFA) proved the purity was 99% (k' = 7.16; linear gradient from 30% CH_3CN - 80% CH_3CN over 20 min) . TLC n-butanol/HOAc/pyridine/H_2O (4:1:1:2, v/v/v/v) showed only one spot under the detection of UV and ninhydrin (R_f 0.68).

2.5 Synthesis of N^{α}-*t*-butyloxycarbonyl-N^{β}-9-fluorenylmethoxycarbonyl-*L*-diaminopropionic acid (5a)

N^{α}-*t*-Butyloxycarbonyl-*L*-diaminopropionic acid **5b** was synthesized by following the procedures described by Waki et al. (1981). Bis[trifluoroacetoxy]-phenyliodine (12.90 g, 30 mmol) was dissolved in 160 mL DMF/H_2O (1:1, v/v). To it was added N^{α}-*t*-butyloxycarbonyl-*L*-asparagine (4.64 g, 20 mmol) at room temperature. After 15 minutes, pyridine (3.23 mL, 40 mmol) was added, and stirring was continued for 3 hours. The solvents were evaporated in a vacuum overnight. The yellowish oily residue was dissolved in H_2O (150 mL). The solution was washed extensively with ether (10 x 100 mL) and evaporated in vacuum with P_2O_5 overnight to a yellowish oil. The oily residue was recrystallized from ether/methanol (small amount) to yield N^{α}-t-butyloxycarbonyl-*L*-diaminopropionic acid **5b** as a white solid (4.38 g, 107%).

N^{α}-*t*-Butyloxycarbonyl-*L*-diaminopropionic acid **5b** (4.10 g, 20.1 mmol) was dissolved in 10% Na_2CO_3 (40 mL). The solution was cooled with stirring in an ice-water bath and to it was added dioxane (22 mL). A solution of 9-fluorenylmethyl chloroformate (5.19 g, 20.2 mmol) in dioxane (30 mL) was added dropwise to the amino acid solution over 30 minutes. The reaction mixture was stirred in an ice-water bath for 1 hour and continually stirred at room temperature

for 2 hours and poured over an ice/water mixture (500 mL). The cooled solution was washed with ether (2 x 150 mL) and acidified to pH 2-3 with 1 N H_2SO_4 in an ice-water bath and extracted rapidly at 0 °C with ethyl acetate (2 x 200 mL). The combined ethyl acetate extracts were washed with water (3 x 100 mL), dried over $MgSO_4$ (anhydrous), filtered and evaporated in vacuum (Stanfield et al., 1990). The resulting white foam (3.41 g) was purified by preparative HPLC with a μBONDAPAK C_{18} column to yield **5a** (2.11 g, 25%) as a white powder after lyophilizing; mp sublimes at 85 - 94 °C (lit. 75 - 100 °C) (Stanfield et al., 1990). NMR (DMSO-d_6) δ 1.36 (s, 9H), 3.31 (m, 2H), 4.03 (m, 1H), 4.35 - 4.12 (m, 3H), 7.00 (d, 1H), 7.47 - 7.23 (m, 4H), 7.69 (d, 2H), 7.89 (d, 2H). $[\alpha]_D^{25}$ -7.8° (*c* 1.1, $CHCl_3$)(lit. +0.20°, *c* 1.0, $CHCl_3$) (Stanfield et al., 1990). HPLC (CH_3CN/H_2O/0.025% TFA) proved the purity was 100% (k' = 6.74; linear gradient from 30% CH_3CN - 80% CH_3CN over 20 min). TLC CH_2Cl_2/MeOH/HOAc (10:1:0.5, v/v/v) showed only one spot under the detection of UV and ninhydrin (R_f 0.51).

III. Syntheses of the α-Factor Analogs

3.1 Synthesis of N^{α}-*t*-butyloxycarbonyl-Tyr (2-BrZ)-phenylacetic acid phenacyl ester (6a)

Potassium fluoride dihydrate (2.80 g, 30 mmol) was added to a rapidly stirred solution of 4-bromomethylphenylacetic acid phenacyl ester (5.20 g, 15 mmol) and N^{α}-*t*-butyloxycarbonyl-Tyr (2-BrZ) (5.00 g, 10 mmol) in CH_3CN (40 mL). The suspension was stirred at room temperature until TLC indicated that the reaction was complete (20 hours). Ethyl acetate (150 mL) and water (150 mL) were added to the reaction mixture to form two phases. The organic phase was washed with

3% $NaHCO_3$ (3 x 150 mL), H_2O (3 x 150 mL), dried over $MgSO_4$ (anhydrous) and evaporated to yield a crude product which was recrystallized from ethyl acetate/cyclohexane in a refrigerator overnight to a purer product **6a** (about 12 g). TLC of CH_2Cl_2 showed that the purity of **6a** was over 95%. The product was used without additional purification to prepare **6b**.

3.2 Synthesis of N^{α}-*t*-butyloxycarbonyl-Tyr (2-BrZ)-phenylacetic acid (6b)

The product **6a** (12 g, about 10 mmol) was dissolved in 70 mL HOAc/H_2O (6:1, v/v). To it was added zinc dust (13.00 g, 200 mmol). The suspension was vigorously stirred at room temperature until TLC showed the disappearance of the starting materal **6b** (8 hours). After filtration, the filtrate was added to H_2O (150 mL), and ethyl acetate (150 mL) and was titrated to pH 1-2 (in aqueous phase). The separated aqueous phase was extracted with ethyl acetate 2 x 100 mL. The combined organic layers were washed by (H_2O 10 x 150 mL), and dried over $MgSO_4$ overnight. The organic solvent was evaporated to yield crude product. The crude was recrystallized from ethyl acetate/cyclohexane in a refrigerator overnight to yield pure product **6b** (4.17 g, 65%); mp 98 - 100 °C. NMR (DMSO-d_6) δ 1.35 (s, 9H), 3.10 - 2.80 (m, 2H), 3.37 (s, 1H), 3.55 (s, 1H), 4.21 (m, 1H), 5.10 (s, 2H), 5.33 (s, 2H), 7.16 (d, 2H), 7.28 (s, H), 7.31 (d, H), 7.45 - 7.32 (m, H), 7.49 (d, 1H), 7.59 (d, 1H), 7.72 (d, 1H). $[\alpha]_D^{25}$ - 7.8° (*c* 0.9, MeOH). HPLC (CH_3CN/H_2O/0.025% TFA) proved the purity was over 99% (k' = 5.43; linear gradient from 40% CH_3CN - 60% CH_3CN over 30 min). TLC CH_2Cl_2/MeOH/HOAc (10:1:0.5, v/v/v) showed only one spot under the detection of UV and ninhydrin (R_f 0.60).

3.3 Synthesis of N^{α}-*t*-butyloxycarbonyl-Tyr (2-BrZ)-phenylacetamido-methyl resin (6c)

Aminomethyl resin (13.17 g, 10 mmol) was put in a reaction vessel and washed successively with CH_2Cl_2 (3 x 70 mL), MeOH (3 x 70 mL) and DMF (4 x 70 mL). The resulting resin was coupled with 6b (6.43 g, 10 mmol) using BOP (4.42 g, 10 mmol) in the presence of DIEA (2 mL) in 50 mL DMF. The reaction vessel was shaken overnight. All reactants were removed by filtration and the resin was thoroughly washed. After a positive Kaiser test (Kaiser et al., 1970), the resin was coupled a second time with 6b (3.22 g, 5 mmol), BOP (2.21 g, 5 mmol) and DIEA (2 mL) in 50 mL DMF for 2 hours. The result of Kaiser test was negative. The derivatized resin then was worked up by washing successively with DMF (4 x 50 mL), CH_2Cl_2 (3 x 50 mL) and MeOH (3 x 90 mL), and the remaining solvents were evaporated in a desiccator under a vacuum overnight. The product (6c) weighed 18.63 g (yield 96%).

3.4 Synthesis of Boc-Pro-Nle-Tyr(2-BrZ)-PAM resin (7a)

The synthesis was performed manually, by placing N^{α}-Boc-Tyr (2-BrZ)-PAM resin (6c)(9.315 g, 5 mmol) into a 150-mL reaction vessel, and initiating the synthetic cycles (Xue et al., 1989). All residues were double-coupled regardless of the Kaiser test result (Kaiser et al., 1970), which was performed prior to and after each coupling step. If the Kaiser test gave a positive result after a second or third coupling, additional coupling or acetylation of the remaining unreacted amino groups was performed. The Boc group was used exclusively for the N^{α}-protection. A typical coupling cycle consisted of the following procedures (15 mL of solvent per gram of resin): 1) CH_2Cl_2, 3 x 1 min; 2) 50% TFA in CH_2Cl_2,

1 x 1 min; 3) 50% TFA in CH_2Cl_2, 1 x 30 min; 4) CH_2Cl_2, 3 x 1 min; 5) Kaiser test; 6) 10% DIEA in CH_2Cl_2, 1 x 2 min; 7) 10% DIEA in CH_2Cl_2, 1 x 5 min; 8) CH_2Cl_2, 3 x 1 min; 9) N^{α}-Boc-amino acid (3 eq) in CH_2Cl_2 added to the vesel followed by DIPC (3 eq), shaken for 3 h; 10) CH_2Cl_2, 6 x 1 min; 11) Kaiser test; 12) 5% DIEA in CH_2Cl_2, 1 x 2 min; 13) CH_2Cl_2, 3 x 1 min; 14) N^{α}-Boc-amino acid (1 eq) in CH_2Cl_2 added to the vessel followed by DIPC (1 eq), shaken for 1 h; 15) CH_2Cl_2, 6 x 1 min; 16) Kaiser test. After Boc-Pro was added onto the peptide chain, the resin was dried to a constant weight in a desiccator under a high vacuum overnight. The product, Boc-Pro-Nle-Tyr(2-BrZ)-PAM resin (7a), weighed 10.270 g (yield 99%).

3.5. Synthesis of Boc-Pro-Gly-Glu(Ofm)-Pro-Nle-Tyr(2-BrZ)-PAM resin (8a)

The synthesis was performed manually, starting from 4.108 g of 7a (2 mmol). The additions of residues Glu, Gly and Pro followed the procedures described above without difficulty. The resulting product (8a) was dried in a desiccator under a high vacuum to a constant weight of 4.940 g (yield 98%).

3.6. Synthesis of Boc-Trp(For)-His(Tos)-Trp(For)-Leu-Gln-Leu-(*D*)Lys(Fmoc)-Pro-Gly-Glu(Ofm)-Pro-Nle-Tyr(2-BrZ)-PAM resin (9a)

The synthesis was performed manually, starting from 2.453 g of 8a (0.993 mmol). The coupling cycles were as previously described except that the cycle immediately following the incorporation of Boc-Gln was as follows: 1) dioxane, 3 x 1 min; 2) 4 N HCl in dioxane, 1 x 1 min; 3) 4 N HCl in dioxane, 1 x 30 min;

4) dioxane, 3 x 1 min; 5) $CHCl_3$, 3 x 1 min; 6) Kaiser test; 7) 10% DIEA in $CHCl_3$, 1 x 2 min; 8) 10% DIEA in $CHCl_3$, 1 x 5 min; 9) $CHCl_3$, 3 x 1 min; 10) CH_2Cl_2, 3 x 1 min; 11) DIPC (3 eq) in CH_2Cl_2 added to the vessel followed by N^{α}-Boc-amino acid (3 eq) in CH_2Cl_2, shaken for 3 h; 12) CH_2Cl_2, 3 x 1 min; 13) Kaiser test; 14) $CHCl_3$, 3 x 1 min; 15) 5% DIEA in $CHCl_3$, 1 x 2 min; 16) $CHCl_3$, 3 x 1 min; 17) CH_2Cl_2, 3 x 1 min; 18) DIPC (1 eq) in CH_2Cl_2 added to the vessel followed by N^{α}-Boc-amino acid (1 eq) in CH_2Cl_2, shaken for 1 h; 19) CH_2Cl_2, 6 x 1 min; 20) Kaiser test. The incorporation of N^{α}-Boc-Leu in position 6, and of N^{α}-Boc-Trp in positions 3 and 1 required a third coupling as revealed by a positive Kaiser test. When a third coupling was required, the HOBt/DIPC accelerated active ester coupling procedure was utilized in a mixture of CH_2Cl_2 and DMF (1:1, v/v). Because the Kaiser test after the third coupling of Trp to position 3 still gave a positive result, the unreacted amino acid was blocked by reaction with acetic anhydride (2 eq) catalyzed by pyridine (about 10 eq) in 40 mL CH_2Cl_2. The product **2a** was washed throughly with DMF, CH_2Cl_2, MeOH and dried in a desiccator under a high vacuum for 2 days, and weighed 3.030 g (yield 78.6% based on the starting amine content on the aminomethyl resin, 0.759 mmol/g).

3.7. Synthesis of cyclo^{7,10}[*D*-Lys^{7}, Glu^{10}, Nle^{12}]α-factor

In order to increase the efficiency of lactam formation, cyclization was carried out prior to the HF cleavage from the resin. The completely assembled tridecapeptide-PAM resin **2a** (1.530 g, 0.501 mmol) was treated with 20% piperidine in 30 mL DMF, 1 x 2 min, 1 x 30 min for deprotection of Fmoc and Ofm from *D*-Lys^{7} and Glu^{10}, respectively. To the reaction vessel BOP coupling reagent (0.751 g, 1.7 mmol) and 1.5% DIEA in 30 mL DMF were added, and the

resulting suspension was shaken for 2.5 hour. The first Kaiser test was positive and a second cyclization was carried out using 0.451 g BOP (1.02 mmol) and 30 mL 1.0% DIEA in DMF overnight, after which the Kaiser test was negative. Previously it had been shown that a purer crude product was obtained if the other side chain protecting groups were deprotected before the HF cleavage (Xue et al., 1989). The Tos group had been removed by HOBt during the accelerated active ester coupling cycle by mistake and the For group had been removed by piperidine during the deprotection of Fmoc and Ofm groups. The Boc protecting group was removed by 48% TFA in CH_2Cl_2 (2% DMS) (30 mL), 1 x 2 min, 1 x 30 min.

The TFA tridecapeptide-PAM resin salt was subjected to HF cleavage. Ten percent anisole was used as the scavenger. About 10 mL HF per gram resin was used for HF cleavage. Cleavage was carried out at -5 to 2 °C for 1 hour. After evaporation of HF under reduced pressure and under the vacuum, the crude product was washed with ethyl ether 3 times, extracted with 25% acetic acid and lyophilized. The crude weighed 200 mg. The overall yield was 32% based on the starting amine content on the aminomethyl resin (0.759 mmol/g). The crude material was analyzed by reversed-phase HPLC on a Waters μBONDAPAK C_{18} column (3.9 mm x 300 mm) utilizing a linear gradient of CH_3CN (0.025% TFA) and H_2O (0.025% TFA) as eluent. One major peak was observed, as shown in Figure 4.

The crude product was dissolved in a mixture of MeOH and CH_3CN(1:1, v/v), and purified by reversed phase, semipreparative HPLC on a Waters μBONDAPAKC_{18} column (19 mm x 150 mm). The product was eluted with a linear gradient of H_2O (0.025% TFA) and CH_3CN (0.025% TFA), from 0 to 80% CH_3CN over 60 min

FIGURE 4: HPLC of the crude (Left) and purified (Right) cyclo^{7,10}[*D*-Lys^{7}, Glu^{10}, Nle^{12}]α-factor (C(4)2)

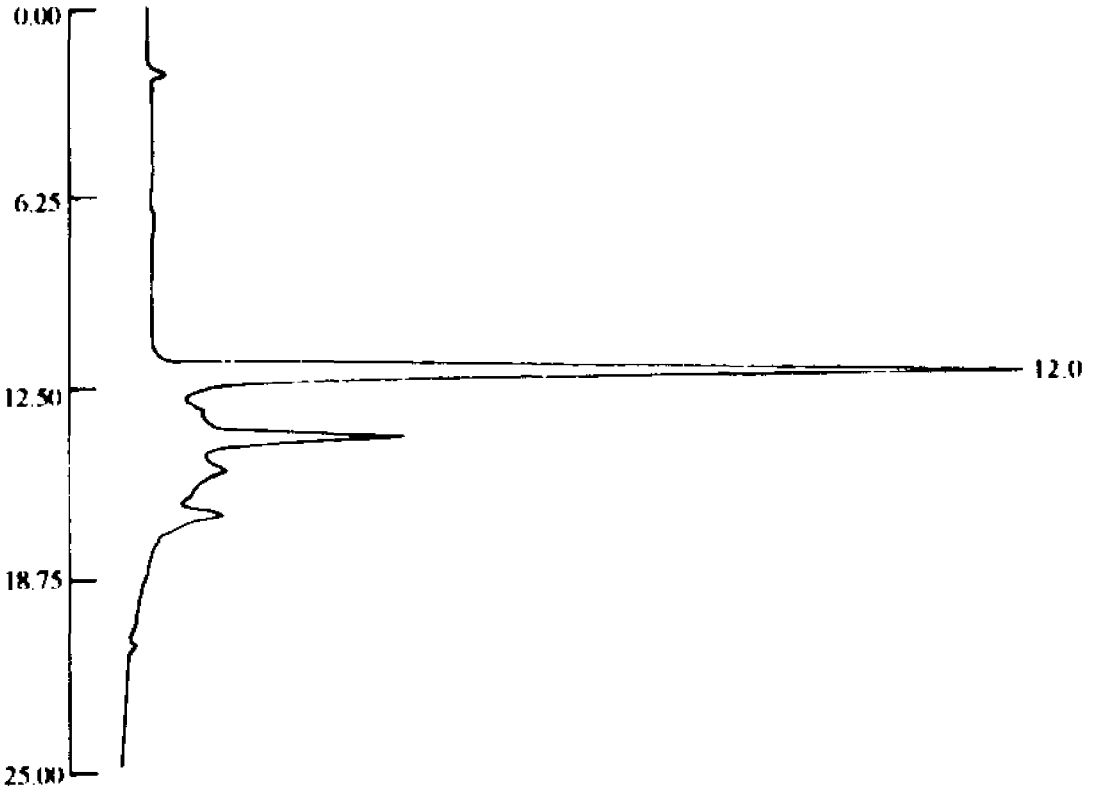
0.00
6.25
12.50
18.75
25.00
12.0


0.00
6.25
12.50
18.75
12.0

at a flow rate of 6 mL/min. The fractions were collected in one-minute intervals and were analyzed by analytical HPLC as described above. The homogeneous fractions (over 99% as judged by HPLC, Figure 4) were combined and lyophilized. The purified material, cyclo^{7,10}[*D*-Lys^{7}, Glu^{10}, Nle^{12}]α-factor, weighed 85 mg (overall yield 13% based on the starting amine content (0.759 mmol/g) on the aminomethyl resin).

The purity of the final product was characterized by HPLC with a different solvent system (linear gradient of MeOH (0.025% TFA) and H_2O (0.025% TFA) and showed that the purity was 97%. The purity of the final product was also analyzed by TLC on silica gel with two developing solvent systems, and only one spot was observed using UV and ninhydrin detection (Table 1). Amino acid analysis gave the amino acid contents which was very close to the calculated values (Table 1). The FABMS spectrum of the final product also showed the correct molecular weight (Table 1).

3.8. Synthesis of linear[*D*-Lys^{7}, Glu^{10}, Nle^{12}]α-factor

The completely assembled tridecapeptide-PAM resin **9a** (0.500 g, 0.164 mmol) was treated with 20% piperidine in 25 mL DMF 1 x 2 min, 1 x 30 min for deprotection of Fmoc and Ofm from *D*-Lys^{7} and Glu^{10} and with 48% TFA in 25 mL CH_2Cl_2(2% DMS), 1 x 2 min, 1 x 30 min for removal of the Boc group from the *N*-terminus. After HF cleavage and lyophilization following the procedures described above, the crude product weighed 200 mg (overall yield of 61% based on the starting amine content on the aminomethyl resin; 0.759 mmol/g). The crude material was analyzed by analytical HPLC utilizing a linear gradient of CH_3CN (0.025% TFA) and H_2O (0.025% TFA) as eluant. One major peak was

Table 1

Chemical and Physical Properties of Cyclic α-Factor Analogs

Peptide	Amino acid analysis										Rf[b]		K'[c]	FAB-MS[d]	Calculated mass (amu)
	Asx	Glx	Gly	His	Leu	Lys	Nle	Pro	Tyr	Trp[a]	Solvent A	Solvent B			
C(4)2	-	1.86	0.94	0.88	2.21	1.02	0.96	2.05	1.07	ND[e]	0.46	0.68	6.92	1649.0	1648.8
C32	-	2.03	1.20	0.91	1.92	-	0.94	2.01	1.07	1.92	0.43	0.65	6.90	1635.0	1634.8
C22	-	1.75	0.97	1.10	2.18	-	0.93	1.93	1.02	2.13	0.44	0.64	6.85	1620.1	1620.8
C12	-	1.82	0.99	1.02	1.86	-	ND	2.11	1.21	ND	0.44	0.68	6.84	1607.4	1606.8
C41	0.92	1.04	1.12	0.89	2.03	0.91	0.98	2.04	1.07	ND	0.51	0.69	7.14	1635.0	1634.8
C31	0.93	0.91	1.01	1.04	1.87	-	ND	2.10	1.15	ND	0.54	0.67	6.99	1621.5	1620.8
C21	1.08	0.88	0.97	1.01	1.80	-	ND	2.09	1.16	ND	0.51	0.66	6.89	1607.3	1606.8
C11	1.16	0.92	0.96	1.01	1.81	-	ND	2.02	1.14	ND	0.51	0.66	6.87	1593.3	1592.8

[a] In two cases (**C32** and **C22**) special care was taken during hydrolysis to obtain the Trp content. In the other peptides, the presence of Trp residues is verified by the FAB-MS values. [b] Solvent system A: butanol/acetic acid/water (4:1:2, v/v/v), solvent system B: butanol/acetic acid/water/pyridine (4:1:2:1, v/v/v/v). Rf values were determined using TLC on silica. [c] K' values were determined for a μBondapak C_{18} column using a 20% - 60% acetonitrile gradient (0.025% TFA) over 20 min. [d] The values represent monoisotopic masses. [e] ND, not done.

FIGURE 5: HPLC of the crude (Left) and purified (Right) [*D*-Lys^{7}, Glu^{10}, Nle^{12}]α-factor (L(4)2)

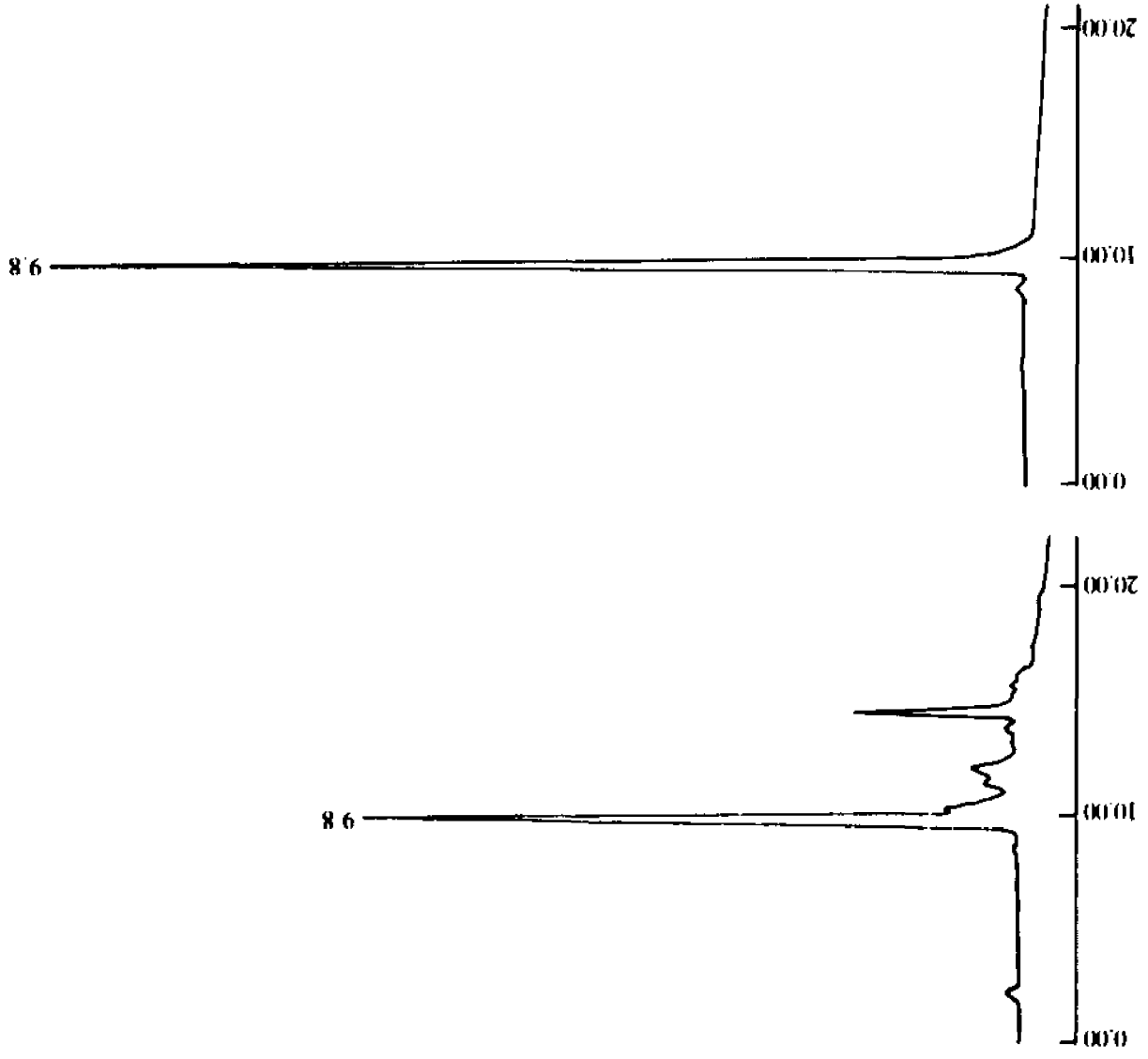
9.8
20.00
10.00
0.00
9.8
20.00
10.00
0.00

observed, as shown in Figure 5.

The crude product was dissolved in a mixture of MeOH and CH_3CN (1:1, v/v), and purified by reversed phase, semipreparative HPLC on a Waters μBONDAPAK C_{18} column (19 mm x 150 mm). The product was eluted with a linear gradient of H_2O (0.025% TFA) and CH_3CN (0.025% TFA), from 0% to 80% CH_3CN over 60 min at a flow rate of 6 mL/min. The fractions were collected in one-minute intervals and were analyzed by analytical HPLC. The homogeneous fractions (over 99% as judged by HPLC, Figure 5) were combined and lyophilized. The purified material, linear[*D*-Lys^7, Glu^{10}, Nle^{12}]α-factor, 25 mg (overall yield 8% based on the starting amine content on the aminomethyl resin) was characterized by HPLC using a linear gradient of MeOH (0.025% TFA) and H_2O (0.025% TFA) as eluent. The purity was 100%. The purity of the final product was also analyzed by TLC on silica gel with two developing solvent systems, and only one spot was observed using UV and ninhydrin detection (Table 2). Amino acid analysis gave ratios that were very close to the calculated values (Table 2). The FABMS spectrum of the final product also showed the correct molecular weight (Table 2).

3.9. Synthesis of Boc-Trp(For)-His(Tos)-Trp(For)-Leu-Gln-Leu-Orn(Fmoc)-Pro-Gly-Glu(Ofm)-Pro-Nle-Tyr(2-BrZ)-PAM resin (10a)

The synthesis was performed manually, starting from 1.160 g of **8a** (0.470 mmol). The coupling cycles were as described in Section 3.6 (this chapter). The incorporation of Boc-His in position 2 required third coupling as revealed by a positive Kaiser test after the second coupling. The resulting product **10a** was washed throughly with DMF, CH_2Cl_2, MeOH and dried in a desiccator under a

Table 2
Chemical and Physical Properties of Linear α-Factor Analogs

Peptide	Amino acid analysis										Rf[b]		K'[c]	FAB-MS[d]	Calculated mass (amu)
	Asx	Glx	Gly	His	Leu	Lys	Nle	Pro	Tyr	Trp[a]	Solvent A	Solvent B			
L(4)2	-	1.93	1.01	0.91	2.22	1.12	0.86	1.97	0.99	ND[e]	0.43	0.59	5.99	1666.9	1666.8
L42	-	2.24	1.03	0.84	1.95	0.98	1.04	1.96	0.96	ND	0.34	0.53	5.33	1666.9	1666.8
L32	-	1.93	1.01	0.89	1.96	-	0.95	2.18	1.09	1.91	0.44	0.59	6.06	1653.0	1652.8
L22	-	1.97	1.04	0.98	2.15	-	0.86	2.07	1.10	1.88	0.45	0.61	6.14	1638.1	1638.8
L12	-	1.77	1.00	1.05	1.87	-	ND	2.13	1.19	ND	0.47	0.63	6.19	1625.4	1624.8
L41	1.07	1.02	1.13	0.88	1.83	1.01	0.84	2.20	1.03	ND	0.48	0.59	6.11	1653.0	1652.8
L31	1.09	0.87	0.97	1.00	1.77	-	ND	2.18	1.13	ND	0.49	0.58	6.11	1639.4	1638.8
L21	1.21	0.98	1.09	1.06	2.02	-	ND	2.35	1.26	ND	0.44	0.60	6.13	1625.3	1624.8
L11	1.08	0.87	0.97	1.01	1.85	-	ND	2.07	1.15	ND	0.47	0.61	6.20	1611.2	1610.8

[a] In two cases (**L32** and **L22**) special care was taken during hydrolysis to obtain the Trp content. In the other peptides, the presence of Trp residues is verified by the FAB-MS values. [b] Solvent system A: butanol/acetic acid/water (4:1:2, v/v/v), solvent system B: butanol/acetic acid/water/pyridine (4:1:2:1, v/v/v/v). Rf values were determined using TLC on silica. [c] K' values were determined for a μBondapak C_{18} column using a 20% - 60% acetonitrile gradient (0.025% TFA) over 20 min. [d] The values represent monoisotopic masses. [e] ND, not done.

high vacuum for 2 days, and weighed 1.640 g (yield 90.1% based on the amine centent of the starting resin, 0.759 mmol/g).

3.10. Synthesis of cyclo^{7,10}[Orn^{7}, Glu^{10}, Nle^{12}]α-factor

Cyclization was carried out before the HF cleavage from the resin. The completely assembled tridecapeptide-PAM resin **10a** (1.00 g, 0.287 mmol) was treated with 20% piperidine to remove the Fmoc and Ofm protecting groups and cyclization was effected using BOP coupling reagent (0.663 g, 1.5 mmol) and 1.5% DIEA in 30 mL DMF overnight as described for the *D*-Lys^{7} analog. Prior to the HF cleavage, the For group had been removed by piperidine during the deprotection of Fmoc and Ofm groups from Orn^{7} and Glu^{10}, the Tos group was removed from His^{2} by 5% HOBt in 20 mL DMF, 60 min, and the Boc protecting group was removed from the N-terminus by 30 mL TFA/CH_2Cl_2/DMS (50/48/2, v/v/v), 1 x 2 min, 1 x 30 min.

The TFA tridecapeptide-PAM resin salt was cleaved as described in section 3.7. After evaporation of HF under reduced pressure and under the vacuum, the crude product was washed with ethyl ether 3 times, extracted with 25% acetic acid and lyophilized. The crude material was analyzed by analytical HPLC using a linear gradient of CH_3CN (0.025% TFA) and H_2O (0.025% TFA) as eluent. One major peak was observed as shown in Figure 6.

The crude product was dissolved in the mixture of H_2O and CH_3CN (1:1, v/v), and purified by reversed phase, semipreparative HPLC on a Waters μBONDAPAK C_{18} column (19 mm x 150 mm). The product was eluted with a linear gradient of H_2O (0.025% TFA) and CH_3CN (0.025% TFA) from 0 to 80%

FIGURE 6: HPLC of the crude (Left) and purified (Right) cyclo^{7,10}[Orn^{7}, Glu^{10}, Nle^{12}]α-factor (**C32**)

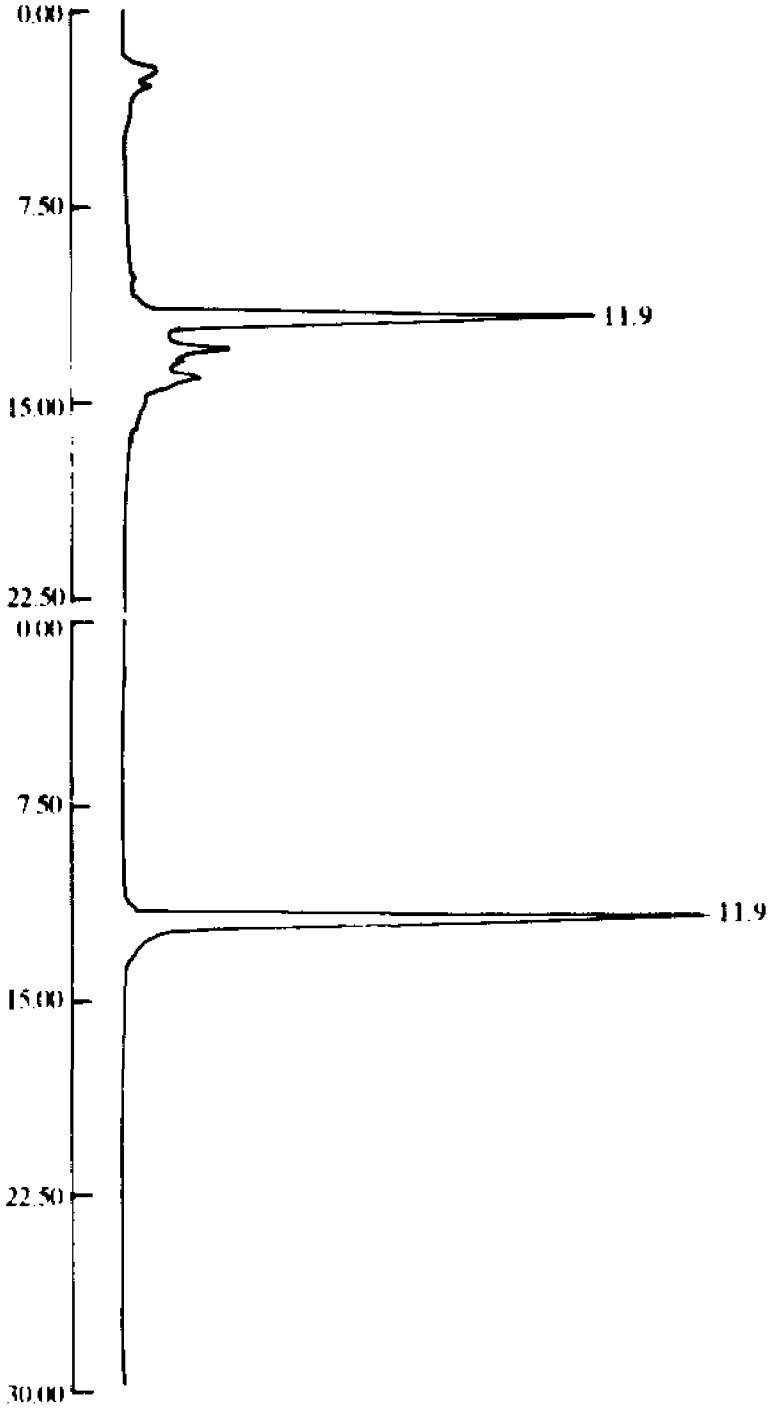

1s

CH_3CN over 60 min at a flow rate of 6 mL/min. The fractions were collected in one minute intervals and were analyzed by analytical HPLC as described above. The homogeneous fractions (over 99% as judged by HPLC, Figure 6) were combined and lyophilized. The purified material, cyclo^{7,10}[Orn^7, Glu^{10}, Nle^{12}]α-factor, 26.4 mg (overall yield 5% based on the starting amine content, 0.759 mmol/g, on the aminomethyl resin) was characterized by HPLC with a linear gradient of MeOH (0.025% TFA) and H_2O (0.025% TFA) as eluent found to be 98% pure. The purity of the final product was also analyzed by TLC on silica gel with two developing solvent systems, and only one spot was observed using UV and ninhydrin detection (Table 1). Amino acid analysis gave the expected values and the FABMS spectrum of the final product also showed the correct molecular weight (Table 1).

3.11. Synthesis of linear[Orn^7, Glu^{10}, Nle^{12}]α-factor

The protecting groups were removed from the completely assembled tridecapeptide-PAM resin **10a** (0.64 g, 0.183 mmol) as described in section 3.8. After HF cleavage and lyophilization following the procedures described above, the crude product weighed 140 mg with an overall yield of 38% based on the starting amine content on the aminomethyl resin (0.759 mmol/g). The crude material was analyzed by reversed-phase HPLC on a Waters μBONDAPAK C_{18} column (3.9 x 300 mm) utilizing a linear gradient of CH_3CN (0.025% TFA) and H_2O (0.025% TFA) as eluent. One major peak was observed as shown in Figure 7.

The crude product was dissolved in a mixture of MeOH and CH_3CN (1:1, v/v), and purified by reversed phase, semipreparative HPLC on a Waters

FIGURE 7: HPLC of the crude (Left) and purified (Right) [Orn^{7}, Glu^{10}, Nle^{12}]α-factor (**L32**)

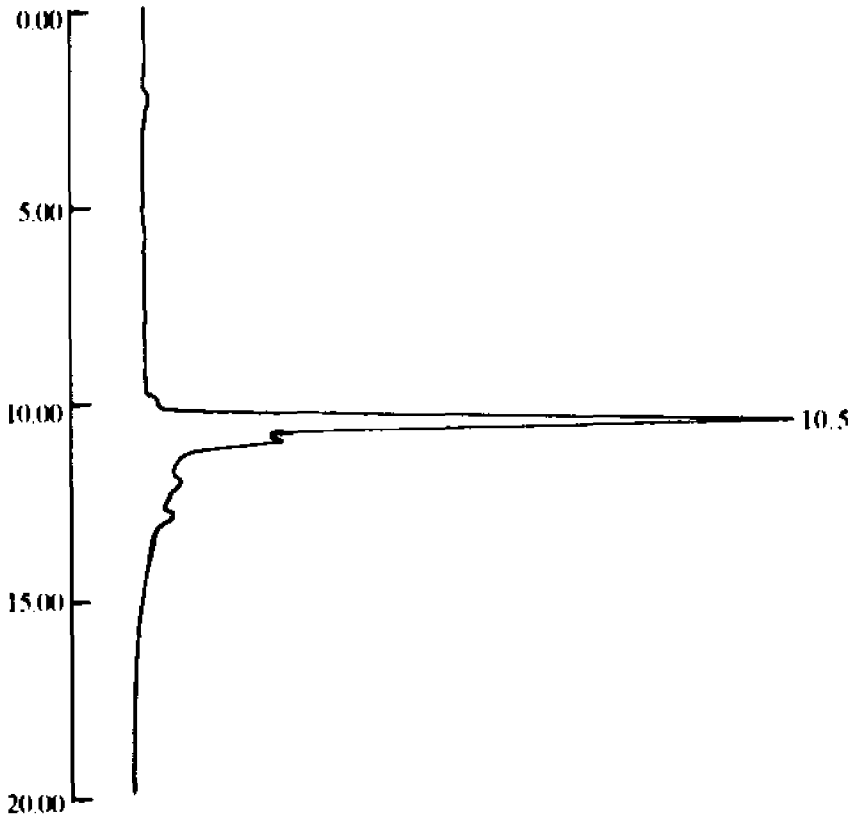
0.00
5.00
10.00
15.00
20.00
10.5

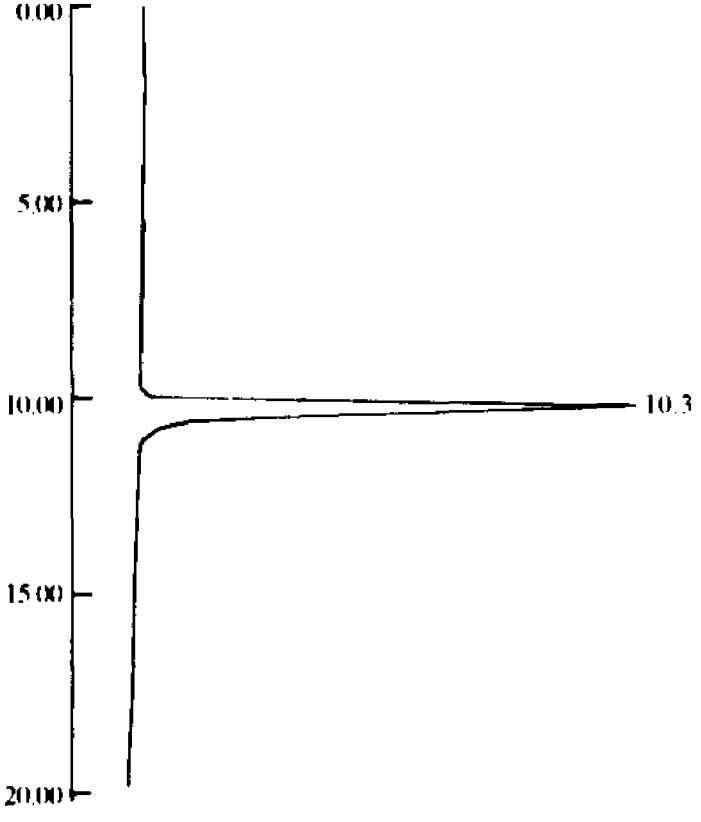
0.00
5.00
10.00
15.00
20.00
10.3

μBONDAPAK C_{18} column (19 mm x 300 mm). The product was eluted with a linear gradient of H_2O (0.025% TFA) and CH_3CN (0.025% TFA), from 0 to 80% CH_3CN over 60 min at a flow rate of 6 mL/min. The fractions were collected in one-minute intervals and were analyzed by analytical HPLC. The homogeneous fractions (over 99% as judged by HPLC, Figure 7) were combined and lyophilized. The purified material, linear[Orn^7, Glu^{10}, Nle^{12}]α-factor, 35.3 mg (overall yield 10% based on the starting amine content (0.759 mmol/g) on the aminomethyl resin) was characterized by HPLC using a linear gradient of MeOH (0.025% TFA) and H_2O (0.025% TFA) as eluent. The purity was 100%. The purity of the final product was also analyzed by TLC on silica gel with two developing solvent systems, and only one spot was observed using UV and ninhydrin detection (Table 2). Amino acid analysis gave ratios which were very close to calculated values (Table 2). The FABMS spectrum of the final product also showed the correct molecular weight (Table 2).

3.12. Synthesis of Boc-Trp(For)-His(Tos)-Trp(For)-Leu-Gln-Leu-Dbr(Fmoc)-Pro-Gly-Glu(Ofm)-Pro-Nle-Tyr(2-BrZ)-PAM resin (11a)

The synthesis was performed manually, starting from 1.3263 g of **8a** (0.537 mmol). The coupling cycles were as previously described. The incorporations of Boc-His in position 2 and Boc-Trp in position 1 needed third coupling as revealed by a positive Kaiser test after the second coupling. The resulting product **11a** was washed thoroughly with DMF, CH_2Cl_2, MeOH and dried in a desiccator under a high vacuum overnight, and weighed 1.8896 g (yield 93.7% based on the amine content of the aminomethyl resin, 0.759 mmol/g).

3.13. Synthesis of cyclo^{7,10}[Dbr^{7}, Glu^{10}, Nle^{12}]α-factor

Cyclization was carried out before the HF cleavage from the resin. The completely assembled tridecapeptide-PAM resin **11a** (1.000 g, 0.2842 mmol) was treated with 20% piperidine to remove the Fmoc and Ofm protecting groups and cyclization was effected using the BOP coupling reagent (0.628 g, 1.42 mmol) and 1.5% DIEA in 20 mL DMF overnight as described in section 3.7. Prior to the HF cleavage, the For groups had been removed from Trp^{1,3} by piperidine during the deprotection of Fmoc and Ofm groups, the Tos group was removed from His^{2} by 5% HOBt in 20 mL DMF, 60 min, and the terminal protecting group Boc was removed by 30 mL TFA/CH_2Cl_2/DMS (50:48:2, v/v/v). 1 x 2 min, 1 x 30 min.

The TFA tridecapeptide-PAM resin salt was cleaved as described for the *D*-Lys7 analog. After evaporation of HF under reduced pressure and under a vacuum, the crude product was washed with ethyl ether 3 times, extracted with 50% acetic acid and lyophilized. The crude product weighed 215.3 mg with an overall yield of 41% based on the starting amine content on the aminomethyl resin (0.759 mmol/g). The crude material was analyzed by reversed-phase HPLC on a Waters μBONDAPAK C_{18} column (3.9 mm x 300 mm) utilizing a linear gradient of CH_3CN (0.025% TFA) and H_2O (0.025% TFA) as eluent. One major peak was observed as shown in Figure 8.

The crude product was dissolved in a mixture of H_2O and CH_3CN (1:1, v/v), and purified by reversed phase, semipreparative HPLC on a Waters μBONDAPAK C_{18} column (19 mm x 150 mm). The product was eluted with a linear gradient of H_2O (0.025% TFA) and CH_3CN (0.025% TFA), from 0 to 80%CH_3CN over 60 min at a flow rate of 6 mL/min. The fractions were collected in one-minute

FIGURE 8: HPLC of the crude (Left) and purified (Right) cyclo^{7,10}[Dbr^{7}, Glu^{10}, Nle^{12}]α-factor (**C22**)

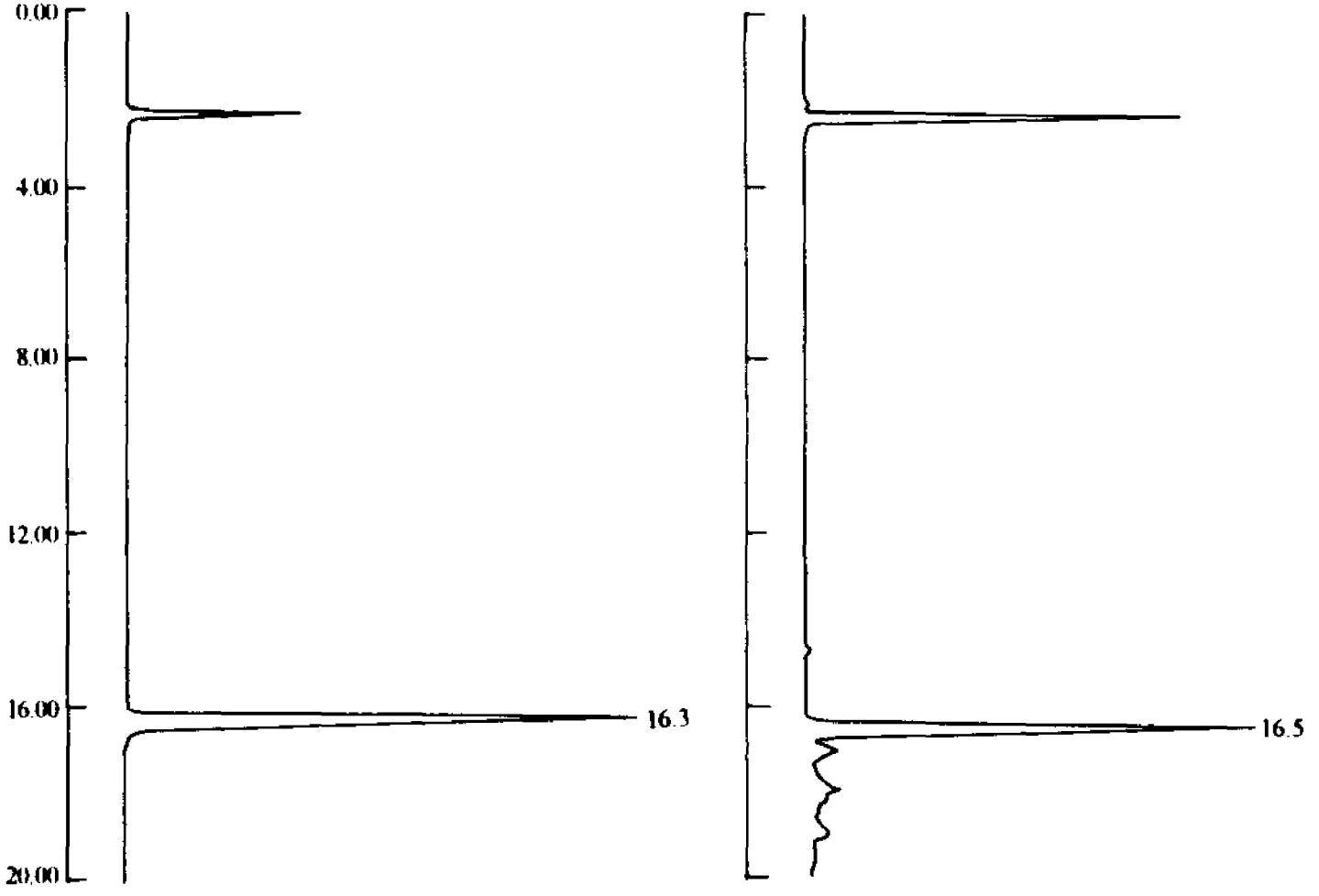
0.00
4.00
8.00
12.00
16.00
20.00
16.3
16.5

intervals and were analyzed by analytical HPLC as described above. The homogeneous fractions (over 99% as judged by HPLC, Figure 8) were combined and lyophilized. The purified material, cyclo^{7,10}[Dbr^{7}, Glu^{10}, Nle^{12}]α-factor, 52 mg (overall yield 9.9% based on the starting amine content, 0.759 mmol/g, on the aminomethyl resin) was characterized by HPLC with a linear gradient of MeOH (0.025% TFA) and H_2O (0.025% TFA) as eluent and found to be 100% pure. The purity of the final product was also analyzed by TLC on silica gel with two developing solvent systems and only one spot was observed using UV and ninhydrin detection (Table 1). Amino acid analysis gave expected values and the FABMS spectrum of the final product also showed the correct molecular weight (Table 1).

3.14. Synthesis of linear[Dbr^{7}, Glu^{10}, Nle^{12}]α-factor

The protecting groups were removed from the completely assembled tridecapeptide-PAM resin **11a** (0.8896 g, 0.2528 mmol) as described in section 3.8. After HF cleavage and lyophilization following the procedures described above, the crude product weighed 196.8 mg with an overall yield of 39% based on the starting amine content on the aminomethyl resin (0.759 mmol/g). The crude material was analyzed by reversed-phase HPLC on a Waters μBONDAPAK C_{18} column (3.9 mm x 300 mm) utilizing a linear gradient of CH_3CN (0.025% TFA) and H_2O (0.025% TFA) as eluent. One major peak was observed as shown in Figure 9.

The crude product was dissolved in a mixture of MeOH and CH_3CN (1:1, v/v), and purified by reversed phase, semipreparative HPLC on a Waters μBONDAPAK C_{18} column (19 mm x 150 mm). The product was eluted with a

FIGURE 9: HPLC of the crude (Left) and purified (Right) [Dbr^{7}, Glu^{10}, Nle^{12}]α-factor (**L22**)

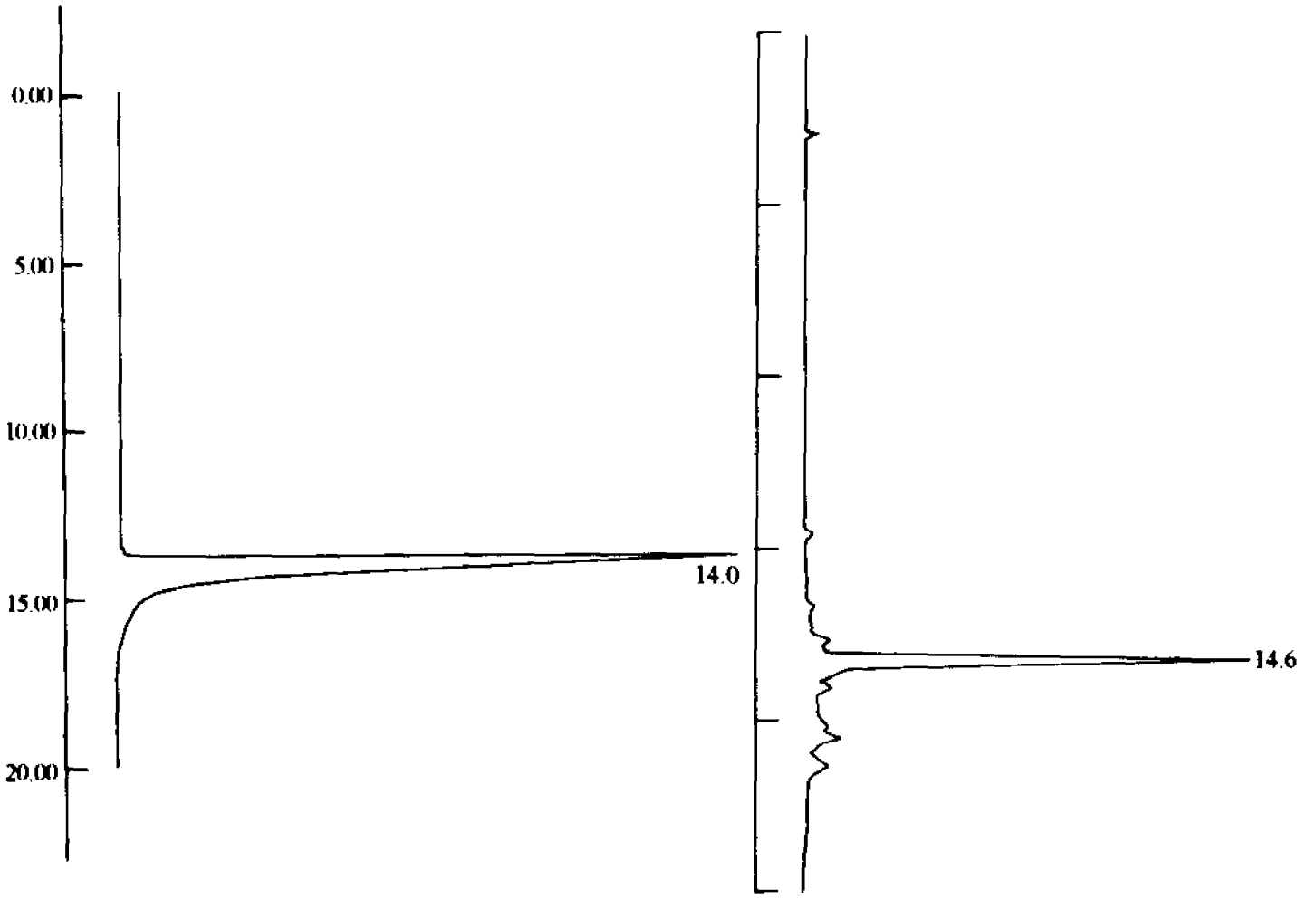
0.00
5.00
10.00
15.00
20.00
14.0
14.6

linear gradient of H_2O (0.025% TFA) and CH_3CN (0.025% TFA), from 0 to 80% CH_3CN over 60 min at a flow rate of 6 mL/min. The fractions were collected in one minute intervals and were analyzed by analytical HPLC. The homogeneous fractions (over 99% as judged by HPLC, Figure 9) were combined and lyophilized. The purified material, linear[Dbr^7, Glu^{10}, Nle^{12}]α-factor, 37.5 mg (overall yield 7.5% based on the starting amine content on the aminomethyl resin) was characterized by HPLC using a linear gradient of MeOH (0.025% TFA) and H_2O (0.025% TFA) as eluent. The purity was 100%. The purity of the final product was also analyzed by TLC on silica gel with two developing solvent systems, and only one spot was observed using UV and ninhydrin detection (Table 2). Amino acid analysis gave ratios which were very close to calculated values (Table 2). The FABMS spectrum of the final product also showed the correct molecular weight (Table 2).

3.15. Synthesis of Boc-Trp(For)-His(Tos)-Trp(For)-Leu-Gln-Leu-Dpr(Fmoc)-Pro-Gly-Glu(Ofm)-Pro-Nle-Tyr(2-BrZ)-PAM resin (12a)

The synthesis was performed manually, starting from 1.027 g of **7a** (0.5 mmol). The coupling cycles were as previously described. The incorporations of Boc-His in position 2 and Boc-Trp in position 1 needed third coupling as revealed by the positive Kaiser test. The resulted product **12a** was washed throughly with DMF, CH_2Cl_2, MeOH and dried in a desiccator under a high vacuum overnight, and weighed 1.629 g (yield 81.3% based on the amine content on the starting aminomethyl resin, 0.759 mmol/g).

3.16. Synthesis of cyclo^{7,10}[Dpr^{7}, Glu^{10}, Nle^{12}]α-factor

The completely assembled tridecapeptide-PAM resin **12a** (1.00 g, 0.287 mmol) was treated with 20% piperidine to remove the Fmoc and Ofm protecting groups and cyclization was effected using the BOP coupling reagent (0.628 g, 1.42 mmol) and 1.5% DIEA in 20 mL DMF overnight as described previously. Prior to the HF cleavage, the For group had been removed from Trp$^{1, 3}$ by piperidine during the deprotection of Fmoc and Ofm groups, the Tos group was removed from His^{2} by 5% HOBt in DMF 20 mL x 60 min and the Boc protecting group was removed by 30 mL TFA/CH_2Cl_2/DMS (50:48:2, v/v/v), 1 x 2 min, 1 x 30 min.

The TFA tridecapeptide-PAM resin salt was subjected to HF cleavage as described in section 3.7. After evaporation of HF under reduced pressure and under a vacuum, the crude product was washed with ethyl ether 3 times, extracted with 50% acetic acid and lyophilized. The crude product weighed 355 mg with an overall yield of 56% based on the starting amine content on the aminomethyl resin (0.759 mmol/g). The crude material was analyzed by analytical HPLC using a linear gradient of CH_3CN (0.025% TFA) and H_2O (0.025% TFA) as eluent. One major peak was observed as shown in Figure 10.

The crude product was dissolved in a mixture of H_2O and CH_3CN (70:30, v/v) and purified by reversed phase, semipreparative HPLC on a Waters μBONDAPAK C_{18} column (19 mm x 300 mm). The product was eluted with a linear gradient of H_2O (0.025% TFA) and CH_3CN (0.025% TFA), from 30 to 45% CH_3CN over 60 min at a flow rate of 6 mL/min. The fractions were collected in one-minute intervals and were analyzed by analytical HPLC as described above. The homogeneous fractions (over 99% as judged by HPLC,

FIGURE 10: HPLC of the crude (Left) and purified (Right) cyclo^{7,10}[Dpr^{7}, Glu^{10}, Nle^{12}]α-factor (C12)

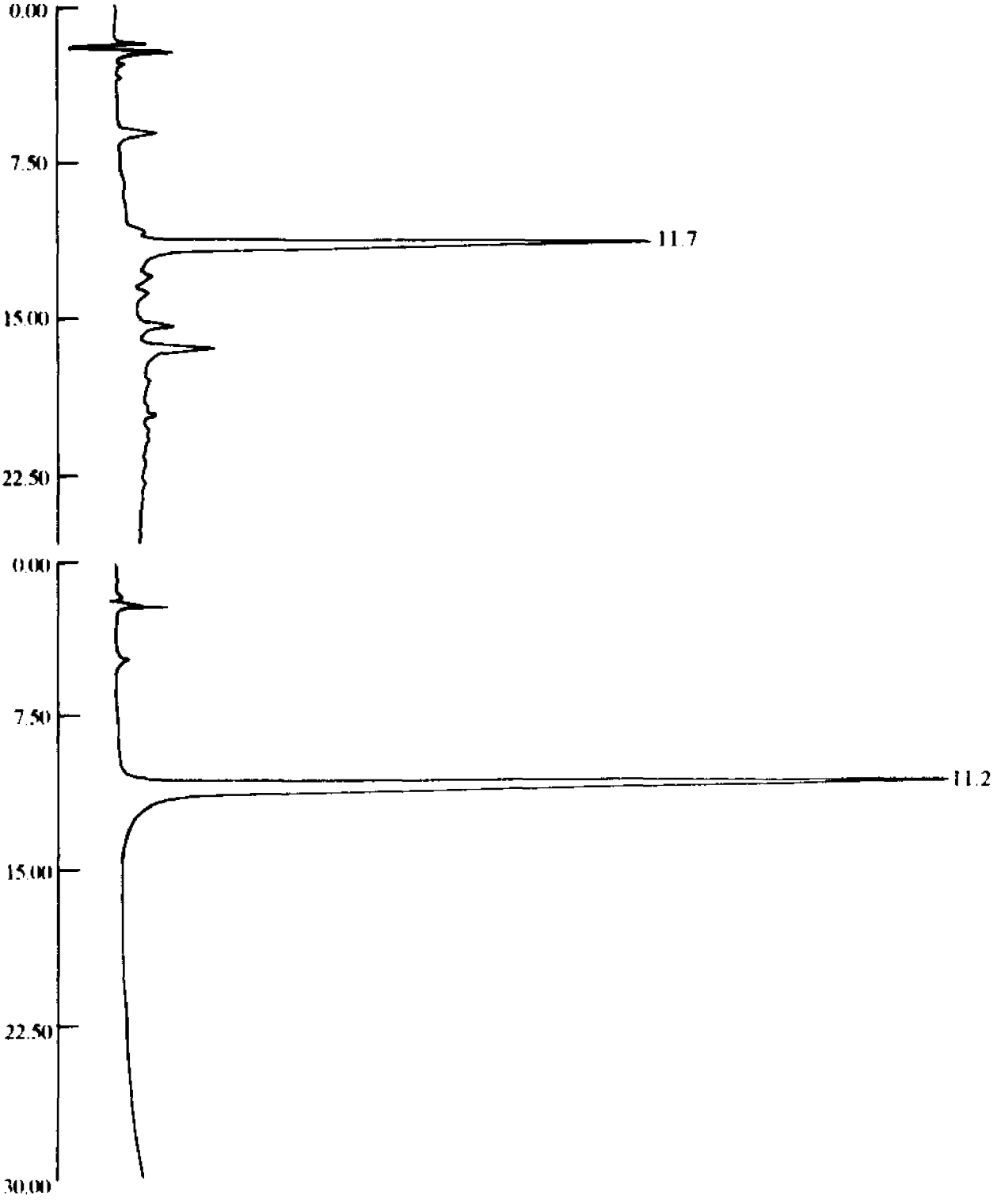
0.00
7.50
11.7
15.00
22.50
0.00
7.50
11.2
15.00
22.50
30.00

Figure 10) were combined and lyophilized. The purified material, cyclo^{7,10}[Dpr^{7}, Glu^{10}, Nle^{12}]α-factor, 55.6 mg (overall yield 8.7% based on the starting amine content , 0.759 mmol/g, on the aminomethyl resin) was characterized by HPLC with a linear gradient of MeOH (0.025% TFA) and H_2O (0.025% TFA) as eluent and found to be 100% pure. The purity of the final product was also analyzed by TLC on silica gel with two developing solvent systems and only one spot was observed using UV and ninhydrin detection (Table 1). Amino acid analysis gave the expected values and the FABMS spectrum of the final product also showed the correct molecular weight (Table 1).

3.17. Synthesis of linear[Dpr^{7}, Glu^{10}, Nle^{12}]α-factor

The protecting groups were removed from the completely assembled tridecapeptide-PAM resin **12a** (0.500 g, 0.1535 mmol) as described in section 3.8. After HF cleavage and lyophilization following the procedures described above, the crude product weighed 176 mg with an overall yield of 58% based on the starting amine content on the aminomethyl resin (0.759 mmol/g). The crude material was analyzed by analytical HPLC using a linear gradient of CH_3CN (0.025% TFA) and H_2O (0.025% TFA) as eluent. One major peak was observed as shown in Figure 11.

The crude product was dissolved in a mixture of H_2O and CH_3CN (75:25, v/v), and purified by reversed phase, semipreparative HPLC on a Waters μBONDAPAK C_{18} column (19 mm x 300 mm). The product was eluted with a linear gradient of H_2O (0.025% TFA) and CH_3CN (0.025% TFA), from 25 to 50% CH_3CN over 60 min at a flow rate of 6 mL/min. The fractions were collected in one-minute intervals and were analyzed by analytical HPLC.

FIGURE 11: HPLC of the crude (Left) and purified (Right) [Dpr^{7}, Glu^{10}, Nle^{12}]α-factor (L12)

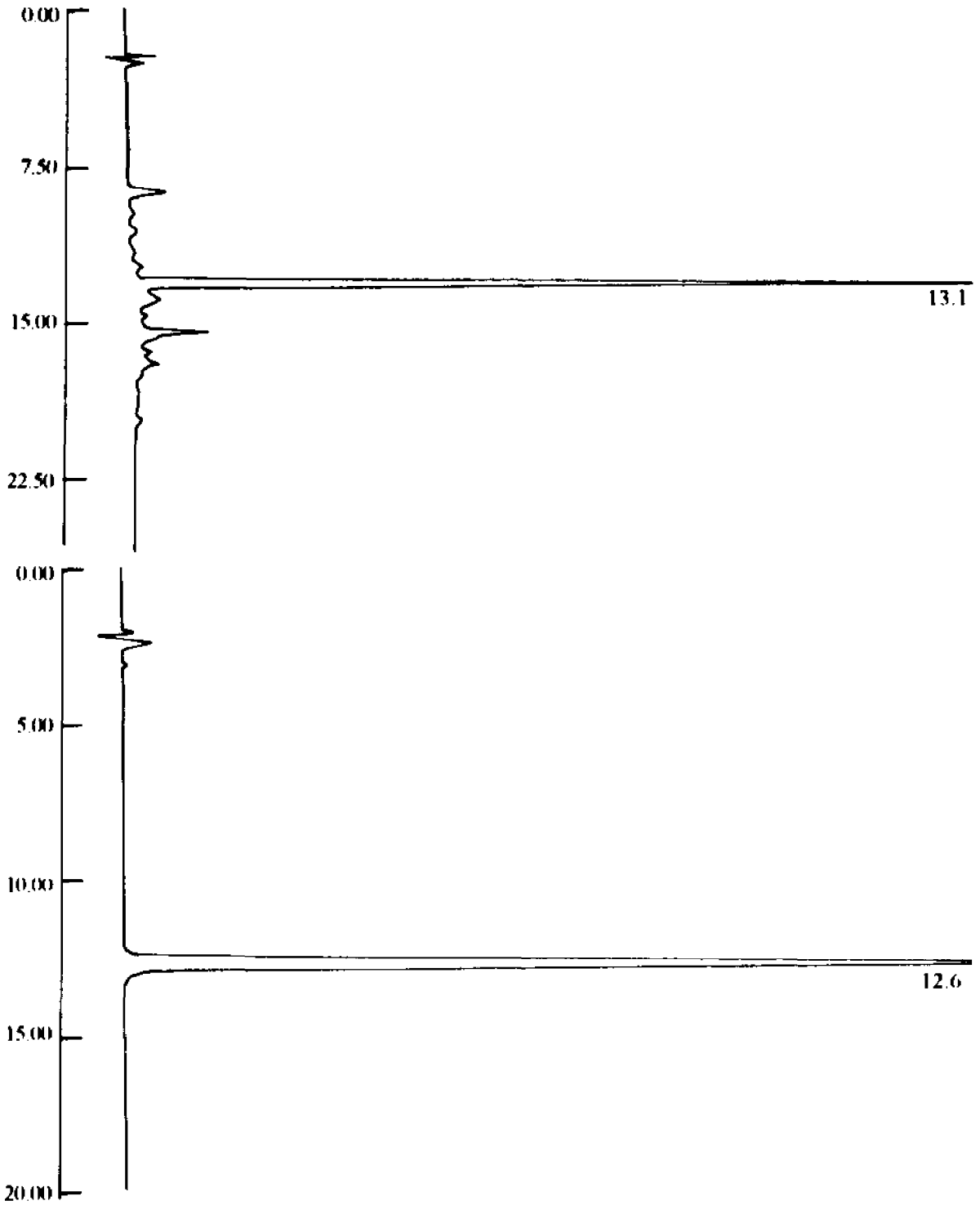
0.00
7.50
13.1
15.00
22.50
0.00
5.00
10.00
12.6
15.00
20.00

The homogeneous fractions (over 99% as judged by HPLC, Figure 11) were combined and lyophilized. The purified material, linear[Dpr^7, Glu^{10}, Nle^{12}]α-factor, 85.3 mg (overall yield 28.3% based on the starting amine content, 0.759 mmol/g, on the aminomethyl resin) was characterized by HPLC using a linear gradient of MeOH (0.025% TFA) and H_2O (0.025% TFA) as eluent and found the purity was 100%. The purity of the final product was also analyzed by TLC on silica gel with two developing solvent systems, and only one spot was observed using UV and ninhydrin detection (Table 2). Amino acid analysis gave the ratios which were very close to the calculated values (Table 2). The FABMS spectrum of the final product also showed the correct molecular weight (Table 2).

3.18. Synthesis of Boc-Pro-Gly-Asp(Ofm)-Pro-Nle-Tyr(2-BrZ)-PAM resin (13a)

The synthesis was performed manually, starting from 4.108 g of 7a (2 mmol). The additions of residues Asp, Gly and Pro were following the procedures described above. The attachments of Boc-Asp(Ofm) and Boc-Pro were needed third coupling. The resulted product (13a) was dried in a desiccator under a high vacuum to a weight of 4.7319 g (yield 94.8% based on the amine content of the starting aminomethyl resin, 0.759 mmol/g).

3.19. Synthesis of Boc-Trp(For)-His(Tos)-Trp(For)-Leu-Gln-Leu-Lys(Fmoc)-Pro-Gly-Asp(Ofm)-Pro-Nle-Tyr(2-BrZ)-PAM resin (14a)

The synthesis was performed manually, starting from 1.5773 g of 7a (0.667 mmol). The coupling cycles were as previously described. The incorporations of Boc-His in position 2 and Boc-Trp in position 1 needed three couplings as

revealed by positive Kaiser test. The resulting product **14a** was washed thoroughly with DMF, CH_2Cl_2, MeOH and dried in a desiccator under a high vacuum for 2 days, and weighed 2.3374 g (yield 92.7% based on the amine content of the starting aminomethyl resin, 0.759 mmol/g).

3.20. Synthesis of cyclo^{7,10}[Lys^7, Asp^{10}, Nle^{12}]α-factor

The completely assembled tridecapeptide-PAM resin **14a** (1.3374 g, 0.3814 mmol) was treated with 20% piperidine for deprotection of Fmoc and Ofm. Cyclization was effected using BOP coupling reagent (0.442 g, 1.0 mmol) and 1.5% DIEA in 20 mL DMF overnight as described for the *D*-Lys^7 analog. Because of the positive Kaiser test, the second cyclization was effected. The side chain and terminal chain protecting groups were removed prior to the HF cleavage. The For group had been removed from Trp by piperidine during the deprotection of Fmoc and Ofm groups. The Tos group was removed from His^2 by 5% HOBt in DMF for 60 min and the terminal protecting group Boc was removed by 30 mL TFA/CH_2Cl_2/DMS (50:48:2, v/v/v), 1 x 2 min, 1 x 30 min.

The TFA tridecapeptide-PAM resin salt was subjected to HF cleavage as described in section 3.7. After evaporation of HF under reduced pressure and under a vacuum, the crude product was washed with ethyl ether 3 times, extracted with 25% acetic acid and lyophilized. The crude weighed 291.6 mg. Overall yield was 41% based on the starting amine content on the aminomethyl resin (0.759 mmol/g). The crude material was analyzed by analytical HPLC using a linear gradient of CH_3CN (0.025% TFA) and H_2O (0.025% TFA) as eluent. One major peak was observed as shown in Figure 12.

FIGURE 12: HPLC spectra of the crude (Left) and purified (Right) cyclo^{7,10}[Asp^{10}, Nle^{12}]α-factor (**C41**)

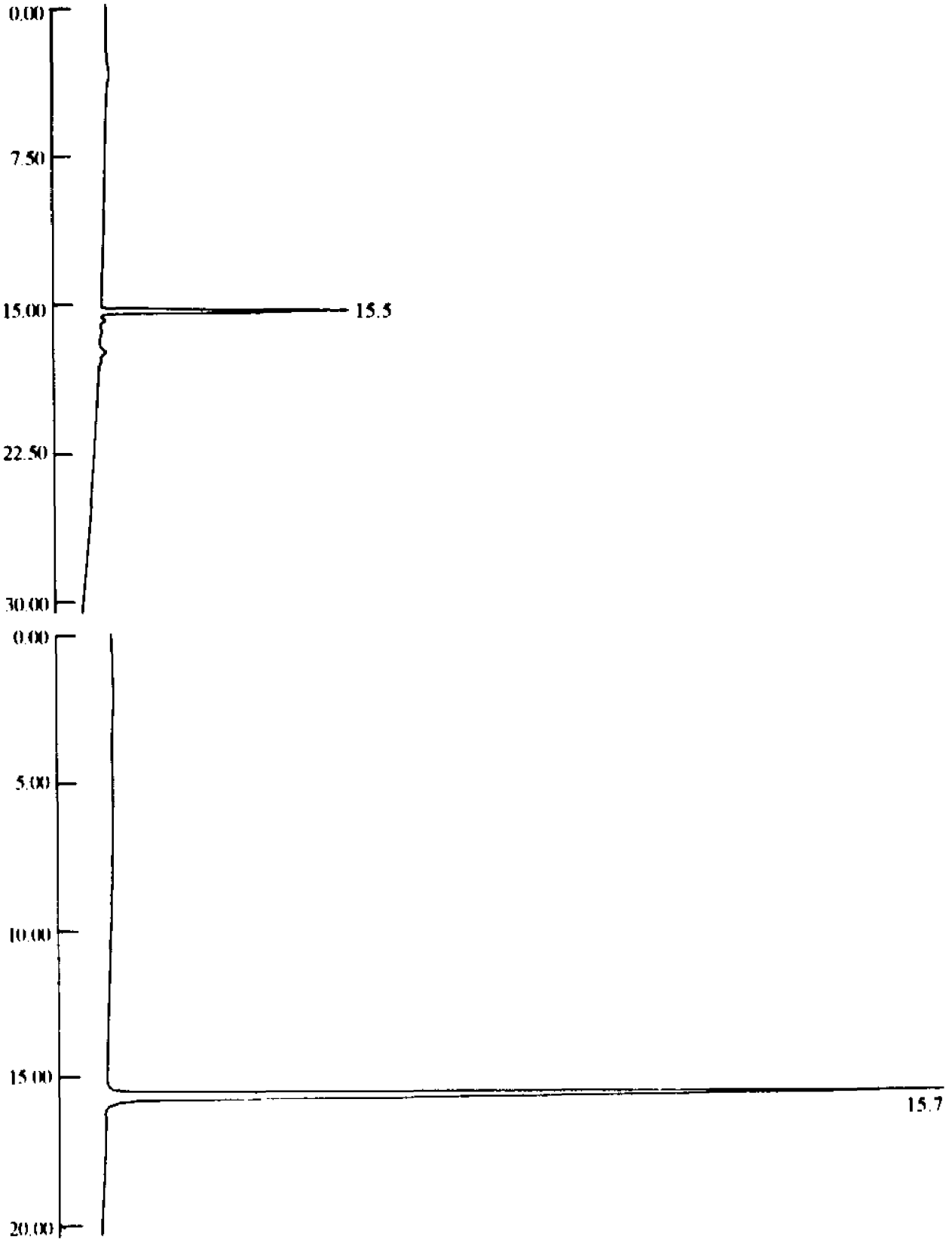
0.00
7.50
15.00
22.50
30.00
15.5
0.00
5.00
10.00
15.00
20.00
15.7

The crude product was dissolved in a mixture of MeOH and CH_3CN (1:1, v/v), and purified by reversed phase, semipreparative HPLC on an equilibrated Waters μBONDAPAK C_{18} column (19 mm x 150 mm). The product was eluted with a linear gradient of H_2O (0.025% TFA) and CH_3CN (0.025% TFA), from 0 to 80% CH_3CN over 60 min at a flow rate of 6 mL/min. The fractions were collected in one minute intervals and were analyzed by analytical HPLC as described above. The homogeneous fractions (over 99% as judged by HPLC, Figure 12) were combined and lyophilized. The purified material, cyclo^{7,10}[Lys^7, Asp^{10}, Nle^{12}]α-factor, 143.3 mg (overall yield 20.0% based on the starting amine content, 0.759 mmol/g, on the aminomethyl resin) was characterized by HPLC with a linear gradient of MeOH (0.025% TFA) and H_2O (0.025% TFA) as eluent and found to be over 99% pure. Purity of the final product was also analyzed by TLC on silica gel with two developing solvent systems and only one spot was observed using UV and ninhydrin detection (Table 1). Amino acid analysis gave expected values and the FABMS spectrum of the final product also showed a correct molecular weight (Table 1).

3.21. Synthesis of linear[Lys^7, Asp^{10}, Nle^{12}]α-factor

The completely assembled tridecapeptide-PAM resin **14a** (1.000 g, 0.2852 mmol) was treated with 20% piperidine in 25 mL DMF 1 x 2 min, 1 x 30 min for deprotection of Fmoc and Ofm, with 5% HOBt in DMF for removal the Tos group from His^2 and with 25 mL TFA/CH_2Cl_2/DMS (50:48:2, v/v/v) 1 x 2 min, 1 x 30 min for removal of the Boc group. After HF cleavage and lyophilization following the procedures described above, the crude product weighed 353.9 mg with an overall yield of 62% based on the starting amine content on the aminomethyl resin (0.759 mmol/g). The crude material was analyzed by analytical

HPLC using a linear gradient of CH_3CN (0.025% TFA) and H_2O (0.025% TFA) as eluent. One major peak was observed as shown in Figure 13.

The crude product was dissolved in a mixture of MeOH and CH_3CN (1:1, v/v), and purified by reversed phase, semipreparative HPLC on a Waters μBONDAPAK C_{18} column (19 mm x 150 mm). The product was eluted with a linear gradient of H_2O (0.025% TFA) and CH_3CN (0.025% TFA), from 0 to 80% CH_3CN over 60 min at a flow rate of 6 mL/min. The fractions was collected in one-minute intervals. The fractions were analyzed by analytical HPLC. The homogeneous fractions (over 99% as judged by HPLC, Figure 13) were combined and lyophilized. The purified material, linear[Lys^7, Asp^{10}, Nle^{12}]α-factor, 27.3 mg (overall yield 4.8% based on the starting amine content, 0.759 mmol/g, on the aminomethyl resin) was characterized by HPLC with a linear gradient of MeOH (0.025% TFA) and H_2O (0.025% TFA) as eluent. The purity was over 98%. The purity of the final product was also analyzed by TLC on silica gel with two developing solvent systems and only one spot was observed using UV and ninhydrin detection (Table 2). Amino acid analysis gave the expected values and the FABMS spectrum of the final product also showed the correct molecular weight (Table 2).

3.22. Synthesis of Boc-Trp(For)-His(Tos)-Trp(For)-Leu-Gln-Leu-Orn(Fmoc)-Pro-Gly-Asp(Ofm)-Pro-Nle-Tyr(2-BrZ)-PAM resin (15a)

The synthesis was performed manually, starting from 1.027 g of 7a (0.500 mmol). The coupling cycles were as previously described. The incorporations of Boc-Asp in position 10, Boc-His in position 2, Boc-Trp in position 1 needed three couplings as revealed by the positive Kaiser test after the second coupling. The

FIGURE 13: HPLC of the crude (Left) and purified (Right) [Asp^{10}, Nle^{12}]α-factor (L41)

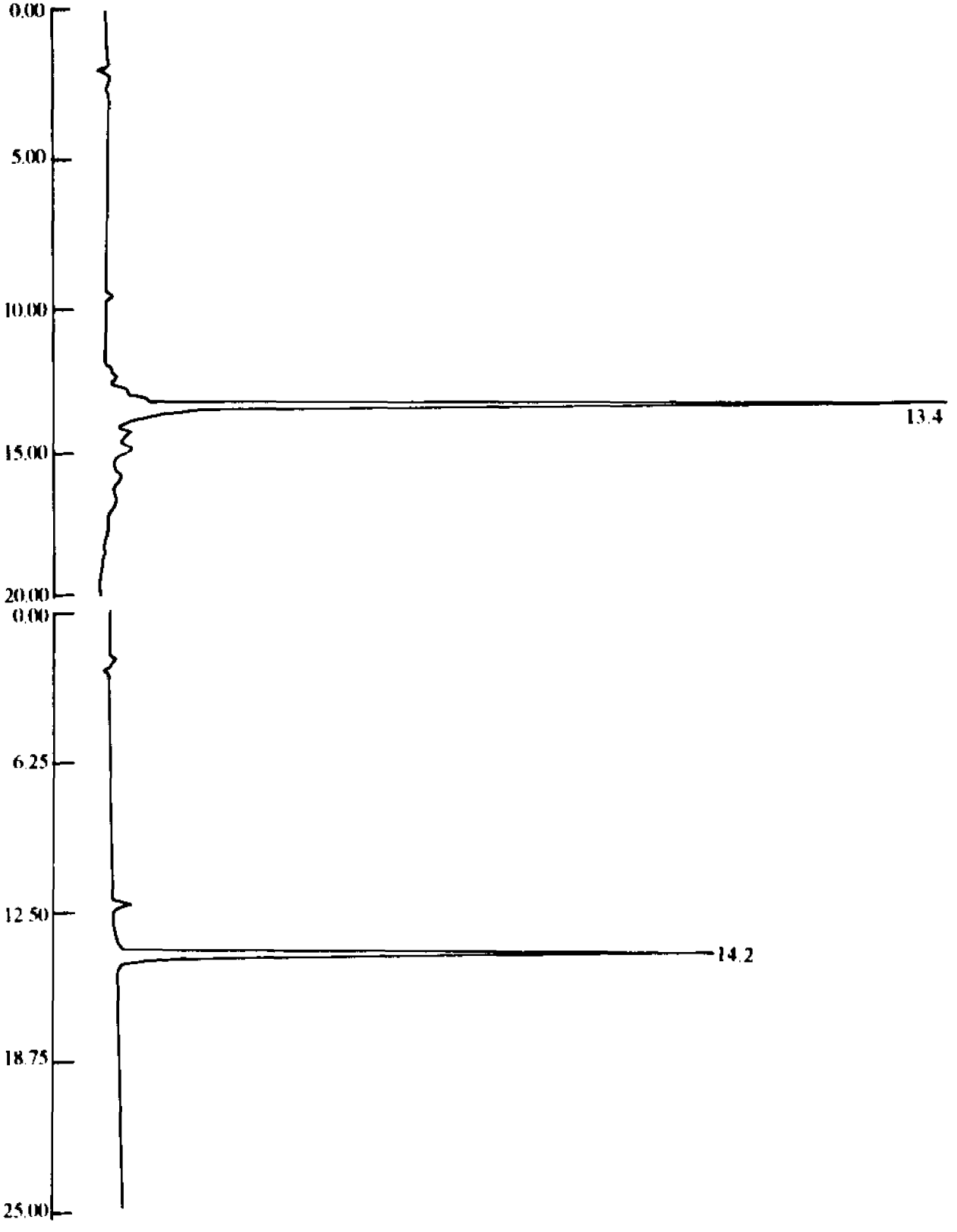
0.00
5.00
10.00
13.4
15.00
20.00
0.00
6.25
12.50
14.2
18.75
25.00

resulting product **15a** was washed thoroughly with DMF, CH_2Cl_2, MeOH and dried in a desiccator under a high vacuum for 2 days, and weighed 1.746 g (yield 88.1% based on the starting amine content, 0.759 mmol/g, on the aminomethyl resin).

3.23. Synthesis of cyclo^{7,10}[Orn^7, Asp^{10}, Nle^{12}]α-factor

The completely assembled tridecapeptide-PAM resin **15a** (1.2460 g, 0.3568 mmol) was treated with 20% piperidine to remove the Fmoc and Ofm protecting groups. To the reaction vessel BOP coupling reagent (0.7885 g, 1.7884 mmol) and 1.5% DIEA in 20 mL DMF were added, and shaken for 4.5 hr. Because of the positive Kaiser test, the reaction mixture was shaken overnight to complete the cyclization. The side chain and terminal chain protecting groups were removed prior to the HF cleavage. The For group had been removed by piperidine during the deprotection of Fmoc and Ofm groups. The Tos group was removed by 5% HOBt in DMF for 60 min and the Boc protecting group was removed by 30 mL TFA/CH_2Cl_2/DMS (50:48:2, v/v/v) 1 x 2 min, 1 x 30 min.

The TFA tridecapeptide-PAM resin salt was cleaved as described in section 3.7. After evaporation of HF under reduced pressure and under the vacuum, the crude product was washed with ethyl ether 3 times, extracted with 50% acetic acid and lyophilized. The crude weighed 335.0 mg. Overall yield was 51% based on the starting amine content on the aminomethyl resin (0.759 mmol/g). The crude material was analyzed by analytical HPLC using a linear gradient of CH_3CN (0.025% TFA) and H_2O (0.025% TFA) as eluent. One major peak was observed as shown in Figure 14.

FIGURE 14: HPLC of the crude (Left) and purified (Right) cyclo^{7,10}[Orn^{7}, Asp^{10}, Nle^{12}]α-factor (C31)

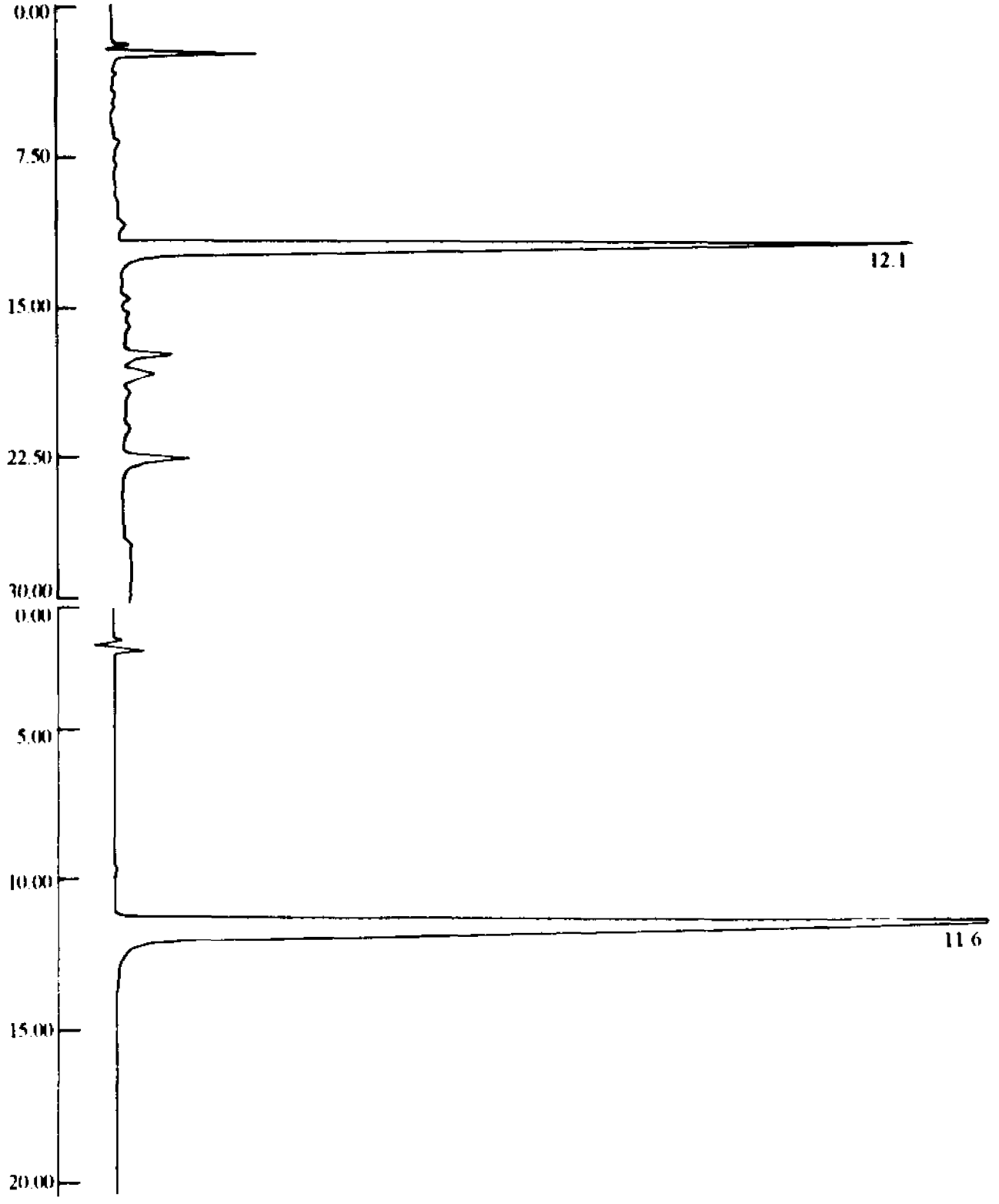
0.00
7.50
12.1
15.00
22.50
30.00
0.00
5.00
10.00
11.6
15.00
20.00

The crude product was dissolved in a mixture of H_2O and CH_3CN (70:30, v/v), and purified by reversed phase, semipreparative HPLC on a Waters μBONDAPAK C_{18} column (19 mm x 300 mm). The product was eluted with a linear gradient of H_2O (0.025% TFA) and CH_3CN (0.025% TFA), from 30 to 45% CH_3CN over 60 min at a flow rate of 6 mL/min. The fractions were collected in one minute intervals and were analyzed by analytical HPLC as described above. The homogeneous fractions (over 99% as judged by HPLC, Figure 14) were combined and lyophilized. The purified material, cyclo^{7,10}[Orn^{7}, Asp^{10}, Nle^{12}]α-factor, 100.1 mg (overall yield 15.2% based on the starting amine content, 0.759 mmol/g, on the aminomethyl resin) was characterized by HPLC with a linear gradient of MeOH (0.025% TFA) and H_2O (0.025% TFA) as eluant. The purity was 99%. The purity of the final product was also analyzed by TLC on silica gel with two developing solvent systems and only one spot was observed using UV and ninhydrin detection (Table 1). Amino acid analysis gave the expected values and the FABMS spectrum of the final product also showed the correct molecular weight (Table 1).

3.24. Synthesis of linear[Orn^{7}, Asp^{10}, Nle^{12}]α-factor

The completely assembled tridecapeptide-PAM resin **15a** (0.500 g, 0.1432 mmol) was treated with 20% piperidine in 25 mL DMF 1 x 2 min, 1 x 30 min for deprotection of Fmoc and Ofm, with 5% HOBt in DMF for removal of the Tos group and with 25 mL TFA/CH_2Cl_2/DMS (50:48:2, v/v/v) 1 x 2 min, 1 x 30 min for removal of the Boc group. After HF cleavage and lyophilizing following the procedures described above, the crude product weighed 182.0 mg with an overall yield of 64% based on the starting amine content on the aminomethyl resin (0.759 mmol/g). The crude material was analyzed by analytical HPLC using a

linear gradient of CH_3CN (0.025% TFA) and H_2O (0.025% TFA) as eluent. One major peak was observed as shown in Figure 15.

The crude product was dissolved in a mixture of H_2O and CH_3CN (75:25, v/v), and purified by reversed phase, semipreparative HPLC on a Waters μBONDAPAK C_{18} column (19 mm x 300 mm). The product was eluted with a linear gradient of H_2O (0.025% TFA) and CH_3CN (0.025% TFA), from 25 to 40% CH_3CN over 60 min at a flow rate of 6 mL/min. The fractions were collected in one-minute intervals and were analyzed by analytical HPLC. The homogeneous fractions (over 99% as judged by HPLC, Figure 15) were combined and lyophilized. The purified material, linear[Orn^7, Asp^{10}, Nle^{12}]α-factor, 45.4 mg (overall yield 16.0% based on the starting amine content, 0.759 mmol/g, on the aminomethyl resin) was characterized by HPLC with a linear gradient of MeOH (0.025% TFA) and H_2O (0.025% TFA) as eluent. The purity was over 97%. The purity of the final product was also analyzed by TLC on silica gel with two developing solvent systems and only one spot was observed using UV and ninhydrin detection (Table 2). Amino acid analysis gave ratios which was very close to calculated values (Table 2). The FABMS spectrum of the final product also showed the correct molecular weight (Table 2).

3.25. Synthesis of Boc-Trp(For)-His(Tos)-Trp(For)-Leu-Gln-Leu-Dbr(Fmoc)-Pro-Gly-Asp(Ofm)-Pro-Nle-Tyr(2-BrZ)-PAM resin (16a)

The synthesis was performed manually, starting from 1.5773 g of 13a (0.667 mmol). The coupling cycles were as previously described. The incorporations of Boc-Dbr in position 7 needed a third coupling as revealed by a positive Kaiser test. The second and the third coupling were using HOBt/DIPC accelerated

FIGURE 15: HPLC of the crude (Left) and purified (Right) [Orn^{7}, Asp^{10}, Nle^{12}]α-factor (L31)

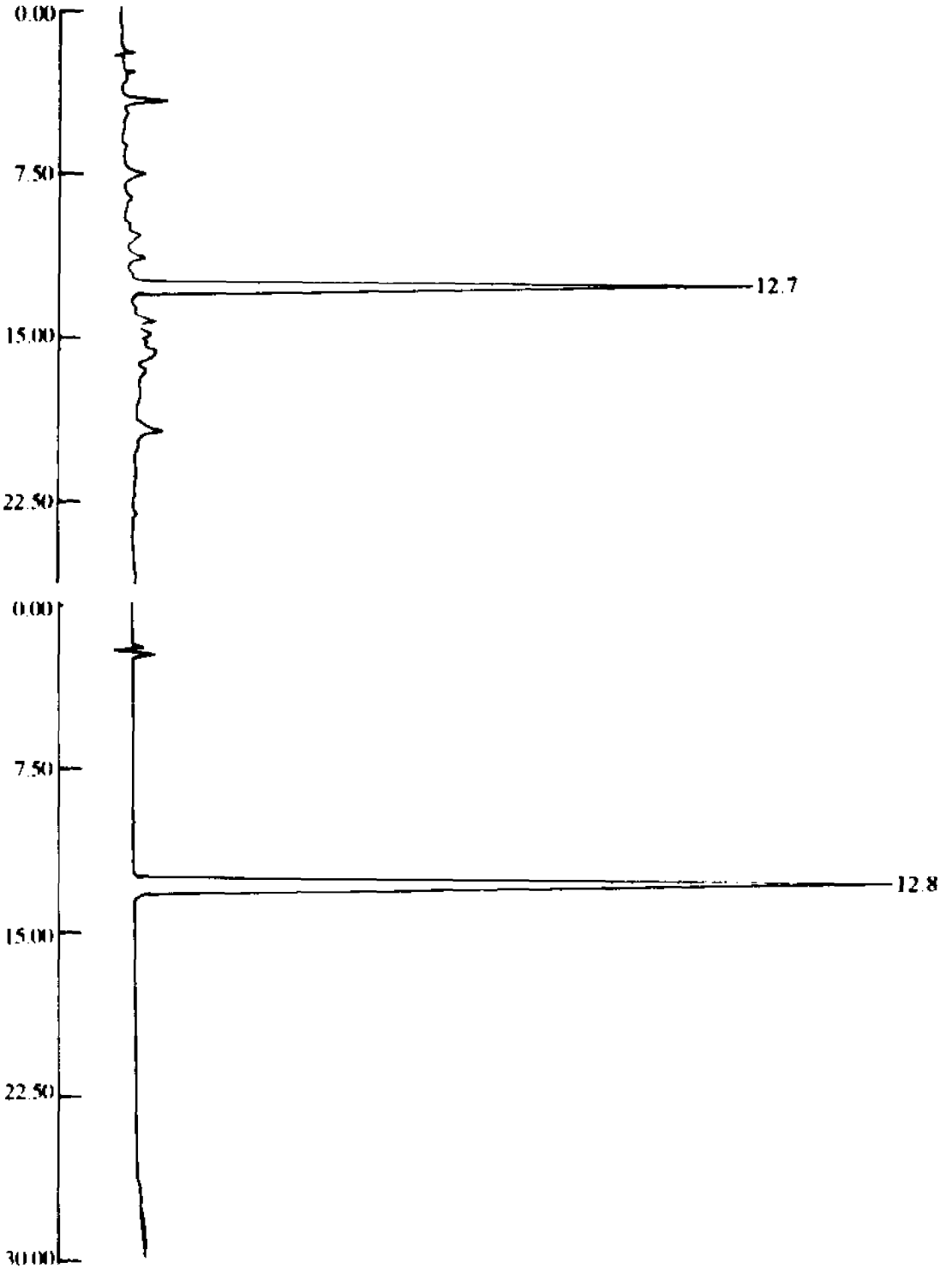
0.00
7.50
12.7
15.00
22.50
0.00
7.50
12.8
15.00
22.50
30.00

active ester. The resulting product **16a** was washed thoroughly with DMF, CH_2Cl_2, MeOH and dried in a desiccator under a high vacuum for 2 days, and weighed 2.3283 g (yield 92.9% based on the starting amine content on the aminomethyl resin, 0.759 mmol/g).

3.26. Synthesis of cyclo^{7,10}[Dbr^7, Asp^{10}, Nle^{12}]α-factor

The completely assembled tridecapeptide-PAM resin **16a** (1.8283 g, 0.5235 mmol) was treated with 20% piperidine for deprotection of Fmoc and Ofm. To the reaction vessel BOP coupling reagent (1.179 g, 2.6675 mmol) and 1.5% DIEA in DMF 30 mL were added, and shaken over night. Because of the positive Kaiser test, the reaction mixture was shaken overnight again to complet the cyclization. The For group had been removed by piperidine during the deprotection of Fmoc and Ofm groups. The Tos group was removed by 5% HOBt in DMF for 60 min and the Boc protecting group was removed by TFA/CH_2Cl_2/DMS (50:48:2, v/v/v) 30 mL x 1 x 2 min, 30 mL x 1 x 30 min.

The TFA tridecapeptide-PAM resin salt was subjected to HF cleavage as described in section 3.7. After evaporation of HF under reduced pressure and under a vacuum, the crude product was washed with ethyl ether 3 times, extracted with 50% acetic acid and lyophilized. The crude weighed 555.6 mg. The overall yield was 58% based on the starting amine content on the aminomethyl resin (0.759 mmol/g). The crude material was analyzed by analytical HPLC using a linear gradient of CH_3CN (0.025% TFA) and H_2O (0.025% TFA) as eluent. One major peak and a significant byproduct were observed as shown in Figure 16.

FIGURE 16: HPLC of the crude (Left) and purified (Right) cyclo^{7,10}[Dbr^{7}, Asp^{10}, Nle^{12}]α-factor (**C21**). Chromatography was performed using the following gradients: (Left) from 20% CH_3CN to 80% CH_3CN in water (0.025% TFA) over 20 min; (Right) from 30% CH_3CN to 45% CH_3CN in water (0.025% TFA) over 20 min.

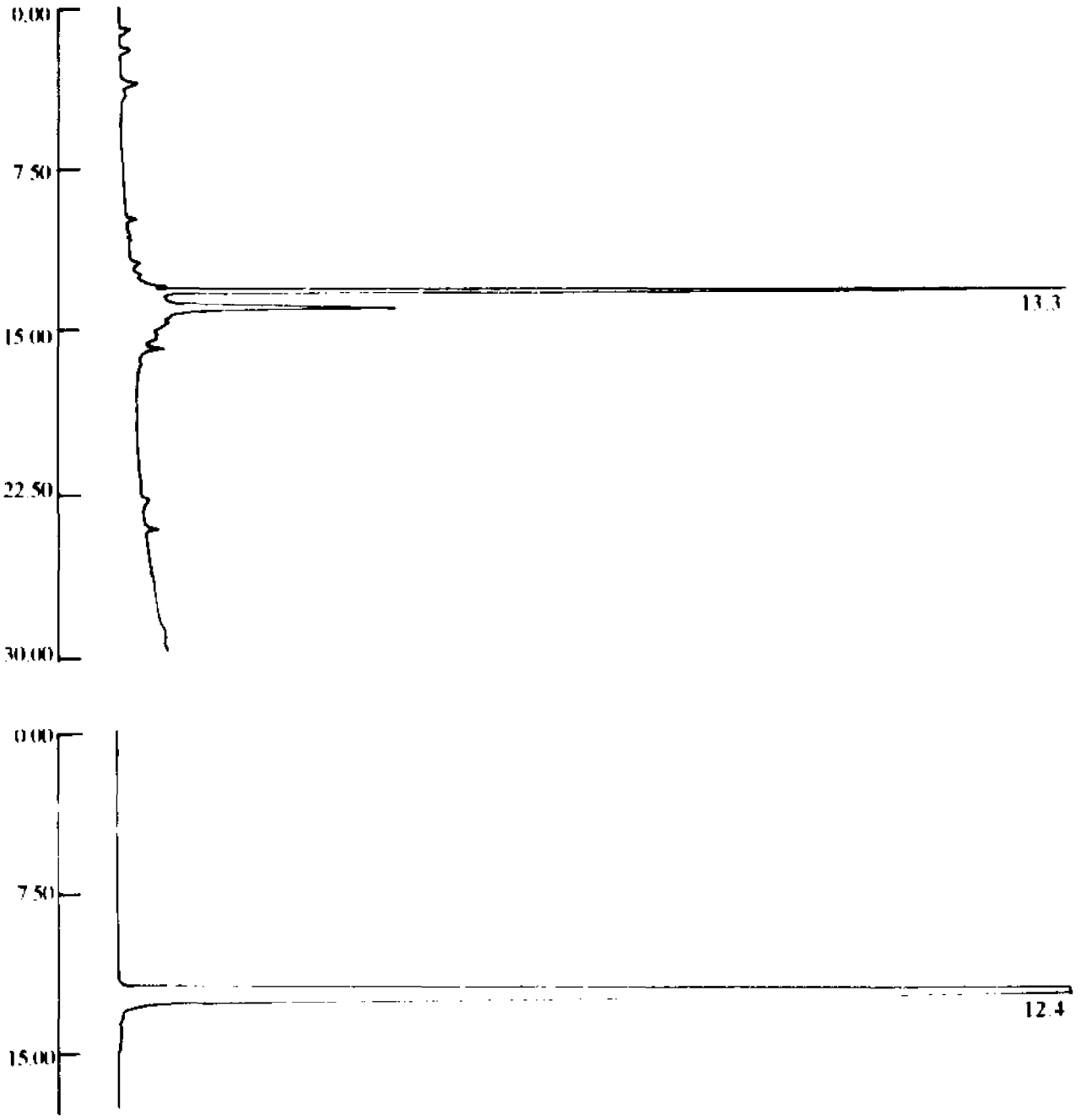
0.00
7.50
15.00
22.50
30.00
13.3
0.00
7.50
15.00
12.4

The crude product was dissolved in a mixture of H_2O and CH_3CN (70:30, v/v), and purified by reversed phase, semipreparative HPLC on a Waters μBONDAPAK C_{18} column (19 mm x 300 mm). The product was eluted with a linear gradient of H_2O (0.025% TFA) and CH_3CN (0.025% TFA), from 30 to 45% CH_3CN over 60 min at a flow rate of 6 mL/min. The fractions were collected in one minute intervals and were analyzed by analytical HPLC as described above. The homogeneous fractions (over 99% as judged by HPLC, Figure 16) were combined and lyophilized. The purified material, cyclo^{7,10}[Dbr^7, Asp^{10}, Nle^{12}]α-factor, 126.9 mg (overall yield 13.2% based on the starting amine content on the aminomethyl resin, 0.759 mmol/g) was characterized by HPLC with a linear gradient of MeOH (0.025% TFA) and H_2O (0.025% TFA) as eluent and found to be 100% pure. The purity of the final product was also analyzed by TLC on silica gel with two developing solvent systems and only one spot was observed using UV and ninhydrin detection (Table 1). Amino acid analysis gave the expected values and the FABMS spectrum of the final product also showed the correct molecular weight (Table 1).

3.27. Synthesis of linear[Dbr^7, Asp^{10}, Nle^{12}]α-factor

The completely assembled tridecapeptide-PAM resin **16a** (0.500 g, 0.1432 mmol) was treated with 20% piperidine in DMF 25 mL x 1 x 2 min, 25 mL x 1 x 30 min for deprotection of Fmoc and Ofm and with TFA/CH_2Cl_2/DMS (50:48:2, v/v/v) 25 mL x 1 x 2 min, 25 mL x 1 x 30 min for removal of the Boc group. After HF cleavage and lyophilization following the procedures described above, the crude product weighed 235.0 mg with an overall yield of 83% based on the starting amine content on the aminomethyl resin (0.759 mmol/g). The crude material was analyzed by analytical HPLC using a linear gradient of CH_3CN (0.025% TFA)

and H_2O (0.025% TFA) as eluent. One major peak was observed as shown in Figure 17.

The crude product was dissolved in a mixture of H_2O and CH_3CN (75:25, v/v), and purified by reversed phase, semipreparative HPLC on a Waters μBONDAPAK C_{18} column (19 mm x 300 mm). The product was eluted with a linear gradient of H_2O (0.025% TFA) and CH_3CN (0.025% TFA), from 25 to 40% CH_3CN over 60 min at a flow rate of 6 mL/min. The fractions were collected in one minute intervals and were analyzed by analytical HPLC. The homogeneous fractions (over 99% as judged by HPLC, Figure 17) were combined and lyophilized. The purified material, linear[Dbr^7, Asp^{10}, Nle^{12}]α-factor, 75.3 mg (overall yield 26.7% based on the starting amine content, 0.759 mmol/g, on the aminomethyl resin) was characterized by HPLC with a linear gradient of MeOH (0.025% TFA) and H_2O (0.025% TFA) as eluent. The purity was 100%. The purity of the final product was also analyzed by TLC on silica gel with two developing solvent systems and only one spot was observed using UV and ninhydrin detection (Table 2). Amino acid analysis gave ratios which were very close to calculated values (Table 2). The FABMS spectrum of the final product also showed the correct molecular weight (Table 2).

3.28. Synthesis of Boc-Trp(For)-His(Tos)-Trp(For)-Leu-Gln-Leu-Dpr(Fmoc)-Pro-Gly-Asp(Ofm)-Pro-Nle-Tyr(2-BrZ)-PAM resin (17a)

The synthesis was performed manually, starting from 1.5773 g of **13a** (0.667 mmol). The coupling cycles were as previously described. The incorporations of Boc-DAPA in position 7, Boc-Leu in position 6 and 4, Boc-Trp in position 3 and Boc-His in position 2 needed three couplings as revealed by the positive Kaiser

FIGURE 17: HPLC of the crude (Left) and purified (Right) [Dbr^7, Asp^{10}, Nle^{12}]α-factor (**L21**)

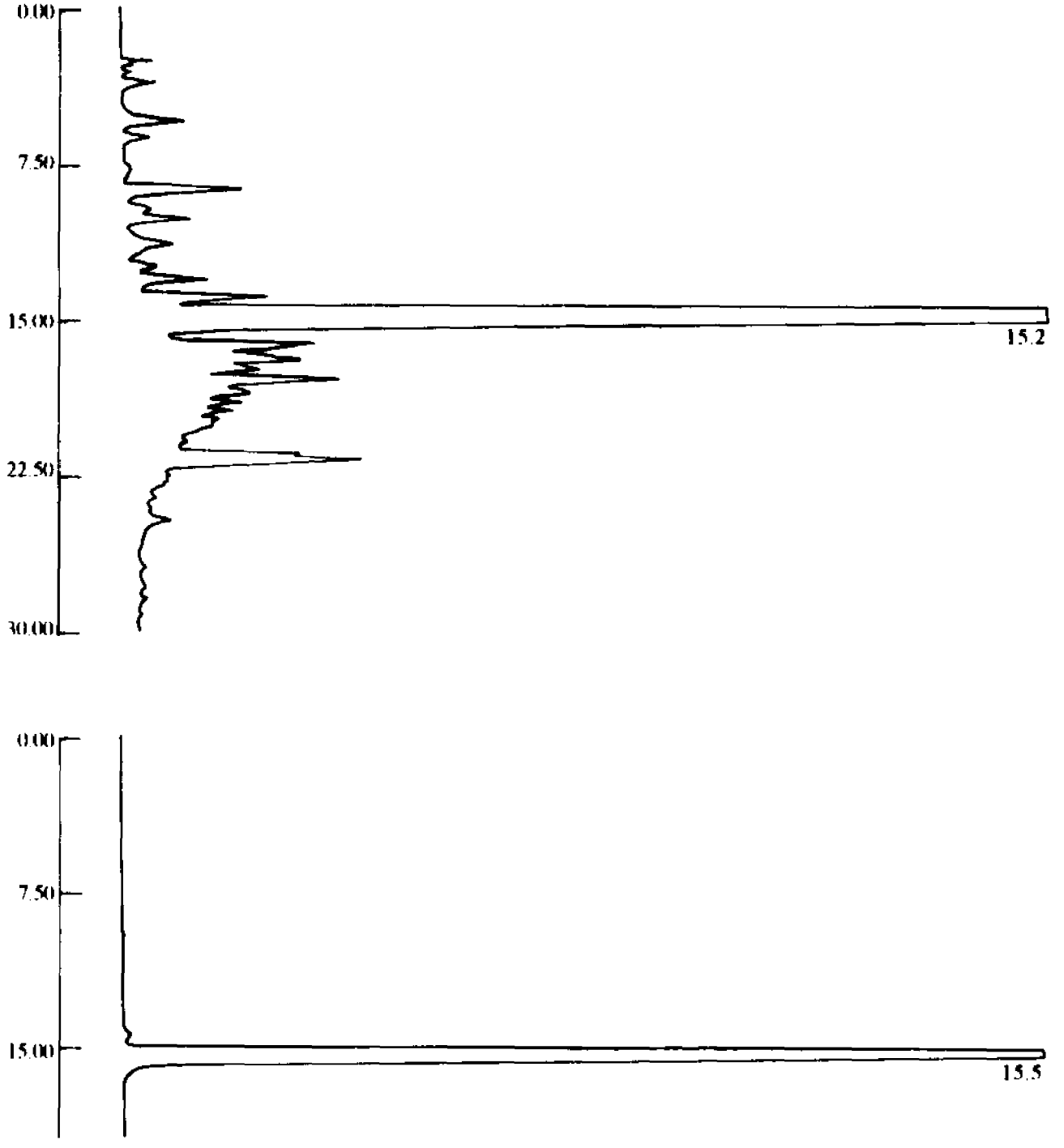
0.00
7.50
15.00
22.50
30.00
15.2
0.00
7.50
15.00
15.5

test. The resulting product **17a** was washed thoroughly with DMF, CH_2Cl_2, MeOH and dried in a desiccator under a high vacuum for 2 days, and weighed 2.1824 g (yield 87.5% based on the starting amine content on the aminomethyl resin, 0.759 mmol/g).

3.29. Synthesis of cyclo^{7,10}[Dpr^7, Asp^{10}, Nle^{12}]α-factor

The completely assembled tridecapeptide-PAM resin **17a** (1.6824 g, 0.5139 mmol) was treated with 20% piperidine for deprotection of Fmoc and Ofm. To the reaction vessel BOP coupling reagent (1.136 g, 2.5695 mmol) and 1.5% DIEA in DMF 30 mL were added, and shaken over night. After the third coupling, the Kaiser test still give a positive result. About 90 - 95% completion was estimated qualitatively. The side chain and the N-terminal protecting groups were removed prior to the HF cleavage by treating with HOBt and TFA.

The TFA tridecapeptide-PAM resin salt was cleaved as described in section 3.7. After evaporation of HF under reduced pressure and under a vacuum, the crude product was washed with ethyl ether 3 times, extracted with 50% acetic acid and lyophilized. The crude weighed 510.3 mg. Overall yield was 55% based on the starting amine content on the aminomethyl resin (0.759 mmol/g). The crude material was analyzed by analytical HPLC using a linear gradient of CH_3CN (0.025% TFA) and H_2O (0.025% TFA) as eluant. One major peak and a significant byproduct (about 11%) were observed as shown in Figure 18.

The crude product was dissolved in a mixture of H_2O and CH_3CN (68:32, v/v), and purified by reversed phase, semipreparative HPLC on a Waters μBONDAPAK C_{18} column (19 mm x 300 mm). The product was eluted with a

FIGURE 18: HPLC of the crude (Left) and purified (Right) cyclo^{7,10}[Dpr^{7}, Asp^{10}, Nle^{12}]α-factor (C11). Chromatography was performed using the following gradients: (Left) from 32% CH_3CN to 57% CH_3CN in water (0.025% TFA) over 20 min; (Right) from 20% CH_3CN to 60% CH_3CN in water (0.025% TFA) over 20 min.

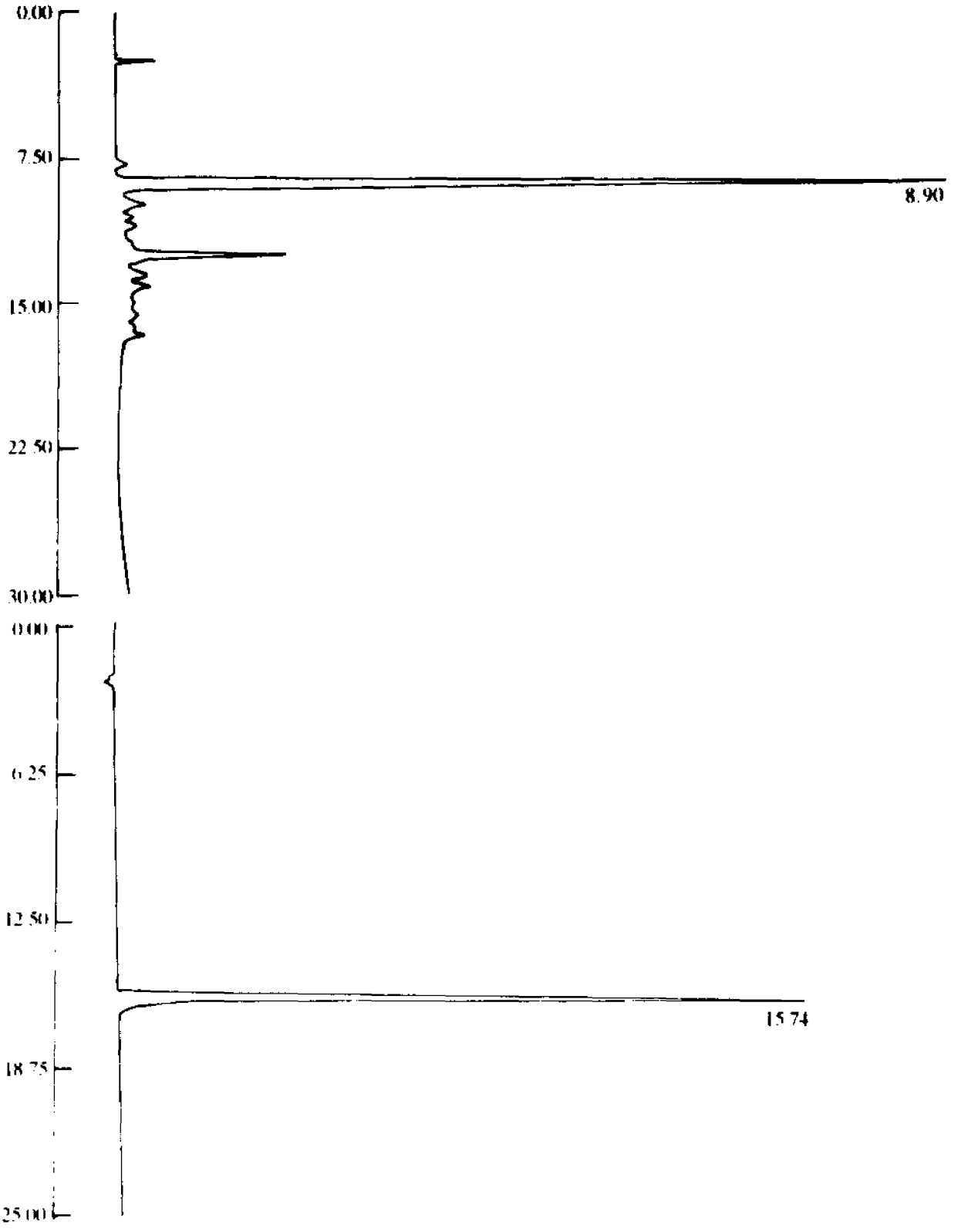
0.00
7.50
8.90
15.00
22.50
30.00
0.00
6.25
12.50
15.74
18.75
25.00

linear gradient of H_2O (0.025% TFA) and CH_3CN (0.025% TFA), from 32 to 57% CH_3CN over 60 min at a flow rate of 6 mL/min. Fractions were collected in one minute intervals and were analyzed by analytical HPLC as described above. The homogeneous fractions (over 99% as judged by HPLC, Figure 18) were combined and lyophilized. The purified material, cyclo^{7,10}[Dpr^7, Asp^{10}, Nle^{12}]α-factor, 143.7 mg (overall yield 15.4% based on the starting amine content on the aminomethyl resin, 0.759 mmol/g) was characterized by HPLC with a linear gradient of MeOH (0.025% TFA) and H_2O (0.025% TFA) as eluent. The purity was over 97%. Purity of the final product was also analyzed by TLC on silica gel with two developing solvent systems and only one spot was observed using UV and ninhydrin detection (Table 1). Amino acid analysis gave the expected values and the FABMS spectrum of the final product also showed a correct molecular weight (Table 1).

3.30. Synthesis of linear[Dpr^7, Asp^{10}, Nle^{12}]α-factor

Before HF cleavage, the side chain and the N-terminal protecting groups were removed by treating **17a** (0.500 g, 0.1527 mmol) with piperidine, HOBt and TFA followed the procedues described before. After HF cleavage and lyophilization following the procedures described above, the crude product weighed 248.0 mg with an overall yield of 83% based on the starting amine content on the aminomethyl resin (0.759 mmol/g). The crude material was analyzed by analytical HPLC using a linear gradient of CH_3CN (0.025% TFA) and H_2O (0.025% TFA) as eluent. One major peak was observed as shown in Figure 19.

The crude product was dissolved in a mixture of H_2O and CH_3CN (75:25, v/v), and purified by reversed phase, semipreparative HPLC on a Waters

FIGURE 19: HPLC of the crude (Left) and purified (Right) [Dpr^{7}, Asp^{10}, Nle^{12}]α-factor (L11)

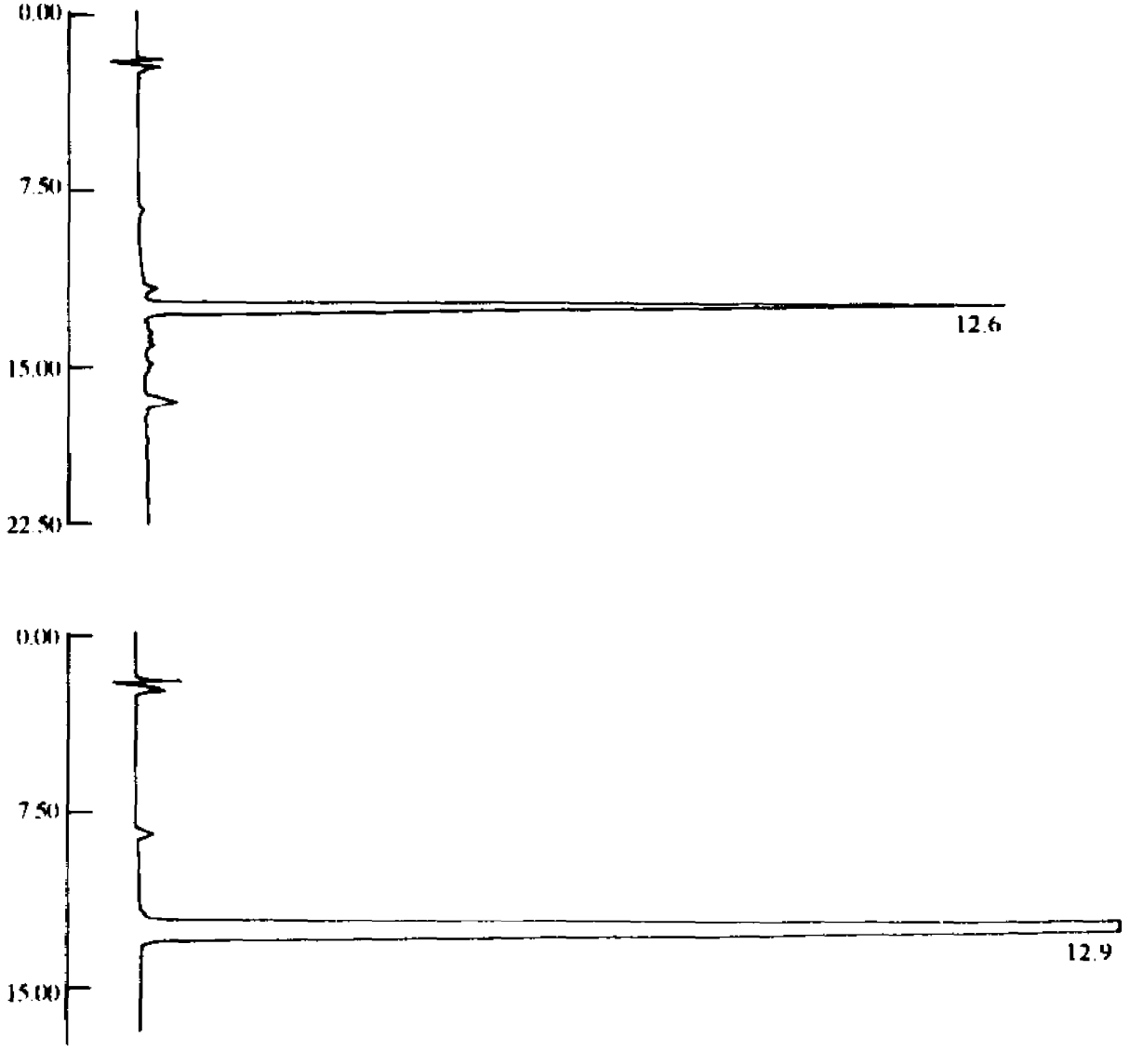
0.00
7.50
12.6
15.00
22.50
0.00
7.50
12.9
15.00

μBONDAPAK C_{18} column (19 mm x 300 mm). The product was eluted with a linear gradient of H_2O (0.025% TFA) and CH_3CN (0.025% TFA), from 25% to 50% CH_3CN over 60 min at a flow rate of 6 mL/min. Fractions were collected in one minute intervals. The fractions were analyzed by analytical HPLC. The homogeneous fractions (over 99% as judged by HPLC, Figure 19) were combined and lyophilized. The purified material, linear[Dpr^7, Asp^{10}, Nle^{12}]α-factor, 105.0 mg (overall yield 35.2% based on the starting amine content, 0.759 mmol/g, on the aminomethyl resin) was characterized by HPLC with a linear gradient of MeOH (0.025% TFA) and H_2O (0.025% TFA) as eluent. The purity was over 97%. The purity of the final product was also analyzed by TLC on silica gel with two developing solvent systems and only one spot was observed using UV and ninhydrin detection (Table 2). Amino acid analysis gave ratios which were very close to calculated values and the FABMS spectrum of the final product also showed the correct molecular weight (Table 2).

IV. Syntheses of the Model Compounds (tetrapeptides)

Two model compounds, Ac-cyclo[Lys-Pro-Gly-Glu]-NH_2 (Tetra **42**) and Ac-cyclo[Orn-Pro-Gly-Glu]-NH_2 (Tetra **32**), were designed to represent the cyclized central regions of the cyclic α-factor analogs, **C42** and **C32** respectively (Figure 3 and Figure 20). Solid phase syntheses of Tetra **42** and Tetra **32** were carried out manually starting with 4-methybenzhydrylamine resin (1 mmol/g) by following the protocol described in Section 3.4 (Chapter 4). Use of 4-methybenzhydrylamine resin resulted in peptide with an amide group at the C-terminal after HF cleavage. Acetylation of the amine terminal was effected following on resin lactamization between the side chains of Lys (or Orn) and Glu. Cyclization followed the procedures described in Section 3.7 (Chapter 4).

FIGURE 20: The structures of Ac-*cyclo*[Lys-Pro-Gly-Glu]-NH_2 (Tetra **42**) and Ac-*cyclo*[Lys-Pro-Gly-Glu]-NH_2 (Tetra **32**)

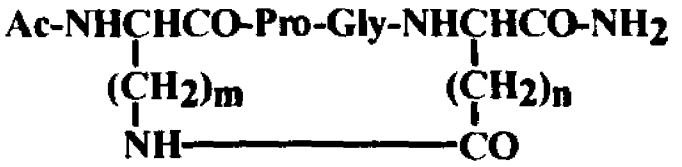

Tetra 42: m = 4; n = 2

Tetra 32: m = 3; n = 2

Acetylation of the terminal amine group was carried out by acetic anhydride (6 equiv) and pyridine (1 equiv) in DMF for 2 h when the peptide chain was still connected on resin. After HF cleavage the crude tetrapeptides were recovered as yellowish white solids (yield, 89% for Tetra **42** and 90% for Tetra **32**). In both crude peptides a significant byproduct was observed in HPLC spectra. The HPLC profile of the crude Tetra **42** is shown in Figure 21(Left). The major byproduct in the crude Tetra **42** was isolated and identified as a cyclic dimer which resulted from interpeptide amide bond formation. This dimer had a molecular ion that was exactly twice that of monomeric lactam (data not shown) and a longer retention time than that of monomer, the desired product (Figure 21; Left).

The crude tetrapeptide was dissolved in the mixture of H_2O/CH_3CN (97:3, v/v) and was purified by reversed phase, semipreparative HPLC on a Waters μBONDAPAK C_{18} column (19 mm x 300 mm). The product was eluted with a linear gradient of CH_3CN/H_2O/TFA (0.025%) from 3 to 55% CH_3CN over 60 min at a flow rate of 6 mL/min. The yields of the purified products were 12% for both Tetra **42** and Tetra **32**. The final products were highly homogenous as judged by analytical HPLC. HPLC spectrum of purified Tetra **42** is shown in Figure 21(Right). Both tetrapeptides were characterized by 1D NMR spectra (Figure 22 for Tetra **42**; Figure 23 for Tetra **32**) which gave the expected resonances and the FABMS spectra which showed the correct molecular weight (453.2 for Tetra **42** and 439.2 for Tetra **32**).

FIGURE 21: HPLC of the crude (Left) and purified (Right) Ac-*cyclo*[Lys-Pro-Gly-Glu]-NH_2 (Tetra **42**)

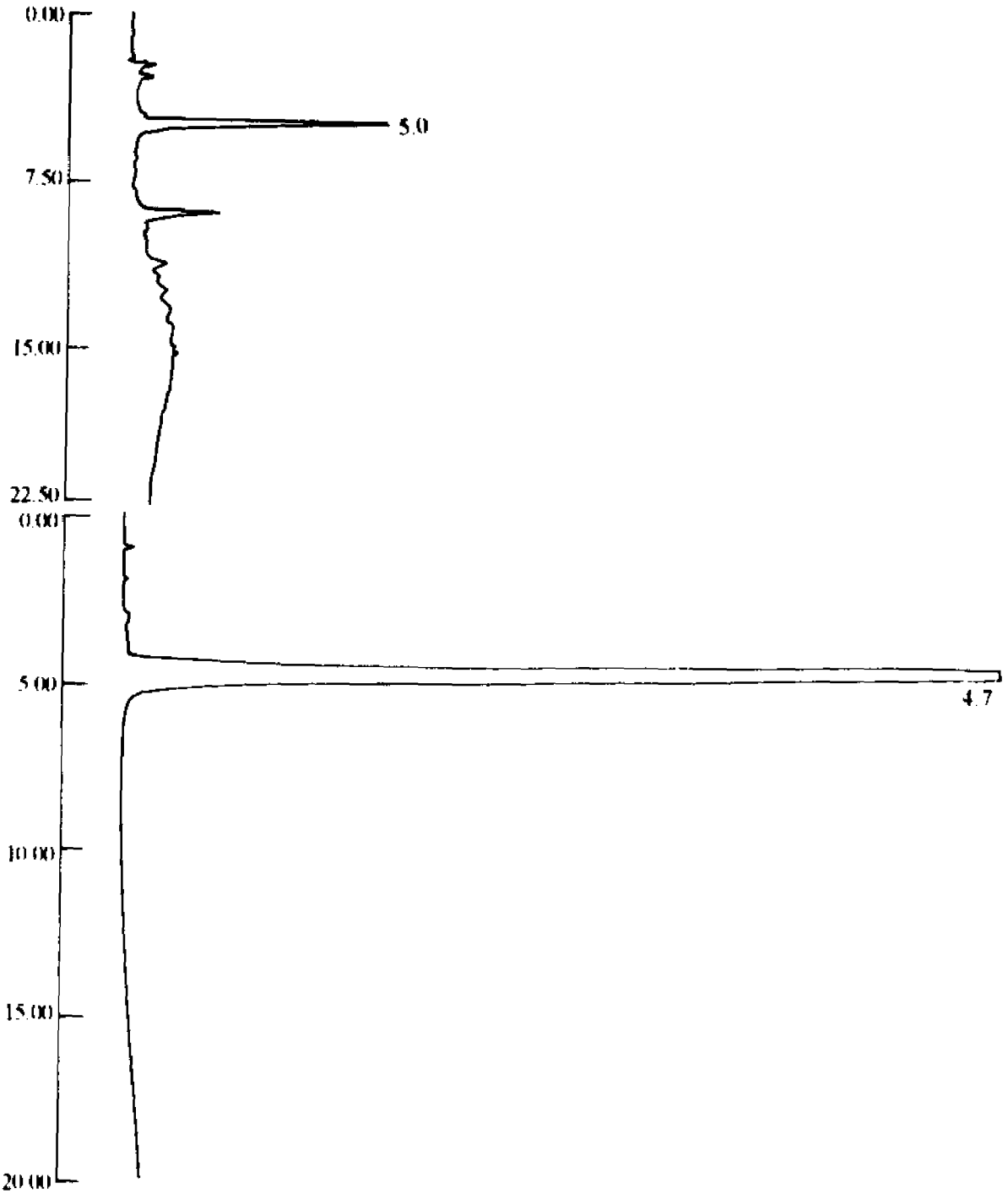
0.00
5.0
7.50
15.00
22.50
0.00
5.00
4.7
10.00
15.00
20.00

FIGURE 22: 1D NMR spectrum of Ac-*cyclo*[Lys-Pro-Gly-Glu]-NH_2 (Tetra **42**) in DMSO (25 °C)

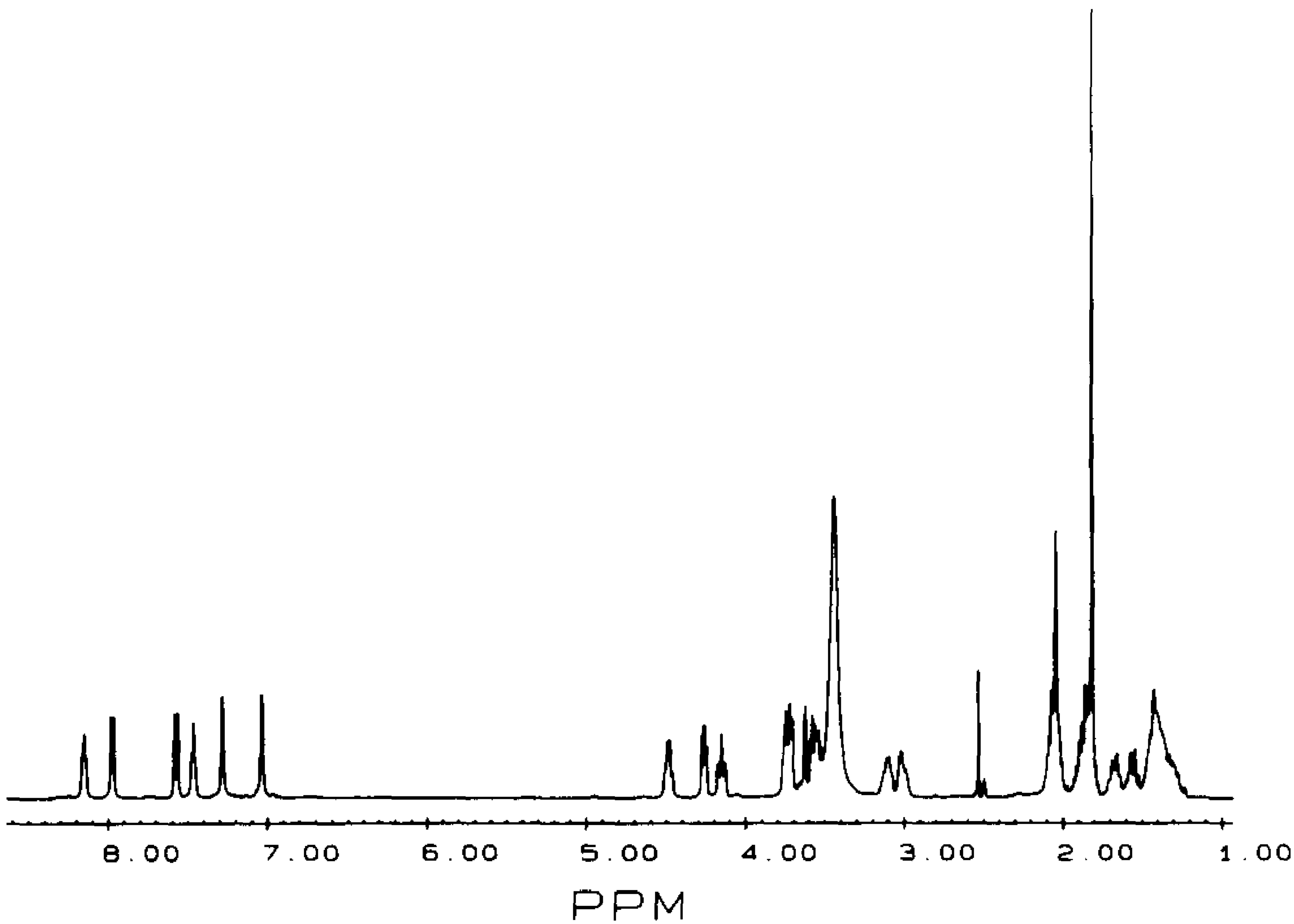
8.00
7.00
6.00
5.00
4.00
3.00
2.00
1.00
PPM

FIGURE 23: 1D NMR spectrum of Ac-*cyclo*[Orn-Pro-Gly-Glu]-NH_2 (Tetra **32**) in DMSO (25 °C)

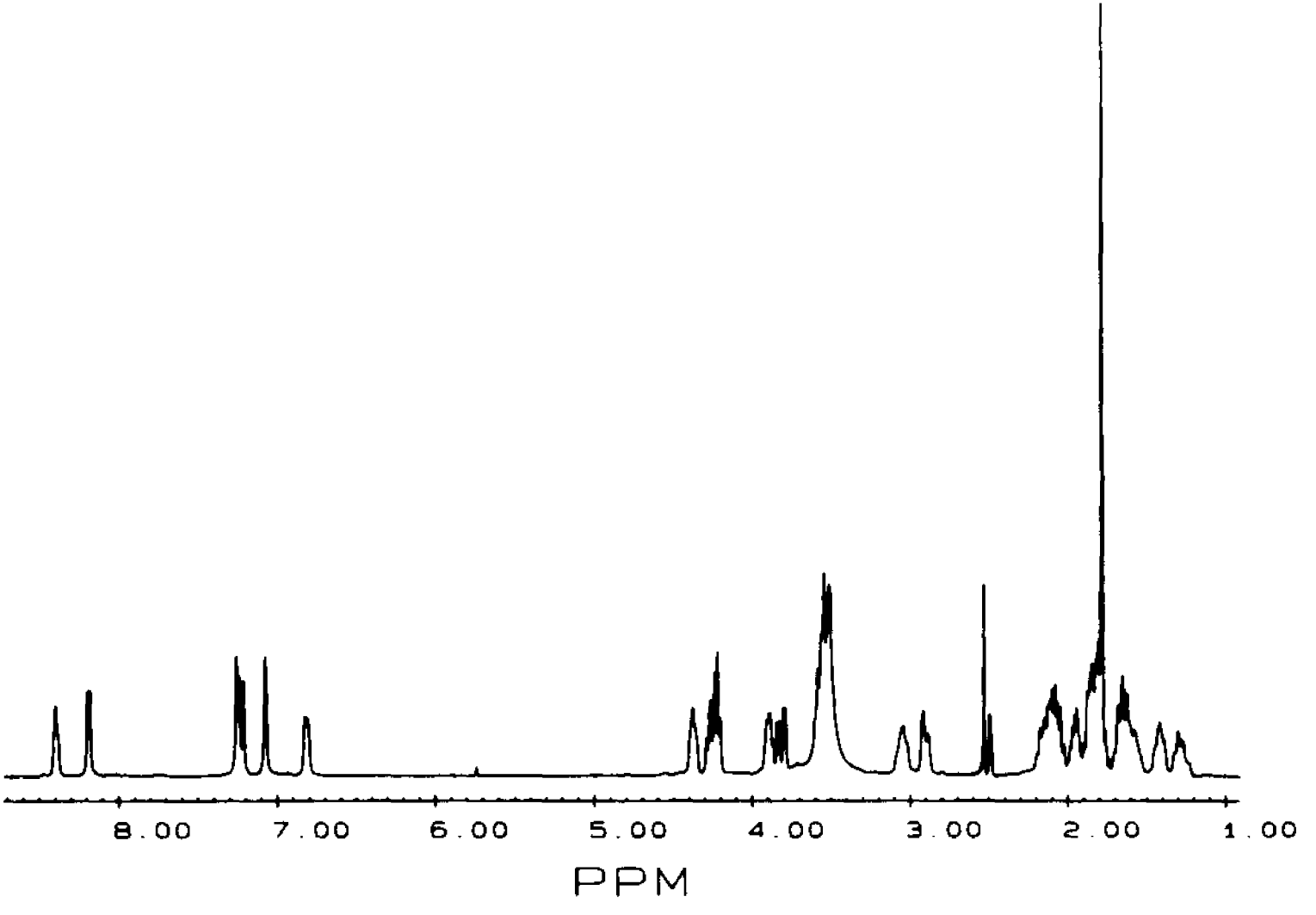
8.00
7.00
6.00
5.00
4.00
3.00
2.00
1.00
PPM

CHAPTER 5

Biological Activity of Cyclic α-Factor Analogs

I. Experimental Methods

1.1. Growth Arrest Assay

The biological activity of the α-factor analogs was assayed in Dr. Becker's laboratory using a growth arrest assay (Halo) as described previously (Raths et al., 1988). Briefly, peptides to be tested were added to sterile filter disks (diameter = 6 mm) placed on a lawn of *S. cerevisiae* RC629. The amount of peptide was systematically lowered until no growth arrest (as indicated by a halo around the disk) was observed. Activity was measured as the diameter (mm) of the growth arrest halo on the lawn of *S. cerevisiae* cells. At least three determinations were made and averaged. The values of each experiment were within 2 mm of each other. All activities were examined using a supersensitive mutant (RC629 [*sst1*]) of *S. cerevisiae*. The sst1 mutation results in the loss of *BAR1* protease, a secreted enzyme, which cleaves the peptide bond between positions 6 and 7 in α-factor (Chan et al., 1982). Thus the biological activities are not influenced by peptide degradation.

1.2. Binding Competition Assay

The binding assay of the α-factor analogs was also assayed in Dr. Becker's laboratory. Competition of bound tritiated [Nle^{12}]α-factor by unlabeled α-factor analogs was assayed against the wild type *S. cerevisiae* strain 4202-15-3 (*MATa*

cryl bar1-1 ade2-1 his 4-580 lys2 tyrl SUP4-3). The reaction was started by the addition of 100 µL of analog/[^{3}H]α-factor mixture (120 µL of appropriate unlabeled α-factor analog mixed with 120 µL of labeled α-factor 9.3 x 10^{-7} M, 9.24 Ci/mmole) to 400 µL of cell suspension. After the reaction was started, two 20 µL samples were removed and counted to determine total amount of radioactivity present. Duplicate reactions were started 3 min. after initial reaction for each analog tested. At 30 min. two 200 µL portions of cell suspension were added separately to 2 mL of YM-1 + i medium and filtered over GM-6 Metricel filters (Gelman Sciences, Inc., Ann Arbor, MI) presoaked in 1% bovine serum albumin. The reaction tubes were then rinsed twice with 2 mL ice-cold YM-1 + i medium, with each rinse filtered over the same filter. Finally, each filter was rinsed twice with 2 mL YM-1 + i medium. The non-specific binding of labeled α-factor to the filters was less than 100 cpm. This represented less than 5% of the total counts. The filters were counted in 5 mL of Budget-solve counting cocktail (Research Products International Corp., Mt. Prospect, IL) (Yang et al., 1995).

II. Biological Activity of the Cyclic and Linear Analogs

2.1 Biological Activity of the Cyclic Analogs

The biological activity is reported in Table 3 as the minimum amount of each peptide causing growth arrest of *S. cerevisiae* RC629. Among the cyclic analogs the series of peptides containing Glu in position 10 had higher potency than the corresponding analogs with Asp this position. For example, **C12** was at least 100-fold more potent than the homologous analog **C11**. The Orn-containing peptides (**C32** and **C31**) were exceptions because the difference in their activity was small. In the Glu-containing peptide series, **C32** was the only cyclic analog which had

Table 3
Bioactivity and Receptor Affinity of Cyclic and Linear α-Factor Analogs

Peptide	Ring size	Bioactivity[a] µg/disk		IC_{50}[c] (M) x 10^7	IC_{50} analog / IC_{50}([Nle^{12}]α-factor
C(4)2	18	>10	(>200)[b]	100	50
C42	18	0.5	(10)	150	75
C32	17	10	(200)	600	300
C22	16	0.5	(10)	2200	1100
C12	15	0.5	(10)	2000	1000
C41	17	>10	(>200)	>10000	>5000
C31	16	10	(200)	45000	22500
C21	15	5	(100)	10000	5000
C11	14	>50	(>1000)	>10000	>5000
L(4)2	-	5	(100)	700	350
L42	-	0.1	(2)	10	5
L32	-	0.1	(2)	30	15
L22	-	0.05	(1)	600	300
L12	-	0.1	(2)	260	130
L41	-	10	(200)	1400	700
L31	-	5	(100)	10000	5000
L21	-	5	(100)	2700	1350
L11	-	5	(100)	10000	5000

[a] The minimum amount of pheromone causing growth arrest of *S. cerevisiae* RC629 The quantities (µg/disk) represent the average of at least three determinations.
[b] The numbers in parentheses are the ratio of the end point amounts for the analog to that of [Nle^{12}]α-factor which caused growth arrest at a minimum of 0.05 µg/disk.
[c] Peptide concentration needed to reduce binding by 50%. IC_{50} of [Nle^{12}]α-factor = 2.0×10^{-7} M.

very low activity (200-fold less than [Nle^{12}]α-factor). No trend was found for the effect on the activity of changing the side chain length of the cyclic analogs. The cyclic analog containing *D*-Lys in position 7, **C(4)2**, was inactive at all concentration tested.

2.2. Biological Activity of the Linear Analogs

Linear analogs having the identical amino acid sequence to those found in the cyclic analogs were evaluated using the same bioassays (Table 3). These peptides differ from the constrained ones in that the amine and carboxyl side chains of residues 7 and 10 are ionizable. Again it was found that the series with Glu at residue 10 was significantly more potent than the corresponding peptides with Asp at this position. For example, **L32** was 50 times more potent than **L31** against strain RC629 (Table 3). Similar activities were found among the Glu-containing analogs and among the Asp-containing peptides.

Comparison of corresponding linear and cyclic analogs shows that the linear peptides were always the most potent. However, the ratio of activities varied from a high of 100 for **L32/C32** to a low 1-2 for **L21/C21** and **L31/C31** (Table 3).

2.3. Competition for Binding to the *STE2* Receptor

The affinity for the α-factor receptor was determined by measuring the competition between the analogs and tritiated [Nle^{12}]α-factor. In all cases the concentration of analog required to displace 50% of the tritiated pheromone from the receptor was at least 5-fold higher than that of [Nle^{12}]α-factor (Table 3). In general the lactam-containing peptides with Glu at position 10 exhibited higher

receptor affinity than those with Asp at this position. This was also true for the corresponding linear homologs. The relative receptor affinities varied from nearly 300-fold (compare **L31** with **L32**) to as low as 5 (compare **C22** with **C21**). As the size of the lactam ring decreases from 18 members to 15 members in the Glu series, the affinity for the receptor decreased by approximately 15-fold. Interestingly, the cyclic compound containing *D*-Lys had a higher affinity for the receptor than the corresponding linear homolog. This is the only case where a cyclic lactam analog was a stronger binder than the linear homolog.

The concept of a ligand binding to a receptor and not elucidating a response has been noted earlier in the literature. The typical example is a pure competitive antagonist which binds strongly to the agonist binding site but does not transduce signal. Less well understood would be a ligand which binds weakly yet results in strong signal transduction. In the present study we observed a clear dissociation between binding and biological potency. Specifically, **L42** and **L22** had nearly identical bioactivities against strain RC629 but the latter compound bound to the receptor 60 times less effectively. Similar phenomena were also observed for the cyclic analogs as comparing **C42** and **C22**. For structurally similar compounds such as **L42** and **L22** to exhibit equal potency and a nearly two orders of magnitude variation in affinity it would require that the poorly bound pheromone (**L22**) be an extremely efficient signal transducer.

CHAPTER 6

Conformational Studies of Peptides

As revealed by biological activity studies (Chapter 5), effects of the lactam ring size on the biological activity are significant, especially in the Glu^{10} series where the activity was reduced 20-fold by decreasing one CH_2 unit in the side chain of residue 7 (compare **C42** with **C32**) (Table 3). Furthermore **C32** is the only analog among the cyclic analogs in the Glu^{10} series which has very low activity. We therefore decided to undertake a comparative conformational analysis of these two cyclic tridecapeptides in order to investigate the stereochemical preferences of these peptides in relation to their biological activities. The following sections will present the conformational studies of two model compounds, Ac-*cyclo*[Lys-Pro-Gly-Glu]-NH_2 (Tetra **42**) and Ac-*cyclo*[Orn-Pro-Gly-Glu]-NH_2 (Tetra **32**), and the conformational analysis of the corresponding cyclic α-factor analogs, cyclo^{7,10}[Glu^{10}, Nle^{12}]α-factor (**C42**) and cyclo^{7,10}[Orn^7, Glu^{10}, Nle^{12}]α-factor (**C32**).

I. NMR Background

1.1. Peak Assignment

The fundamental requirement for any NMR study is the assignment of the observed resonances. The major task in an NMR assignment is to recognize the individual amino acid residues and to identify their specific sequences in the peptide chain.

Conventional COSY, COSY-45 and DQF-COSY experiments are used primarily for the first goal., The connectivities between the scalar coupled vicinal protons within a residue are observable in the COSY spectrum (Nagayama et al., 1980; Bax and Freeman, 1981). Many amino acid residues have unique connectivity patterns for the side chain resonances, which enable one to identify the type of residue. Those that do not have unique connectivity patterns can be discerned by either their chemical shifts or using sequential NOEs. In some cases, the connectivity patterns are not easily recognized because some cross peaks are very close to the diagonal and are often masked by the pronounced tails of the intense diagonal peaks due to their similar chemical shifts. COSY-45 (Friebolin, 1991) and DQF-COSY (Bodenhausen et al., 1981; Piantini et al., 1982) experiments are used to improve the spectral resolution by either reducing the intensity of the diagonal peaks or removing the large dispersive tails by applying the phase-sensitive mode.

Another major limitation of the COSY experiment, which is not overcome by COSY-45 or DQF-COSY, is the inability to resolve connectivities due to resonance degeneracy such as that of overlapped αCHs. This problem can often be solved by relayed-COSY experiment (Wagner, 1983). In such an experiment cross peaks can be observed between spins such as NH and βCH which are not directly scalar coupled but which share a mutual coupling partner (αCH). Thus, it allows one to identify the corresponding pairs of NHs and βCHs unambiguously (Wüthrich, 1986).

The latterly developed TOCSY experiment is far superior to the above experiments. In such an experiment, all pairs of nuclei within the same residue can show cross-peaks if an appropriate mixing time is applied. If a short mixing

time (<0.1/J) is used, only direct scalar connectivities will be observed (Braunschweiler et al., 1983; Bax and Davis, 1985). Thus, the TOCSY experiment allows one to identify the amino acids based on only one 2D experiment. In addition the phase-sensitive spectrum is free of dispersion mode signals, and leads, therefore, to high spectral resolution (Braunschweiler et al., 1983).

To complete the distinction between residues with similar connectivity patterns, sequence-specific assignments can be made by a combination of COSY and NOESY experiments. Specifically one can identify the neighboring residues by sequential NOE connectivities $d_{\alpha N}$ (i, i+1) or d_{NN} (i, i+1) or possibly $d_{\beta N}$ (i, i+1). Together with the NOESY, the COSY experiment allows the established sequence-specific segment to be related to the next segment through the scalar coupling $d_{\alpha N}$ (i, i) (Würthrich, 1986).

The simplest pulse sequences for the above NMR experiments are presented schematically in Figure 24.

1.2. NOE Analysis

The NOESY experiment has become one of the most important tools for determination of molecular conformation in solution. The cross peaks in the NOESY spectrum reveal closely spaced protons (less than 5-6 Å). The stronger the NOE cross peak is, the closer the two spins are in space. The limitation of the NOESY experiment is that NOE is known to be sensitive to molecular motion. For example, the dependence of maximum homonuclear NOE enhancement on correlation time τ_c is shown in Figure 25 (Neuhaus and Williamson, 1989). For large molecules (where $\omega\tau_c > 1.12$), NOESY cross peaks are in the same phase as

FIGURE 24: The pulse sequences for 2D NMR experiments used

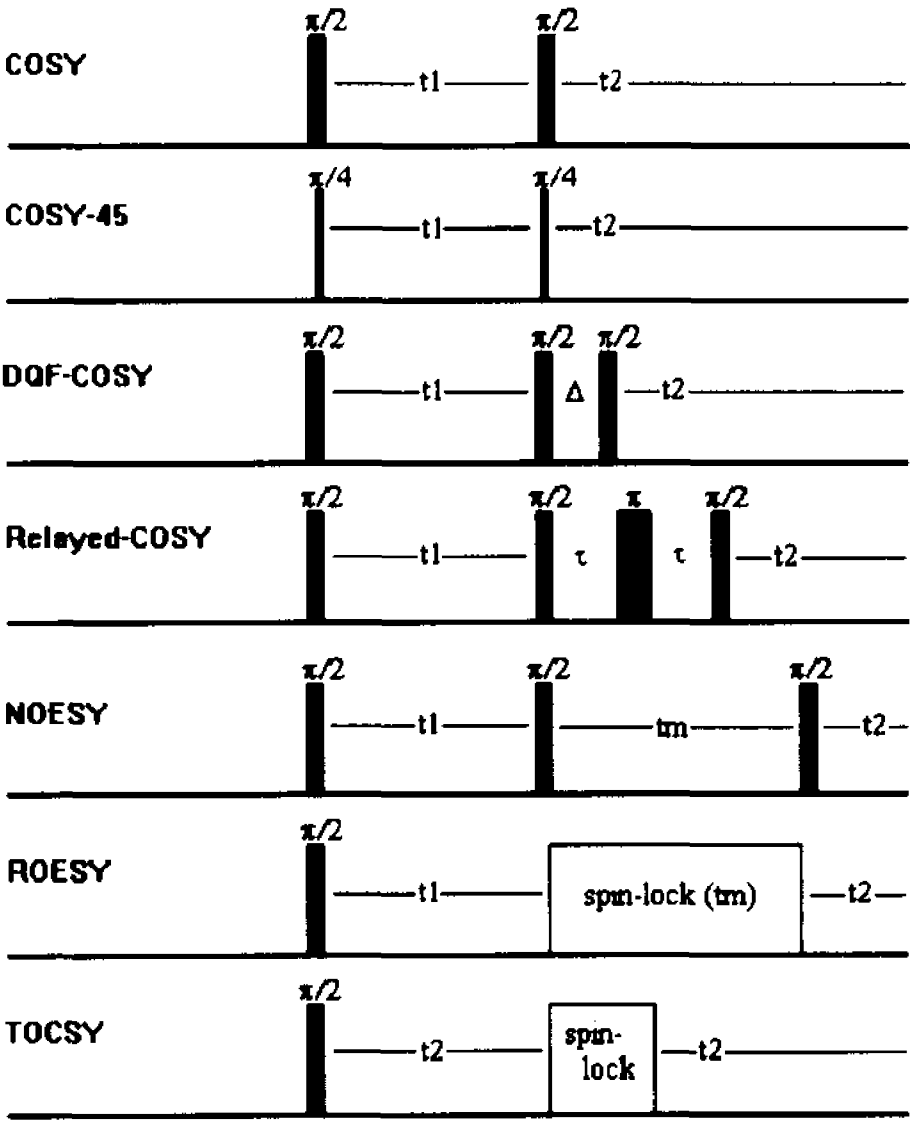
COSY
π/2
t1
π/2
t2
COSY-45
π/4
t1
π/4
t2
DQF-COSY
π/2
t1
π/2
Δ
π/2
t2
Relayed-COSY
π/2
t1
π/2
τ
π
τ
π/2
t2
NOESY
π/2
t1
π/2
tm
π/2
t2
ROESY
π/2
t1
spin-lock (tm)
t2
TOCSY
π/2
t2
spin-lock
t2

FIGURE 25: Dependence of the maximum homonuclear NOE on $\omega\tau_c$ (Data from Neuhaus and Williamson, 1989)

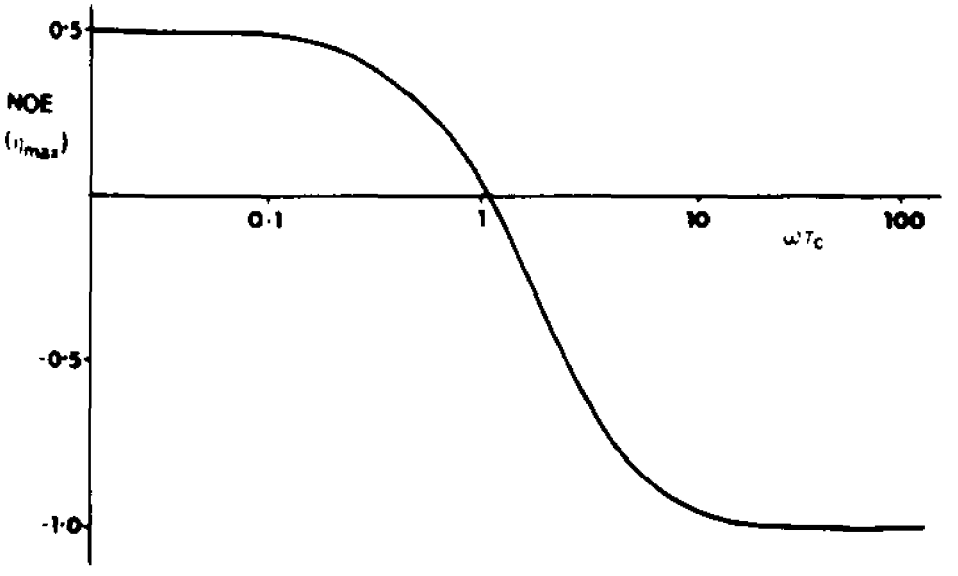
0·5
NOE
(η_{max})
0·1
1
10
100
$\omega\tau_c$
-0·5
-1·0

the diagonal. For small and fast tumbling molecules (where $\omega\tau_c < 1.12$), NOESY cross peaks are in the opposite phase of the diagonal. When the correlation time τ_c approaches the inverse of the Larmor frequency ω of the protons (or $\omega\tau_c \approx 1.12$), the NOE cross peaks intensities often approach zero and this situation often occurs for medium-size molecules (MW ≈ 200-2000) (Kessler et al., 1987; Neuhaus and Williamson, 1989). For the latter case the ROESY experiment is advantageous because the cross-relaxation is less sensitive to the correlation time τ_c and the NOE remains in the opposite phase of the diagonal irrespective of the value of τ_c and ω (Bax and Davis, 1985; Kessler et al., 1987).

Quantitative NOE analysis has been used to obtain structural information pertaining to various molecules. Distances derived from quantitative NOEs have been used to generate 3D molecular structures. A variety of procedures have been suggested for quantitative NOE analysis using 2D NOESY experiments (Kessler et al., 1982; Williamson et al., 1985; Olejniczak et al., 1986; Esposito et al., 1988; Fejzo et al., 1990). Among them, the initial build-up rate approximation method probably is the most frequently used method for quantitative NOE analysis. Although this method is correct only for two spin systems (Bruch et al., 1984; Stradley et al., 1990), it may result in a good approximation for multiple spins when the cross correlation between the spins is negligible and a high irradiation power is used (Noggle et al., 1974). If all dipolar interactions in a molecule can be characterized by a single correlation time, the equation: $(r_{ij}/r_{kl})^6 = \sigma_{kl}/\sigma_{ij}$ is valid (where σ_{ij} and σ_{kl} are the cross-relaxation rates between nuclei **i** and **j** and between nuclei **k** and **l** respectively) (Stradley et al., 1990; Perczel et al., 1991). Since the initial build-up of the NOE cross peak intensity (I) is proportional to the cross-relaxation rate (σ) under the initial rate approximation (Neuhaus and Williamson, 1989; Saultis and Liepins, 1990), the internuclear

distance r_{ij} can be estimated by equation of $(r_{ij}/r_{kl})^6 = I_{kl}/I_{ij}$ if the distance r_{kl} between nuclei k and l is known.

II. Circular Dichroism

Circular dichroism (CD) measurements have been used extensively to evaluate the conformation of proteins and peptides in solution. Accurate optical parameters, such as the mean residue ellipticities of α-helical, β-sheet and random conformations at wavelengths of 208 nm or 222 nm, have been deduced from either synthetic polypeptides (Greenfield and Fasman, 1969; Brahms et al., 1980) or from reference proteins with known structures (Provencher et al., 1981; Compton et al., 1986; Johnson, 1990; Perczel et al., 1992). Using these parameters one can calculate the content of these secondary structures in proteins and/or peptides. The CD patterns for Venkatachalam's β-turn structures (Venkatachalam, 1968) have been calculated by Woody (1974). By deconvolution of the CD curves of ten selected β-turn model compounds, Perczel et al., (1991) attempted to calculate the pure component CD spectra of type I and type II β-turns. Their study showed that the ratios of the major β-turn types agreed with those from their quantitative NOE analysis. However their deconvolution attempts yielded pure component CD curves which did not agree with those predicted by Woody (1974). The CD spectrum of a γ-turn is similar to that of the β-turn. However, the trough in the CD spectrum of a γ-turn structure shifts to a longer wavelength as compared to that of the β-turns(Madison et al., 1974; Deber et al., 1976; Madison et al., 1977). Despite all of the above efforts the correlation between the CD spectrum and the turn type is not as successful as the correlations of CD with the α-helical and β-sheet conformations. Nevertheless, CD has proved to be a very

useful technique to ascertain the secondary structure of a protein and/or peptide in solution.

III. Methods to Study Turn Conformations

As stated before (Chapter 2, Section VI), the Pro-*D*-Ala sequence favors a type II β-turn and the Pro-*L*-Ala sequence favors a type I β-turn (Venkatachalam, 1968; Aubry et al., 1985; Rose et al., 1985). Since a glycyl residue can be considered to be equivalent to either a *D* or an *L* configuration, the Pro-Gly sequence might be expected to adopt both type I and type II β-turn conformations. In fact a Pro-Gly sequence has been found in both type I and type II β-turns (Chandrasekaran et al., 1973; Crawford et al., 1973; Chou and Fasman, 1977; Ballardin et al., 1978). β-Turns are also called "reverse turns" in which the direction of the polypeptide chain changes by 180° through four consecutive amino acid residues. Originally three types of β-turns (I, II and III) were defined by the dihedral angles (ϕ, ψ) of the two corner residues i+1 and i+2. It was predicted that these turns are composed of all trans peptide bonds and are stabilized by an intramolecular 1←4 hydrogen bond (Venkatachalam, 1968; Crisma et al., 1984). The conventional detection and characterization of a β-turn by the NMR technique has depended on the following evidence: (1) the detection of an intramolecular hydrogen bond from the amide proton of the i+3 residue to the carbonyl of the i residue; (2) certain short diagnostic NOE distances; (3) the value of the $^{3}J_{N\alpha}$ coupling constant for the i+2 residue (Aubry et al., 1985; Dyson et al., 1988); (4) the chemical shift for the αCH of residue i+2 in NMR, especially in ^{13}C NMR (Pease and Watson, 1978; Bruch et al., 1985; Bach and Gierasch, 1986; Spatola et al., 1986; Stroup et al., 1992).

A number of methods can be used to determine a potential intramolecular hydrogen bond. The two most common methods are measurement of the temperature dependence of the proton chemical shift and of the deuterium proton exchange rates (Kopple and Ohnishi, 1969; Ohnishi and Urry, 1969). There are other complementary methods such as using ^{13}C NMR to measure the solvent dependence for the carbonyl (Urry et al., 1974) or using the TFA containing solvent mixture to measure the solvent dependence of the proton chemical shift (Pitner et al., 1972). The characteristic interproton distance in standard type I and type II β-turns for an *L*-Pro-*L*-Xxx sequence in the i+1 and i+2 positions have been reported (Stradley et al., 1990) and are shown in Table 4. It has also been demonstrated that a small value of $^{3}J_{N\alpha}$ (4.5 Hz) for the i+1 residue and a larger value of $^{3}J_{N\alpha}$ (9.0 Hz) for the i+2 residue corresponded to a Type II β-turn and a Type I β-turn, respectively, using model dipeptides (Aubry et al., 1985).

Table 4
Internuclear Distances in Standard Type I and Type II β-turns and in the γ-turn

	type I β-turn[a]	type II β-turn[a]		γ-turn[b]
αCH_{i+1}-NH_{i+2}	3.5 Å	2.1 Å	αCH_i-NH_{i+1}	2.1 Å
αCH_{i+2}-NH_{i+2}	2.9 Å	2.3 Å	αCH_{i+1}-NH_{i+1}	2.5 Å
αCH_{i+2}-NH_{i+3}	3.3 Å	3.3 Å	αCH_{i+1}-NH_{i+2}	2.5 Å
NH_{i+2}-NH_{i+3}	2.4 Å	2.5 Å	αCH_{i+2}-NH_{i+2}	2.5 Å
δCH_P-NH_{i+2}	2.7 Å	5.5 Å	NH_{i+1}-NH_{i+2}	NONE

[a]Distances are taken from Table V (Stradley et al., 1990). [b]Distances are taken from Table IV (Stroup et al., 1992)

IV. Materials and Methods

All NMR samples were contained in Wilmad 528-pp (5 mm) NMR tubes. Samples were dried overnight with an Abderhalden drying pistol at 65 °C to remove loosely bound water carried over from lyophilization. Peptides in DMSO-d_6 (99.99%) had a concentration of 5.0 mg/0.5 mL (about 5 mM for tridecapeptides and about 20 mM for tetrapeptides) for all NMR measurements. In order to detect possible aggregation one of the tetrapeptides (Tetra **42**) and one of the cyclic tridecapeptides (**C32**) were examined by NMR using 5-fold, 10-fold and 50-fold lower concentrations. The chemical shifts were found to vary no more than 0.02 ppm and the profile of the 1D ^{1}H NMR remained the same. Therefore it was unlikely that the peptides aggregated at the concentration used in our investigation. The NMR spectra were acquired on a Bruker 200 MHz spectrometer or a 400 MHz JEOL GX-400 spectrometer or a Varian 500 MHz spectrometer. Data processing was performed on a Sun Sparc IPX workstation utilizing the NMRi 1.2.1 software package or on a Sun Sparc IPX workstation utilizing the VNMR version 4.3 software package. All spectra were accumulated at 25 °C unless otherwise noted. Chemical shifts are reported relative to the residual proton resonance of DMSO at 2.49 ppm. Typically, one-dimensonal ^{1}H NMR spectra were acquired with 16 K points over a spectral width of ~5000 Hz. Usually an exponential multiplication with 0.3-0.5 Hz line broadening was applied prior to Fourier transformation.

The 2D spectra were generally recorded with 1K or 2K data points, 256 or 512 t_1 increments with 8-32 scans per t_1 value or 64-128 scans per t_1 value (on the 200 MHz instrument only), and the post aquisition delays of 1.0-2.0 s to ensure uniform recovery of the signals. The spectral width was 4000-5000 Hz in both

dimensions. All free induction decays were multiplied by a shifted sine-bell window functions in the F1 dimension and a shifted squared sine-bell in the F2 dimension. COSY, COSY-45 and Relayed-COSY were aquired in the absolute-value mode. DQF COSY, NOESY, ROESY were performed in the phase-sensitive mode. In all cases the t_1 dimension was zero-filled in order to obtain a 1K x 1K or a 2K x 2K spectrum of real data. In the ROESY experiment the carrier frequency was set to the position near the most down-field αCH and the lowest possible value of the spin-locking power (about 3 KHz) was used in order to reduce the Hartmann-Hahn effect (Bax and Davis, 1985). All peptides were studied in DMSO-d_6 solution.

The CD measurements were performed on a Jasco J-500 spectropolarimeter using circular quartz cells, with a path length of 0.01 cm at ambient temperature (~25 ^{o}C). The instruments was calibrated with D-(+)-10-camphorsulfonic acid. Spectra were obtained in the range of 190 nm to 260 nm, at a scan speed of 20 nm/min and using a time constant of 16 s. Peptide solutions were prepared in HPLC grade solvents. All spectra were corrected by subtracting the solvent absorption recorded under identical conditions. The CD spectra are reported in terms of molar ellipticity $[\theta]_M$ (deg.cm^2.dmol^{-1}), where the actual molecular weight of the peptide and not the mean residue molecular weight was used to calculate the molecular ellipticity.

V. Conformational Analysis of the Tetrapeptides

5.1. Circular Dichroism

Two model compounds (Tetra **42** and Tetra **32**) which represent the cyclized central regions of **C42** and **C32**, respectively, were synthesized as described earlier (Chapter 4, Section IV). The CD spectra of these tetrapeptides were measured in water by scanning the region of characteristic electronic absorption bands for amide groups between 190-260 nm. The experimental data are reported in Figure 26. In the CD spectrum of Tetra **42**, the extrema are seen at 198 nm, $[\theta]_{198}$ = +22900 deg.cm^2/dmol and at 225 nm, $[\theta]_{225}$ = -6300 deg.cm^2/dmol with a crossover point at 212 nm. The CD of Tetra **32** have extrema at 199 nm, $[\theta]_{199}$ = +30500 deg.cm^2/dmol and at 225 nm, $[\theta]_{225}$ = -14500 deg.cm^2/dmol with a crossover point at 213 nm. These curves are similar to those predicted by Woody (1974) for the type II β-turn of Venkatachalam (1968), where the peak and trough were predicted to be at 200-210 nm and ~225 nm, respectively.

A comparison of the spectra of both peptides (Figure 26) reveals that the magnitude of the ellipticities in Tetra **42** are smaller than those in Tetra **32**. The decrease of band intensities suggests an increase of conformational mobility in Tetra **42** (Perczel et al., 1991). A relatively broad minimum (between 218-232 nm) observed in the CD spectrum of Tetra **42** in water may have resulted from addition of two minima, a minimum of 225 nm from a β-turn and a minimum of 227-235 nm due to a 1←3 hydrogen bond in a γ-turn (Venkatachalam, 1968; Madison et al., 1977; Pease and Watson, 1978). In comparison Tetra **32** exhibits a sharper CD minimum at 225 nm. Compared with the CD in water, a red-shifted

FIGURE 26: Circular dichroism spectra of Ac-*cyclo*[Orn-Pro-Gly-Glu]-NH_2 (Tetra **32**) (Left) and Ac-*cyclo*[Lys-Pro-Gly-Glu]-NH_2 (Tetra **42**) (Right) in water (1.0 mg/mL)

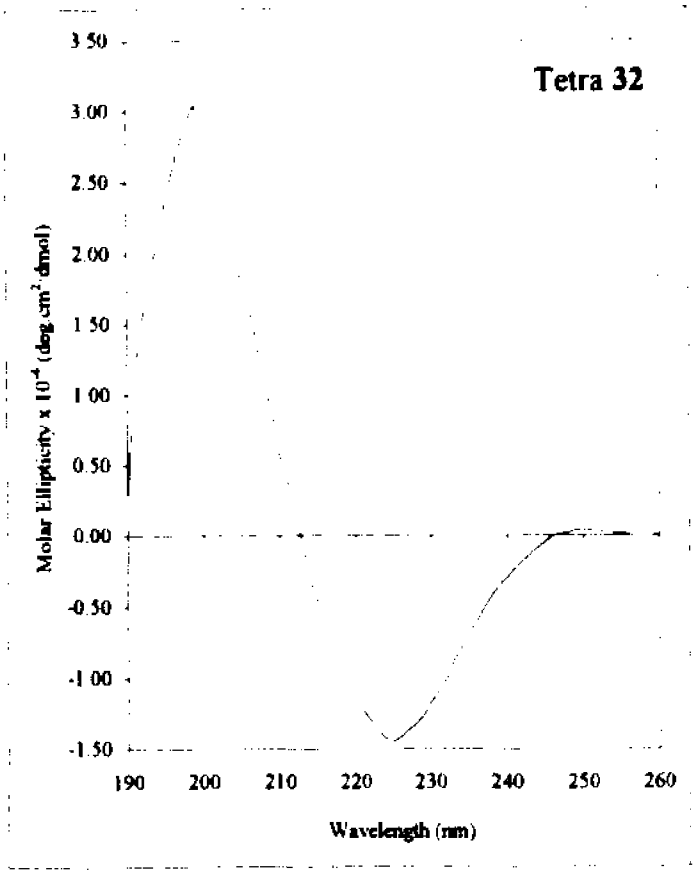
Tetra 32
3.50
3.00
2.50
2.00
1.50
1.00
0.50
0.00
-0.50
-1.00
-1.50
Molar Ellipticity x 10⁻⁴ (deg.cm².dmol)
190
200
210
220
230
240
250
260
Wavelength (nm)

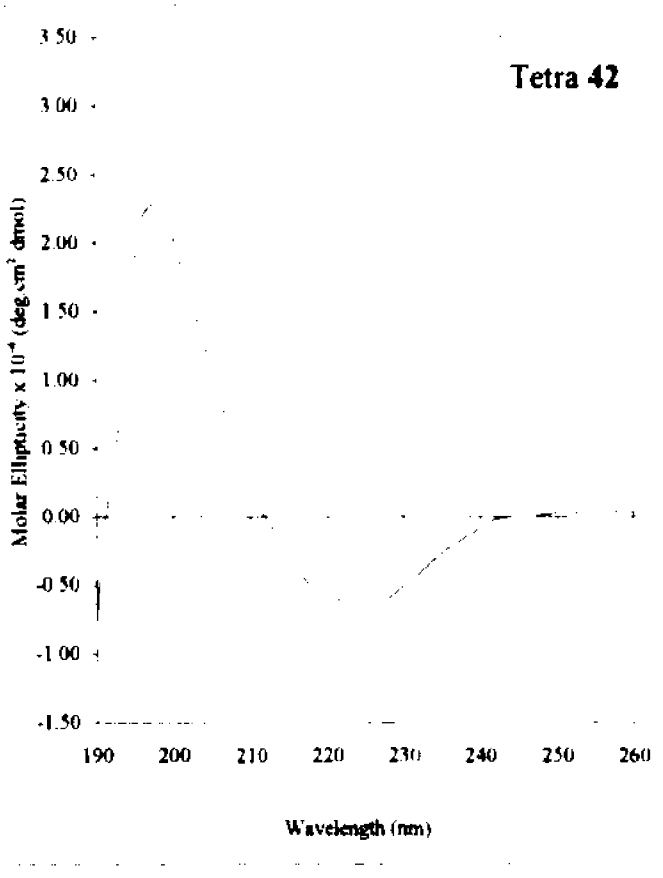
Tetra 42
3.50
3.00
2.50
2.00
1.50
1.00
0.50
0.00
-0.50
-1.00
-1.50
Molar Ellipticity x 10⁻⁴ (deg.cm².dmol)
190
200
210
220
230
240
250
260
Wavelength (nm)

CD minimum (~ 9-15 nm) was observed in the CD spectrum in TFE or MeOH for Tetra **42**. In contrast the shift of the CD minimum with these solvents was much less significant for Tetra **32** (Rao, personal communication). These results may indicate that there is more conformational mobility in Tetra **42** than in Tetra **32**. The CD spectrum of Tetra **32** is consistent with a type II β-turn conformation. For Tetra **42** a γ-turn may be present in addition to a type II β-turn. Because a red-shift in the CD minimum was not significant when Tetra **32** was studied in organic solvents, it is likely that for Tetra **42** the change of CD profile observed for this peptide in organic solvents is due to the conformational interconversion between the β- and γ-turn and is not a solvent effect.

5.2. Resonance Assignment of the Tetrapeptides

The chemical shifts for backbone protons (NH and αCH) and βCHs of both Tetra **42** and Tetra **32** in DMSO-d_6 were assigned unambiguously by a combination of COSY, 45-COSY, Relayed-COSY and DQF-COSY run on a Bruker 200 MHz instrument and were confirmed by sequential NOEs in their ROESY spectra (data not shown). The unequivocal assignment of the side chain protons was accomplished using TOCSY from a JEOL 400 MHz instrument. The TOCSY spectrum of Tetra **42** with the coupling pattern of Lys is shown in Figure 27. Assignments for all protons of both cyclic tetrapeptides are listed in Table 5 and Table 6.

FIGURE 27: TOCSY spectrum of Ac-*cyclo*[Lys-Pro-Gly-Glu]-NH_2 (Tetra **42**) in DMSO (25 °C; 10 mg/mL). The spin system of Lys is shown (solid line)

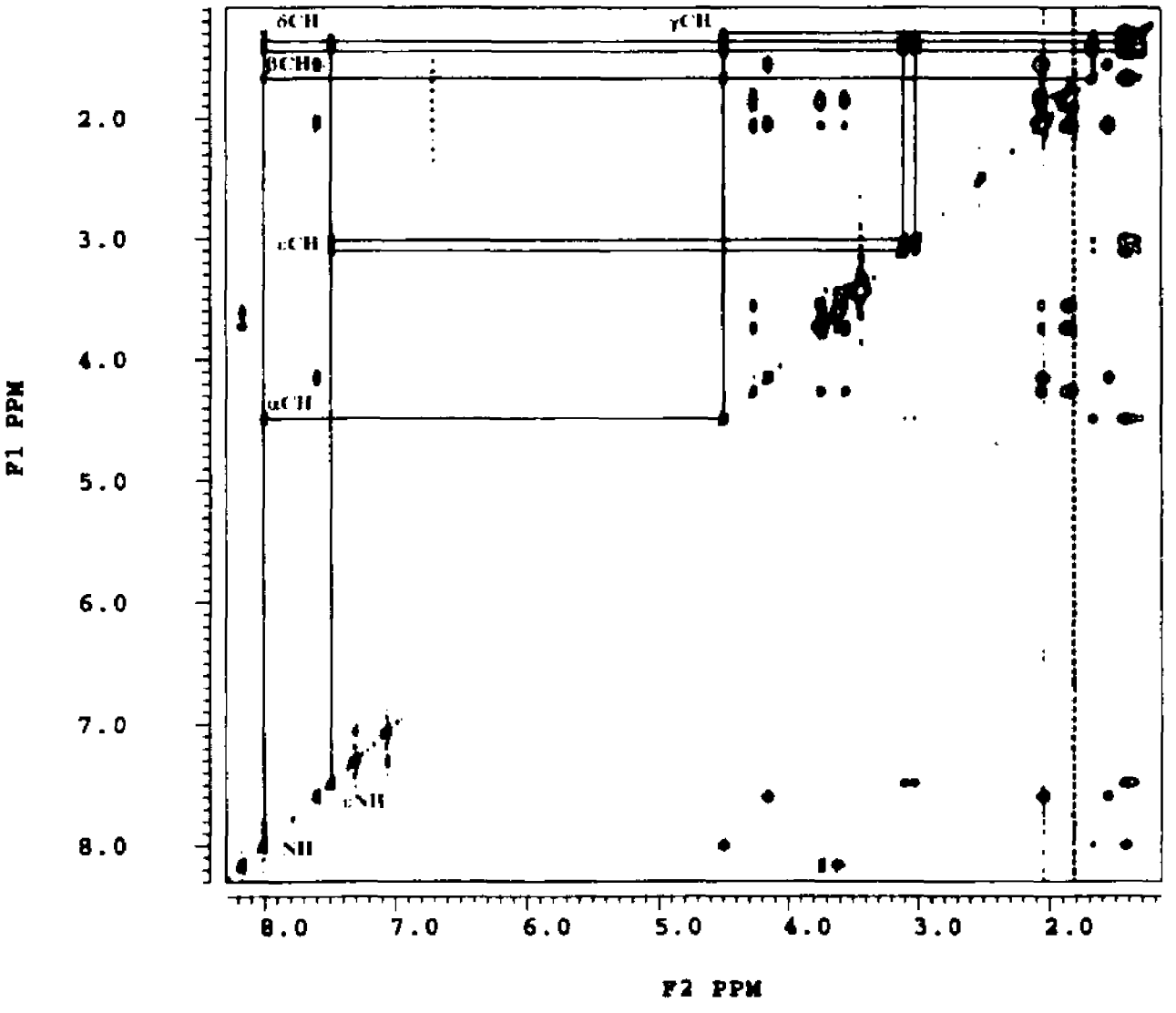
δCH
γCH
βCHa
βCHb
αCH
αCH
εNH
NH
2.0
3.0
4.0
5.0
6.0
7.0
8.0
F1 PPM
8.0
7.0
6.0
5.0
4.0
3.0
2.0
F2 PPM

Table 5
^{1}H Assignments for Ac-*cyclo*[Lys-Pro-Gly-Glu]-NH_2 (Tetra **42**) in DMSO (25°C)

	αNH	αH	βH	γH	δH	εH	εNH
Lys	8.00	4.48	1.66	1.29	1.37	3.12	7.48
			1.41			3.05	
Pro		4.26	2.06	1.86	3.74		
			1.90		3.55		
Gly	8.17	3.73					
		3.61					
Glu	7.59	4.15	1.54	2.04			
CH_3	1.85						
NH_2	7.30						
	7.05						

* Chemical shifts given in parts per million (ppm) using DMSO (2.49 ppm) as the internal standard

Table 6
^{1}H Assignments for Ac-*cyclo*[Orn-Pro-Gly-Glu]-NH_2 (Tetra **32**) in DMSO (25°C)

	αNH	αH	βH	γH	δH	δNH
Orn	8.24	4.38	1.64;1.57	1.41;1.28	3.05;2.90	6.88
Pro		4.23	2.10;1.94	1.87;1.79	3.91;3.57	
Gly	8.45	3.81;3.53				
Glu	7.24	4.27	1.85;1.64	2.19;2.06		
CH_3	1.80					
NH_2	7.27;7.08					

* Chemical shifts given in parts per million (ppm) using DMSO (2.49 ppm) as the internal standard

5.3. Temperature Dependence and Qualitative NOE Studies

The 1D proton NMR spectra (Figure 22 and Figure 23) of Tetra **42** and Tetra **32** in DMSO-d_6 show a single resonance for each type of proton, demonstrating that in this solvent either there is one major conformer or that different conformers experience rapid conformational exchange with the exchange rates faster than the difference in their chemical shifts. The $^3J_{N\alpha}$ coupling constants in both peptides are reported in Table 7. Amide proton temperature coefficients ($d\delta/dT$) for the tetrapeptides were measured over the range of 293 K - 338 K in DMSO-d_6 and are reported in Table 8. The $d\delta/dT$ of the Glu amide proton in Tetra **32** is very low (-0.90 ppb/k), which indicates that this proton is involved in strong intramolecular hydrogen bonding or is solvent shielded (Kessler, 1982). The presence of a deeply buried NH is unlikely in a small molecule like Tetra **32** (Perczel et al., 1991). This low $d\delta/dT$ value (-0.90 ppb/k) suggests that the Glu NH is involved in a 1←4 hydrogen bonding which is indicative of the presence of a type I or a type II β-turn structure in Tetra **32** (Torchia et al., 1972; Pease and Watson, 1978; Stroup et al., 1987). Another low value of $d\delta/dT$ (-2.28 ppb/K) is observed for the δ NH of Orn in Tetra **32**. This value indicates that the side chain amide proton of the ith residue (Orn) also participates in an intramolecular hydrogen bond (Kemp and McNamara, 1981). No very low $d\delta/dT$ values are found for any of the NHs in Tetra **42**. Two relatively low values of $d\delta/dT$ are found for the Gly NH (-3.14 ppb/K) and the Glu NH (-4.80 ppb/K) in this peptide. The absolute values of $d\delta/dT$, smaller than 4 ppb/K, are generally interpreted as weak but significant participation of NH's in intramoleculer hydrogen bonds (Stradley, et al., 1990; Perczel et al., 1991). Therefore in Tetra **42**, the Gly NH may be involved in a weak hydrogen bond and the Glu NH may be partially intramolecularly hydrogen bonded (Kemp and McNamara, 1981).

Table 7

$^3J_{\alpha NH}$ Coupling Constants (Hz) for Tetra **42** and Tetra **32** in DMSO (25 °C)

	Tetra **42**	Tetra **32**
αN (Gly)	5.49 (t)	5.70 (t)
αN (Lys or Orn)	7.94 (d)	6.87 (d)
αN (Glu)	9.16 (d)	9.39 (d)
εN (Lys) or δN (Orn)	5.19 (t)	3.25(d) and 6.86(d)
NH_2	48.82 (d)	35.13 (d)

Table 8

Amide Proton Temperature Coefficients (ppb/K) for Tetra **42** and Tetra **32** in DMSO

NH	Tetra **42**	NH	Tetra **32**
Lys	-7.0	Orn	-7.4
Lys εNH	-5.9	Orn δNH	-2.3
Gly	-3.1	Gly	-6.8
Glu	-4.8	Glu	-0.9

The conventional NOESY experiment was not useful for these model compounds because either the NOE cross peaks were absent or very weak in the NOESY spectra (mixing time varies from 600 ms to 100 ms) of these cyclic tetrapeptides. The NOESY experiment is known to be sensitive to molecular motion. Therefore, under the experimental conditions used these peptides must have an unfavorable correlation time which leads to the nearly zero NOEs. As an alternative approach the rotating frame NOESY (or ROESY) experiment was performed on both tetrapeptides (Figure 28 and Figure 29). For both peptides strong NOE cross peaks were observed between the Lys αCH and the Pro δCH in Tetra **42** or between the Orn αCH and the Pro δCH in Tetra **32** (Figure 28 and Figure 29). This NOE connectivity indicates that the Xxx-Pro amide bond is predominantly *trans* (Wüthrich, 1986).

For Tetra **32** the strongest interresidue NOE in the αCH-NH region is observed between the Gly NH and the Pro αCH (Figure 30, Left). The medium NOE between the Gly αCH and NH and weaker NOE between the Gly NH and Glu NH (Figure 30, Left; and Figure 31, Left) are expected for a type II β-turn conformation around Pro-Gly in Tetra **32**. As shown in Table 4 the internuclear distances between αCH (i+2) and NH (i+2) and between NH (i+2) and NH (i+3) were determined to be 2.3 Å and 2.5 Å, respectively, in a standard type II β-turn for a Pro-Xxx sequence in a cyclic pentapeptide (Stradley et al., 1990). The other characteristic interproton distances, such as the separation between the Gly αCH and Glu NH appears very weak, and the separation between the δCH of Pro and Gly NH is not observed in our experiment. Therefore, these distances presumably are larger than 3.0 Å, which is consistent with the presence of a type II β-turn and absence of a type I β-turn (Table 4). The small dδ/dT value (-0.90 ppb/K) for the

FIGURE 28: The 500 ms ROESY spectrum of Ac-*cyclo*[Lys-Pro-Gly-Glu]-NH_2 (Tetra **42**) in DMSO (25 °C)

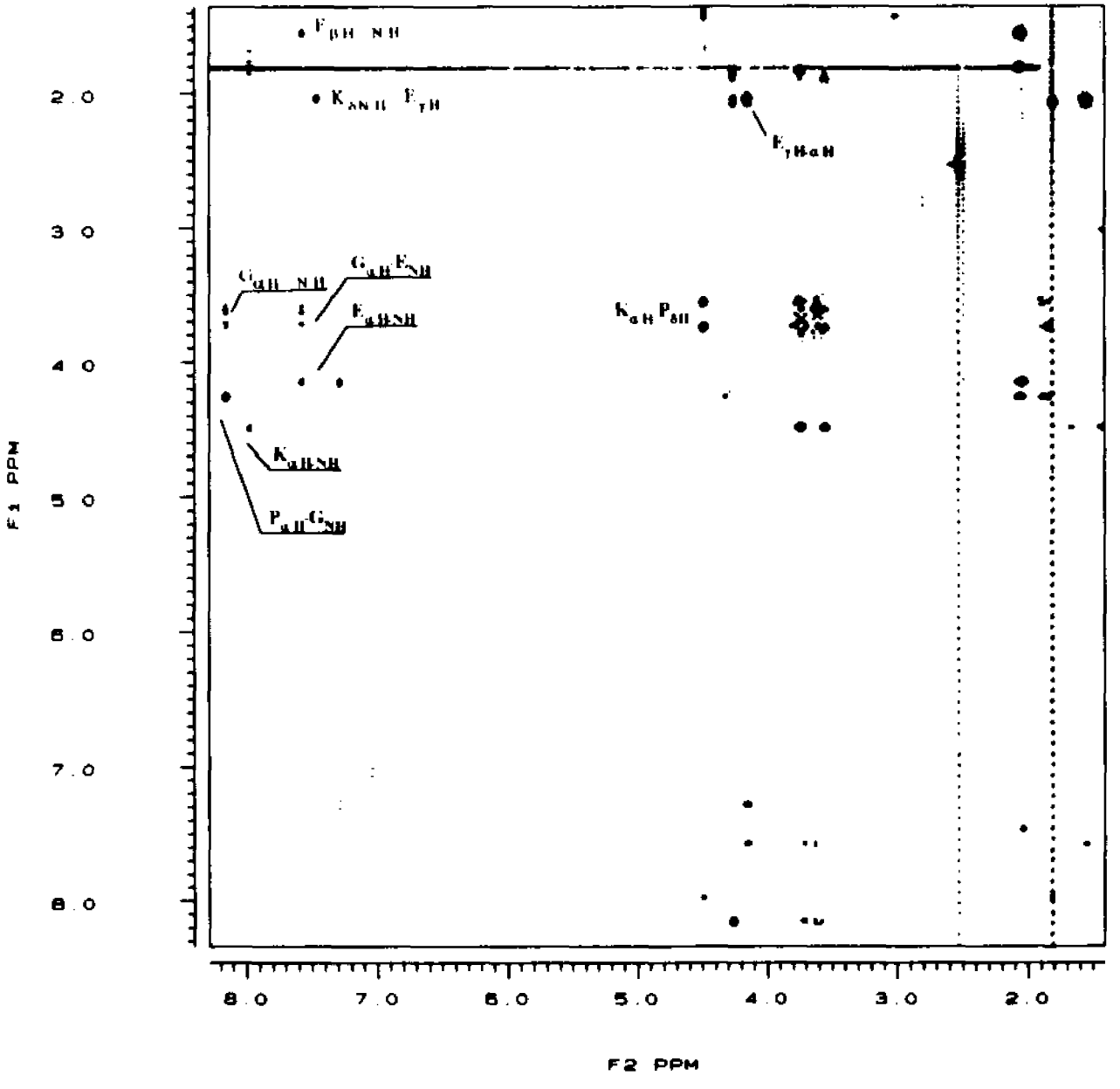
F1 PPM
2.0
3.0
4.0
5.0
6.0
7.0
8.0
8.0
7.0
6.0
5.0
4.0
3.0
2.0
F2 PPM

FIGURE 29: The 500 ms ROESY spectrum of Ac-*cyclo*[Orn-Pro-Gly-Glu]-NH_2 (**Tetra 32**) in DMSO (25 °C)

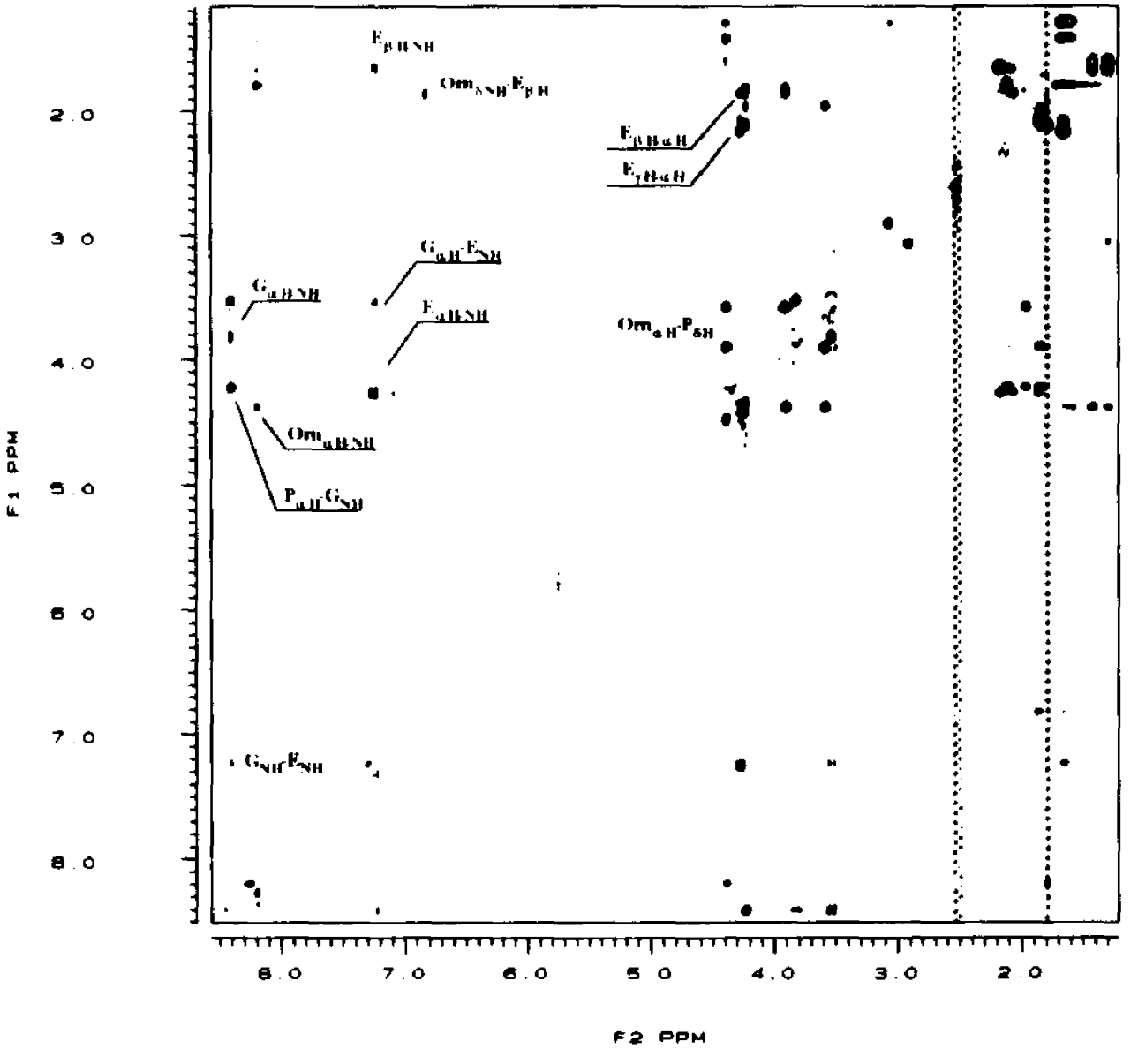
F1 PPM
2.0
3.0
4.0
5.0
6.0
7.0
8.0
F2 PPM
8.0
7.0
6.0
5.0
4.0
3.0
2.0

FIGURE 30: The αCH-NH regions of the 500 ms ROESY spectra of Ac-*cyclo*[Orn-Pro-Gly-Glu]-NH_2 (Tetra **32**) (Left) and Ac-*cyclo*[Lys-Pro-Gly-Glu]-NH_2 (Tetra **42**) (Right) in DMSO

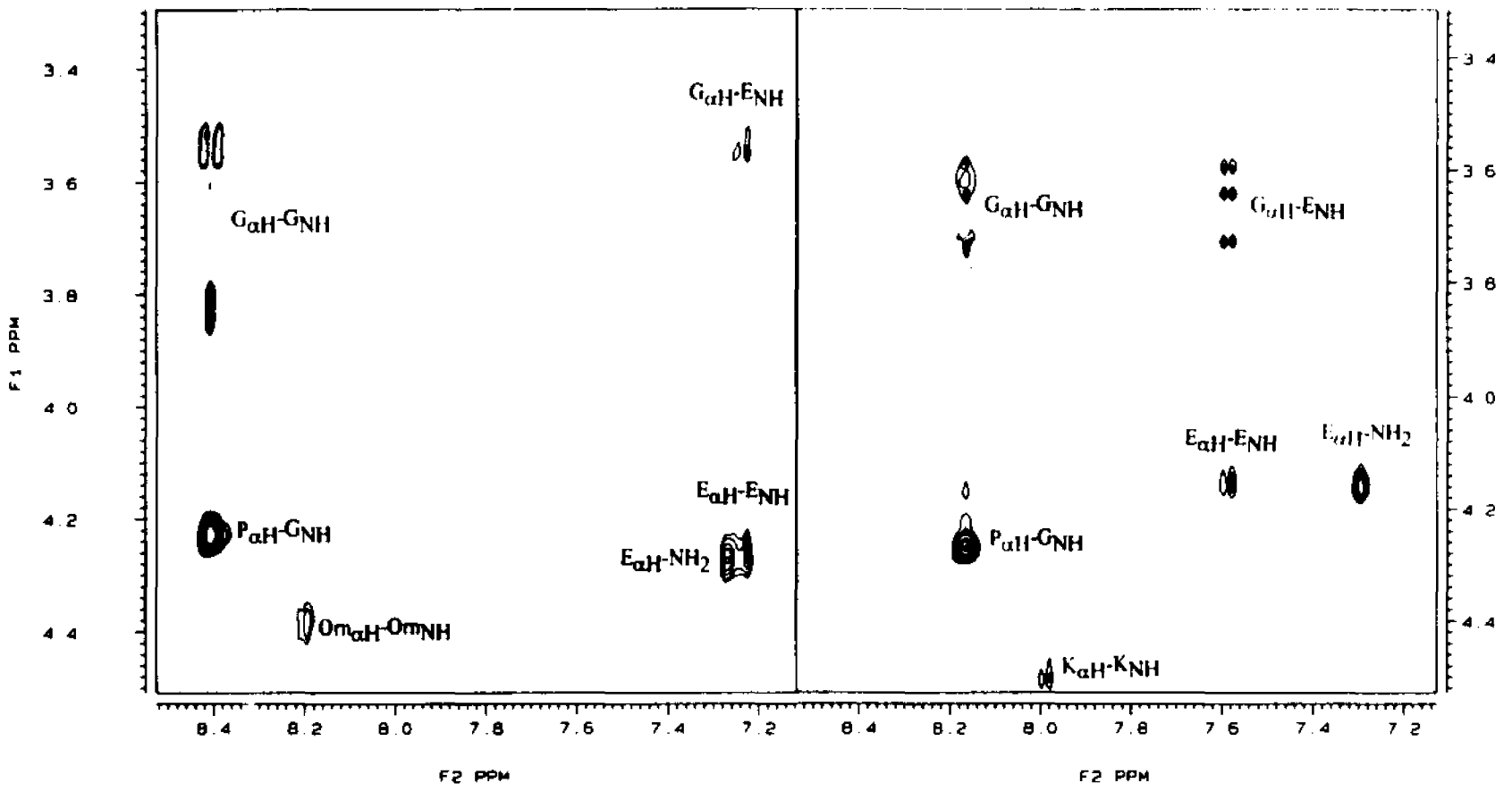
F1 PPM
3.4
3.6
3.8
4.0
4.2
4.4
$G_{\alpha H}$-G_{NH}
$G_{\alpha H}$-E_{NH}
$P_{\alpha H}$-G_{NH}
$E_{\alpha H}$-E_{NH}
$E_{\alpha H}$-NH_2
$Om_{\alpha H}$-Om_{NH}
$K_{\alpha H}$-K_{NH}
8.4
8.2
8.0
7.8
7.6
7.4
7.2
F2 PPM

FIGURE 31: The NH-NH regions of the 500 ms ROESY spectra of Ac-*cyclo*[Orn-Pro-Gly-Glu]-NH_2 (Tetra **32**) (Left) and Ac-*cyclo*[Lys-Pro-Gly-Glu]-NH_2 (Tetra **42**) (Right) in DMSO

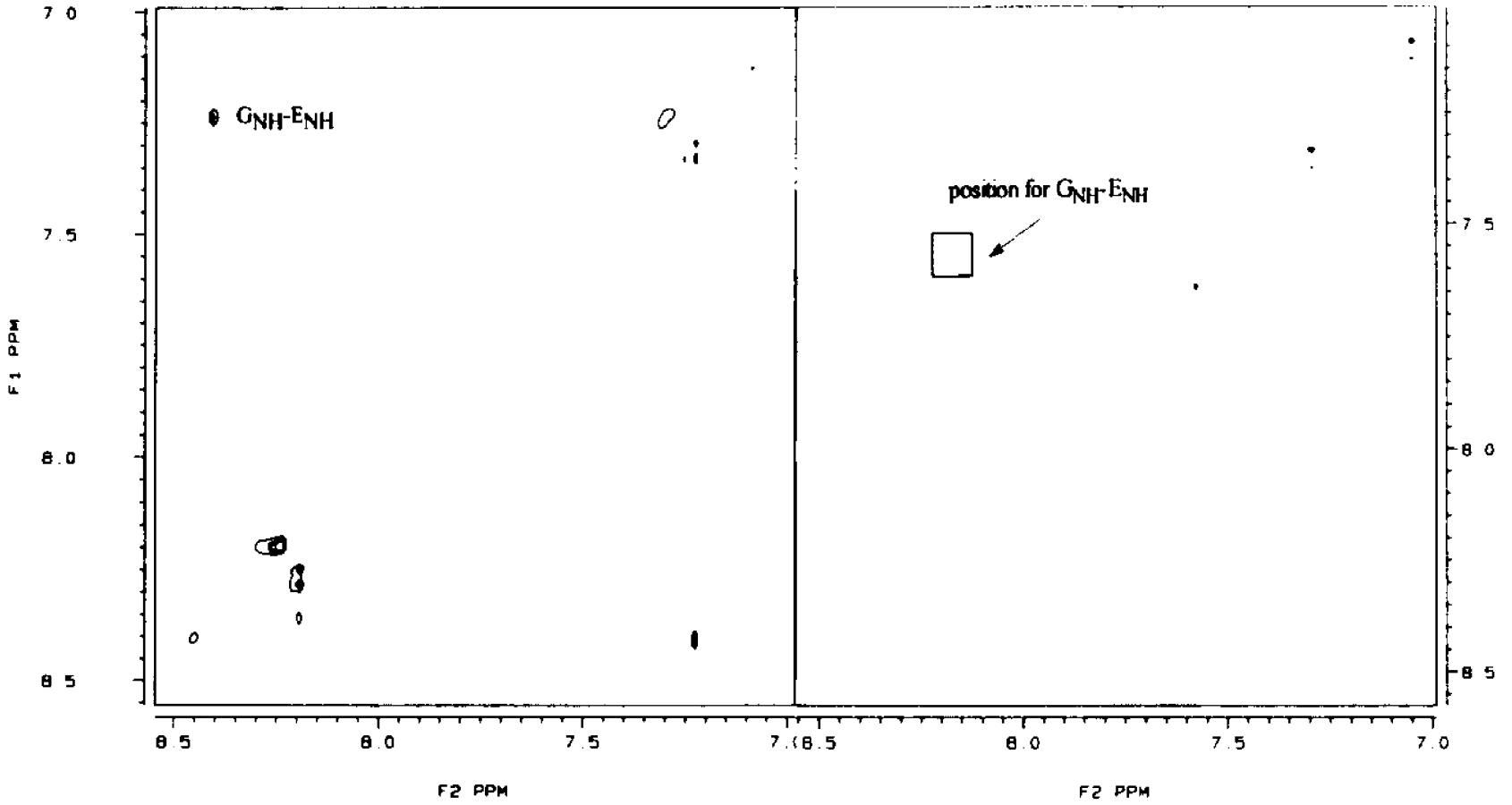
7.0
7.5
8.0
8.5
F1 PPM
GNH-ENH
position for GNH-ENH
8.5
8.0
7.5
7.0
F2 PPM
8.5
8.0
7.5
7.0
F2 PPM

Glu NH provides additional evidence for the existence of a type II β-turn conformation in Tetra **32**.

For Tetra **42** the very large NOE between the Gly NH and the Pro αCH and the absence of an NOE between the Gly NH and Pro δCH (Figure 30, Right; Table 4) are indicators for the presence of a type II β-turn and the absence of a type I β-turn conformation around Pro-Gly (Wüthrich, 1986; Stradley et al., 1990). The small (5.49 Hz) $^{3}J_{N\alpha}$ coupling constant of Gly is additional evidence for the absence of a type I β-turn conformation which should have a $^{3}J_{N\alpha}$ value of 9 Hz for Gly (Wagner et al., 1986). However, the NOEs between the Gly αCH and Glu NH is stronger and the NOE between the Gly NH and Glu NH is weaker than expected in a type II β-turn (Figure 30, Right; Figure 31, Right; and Table 4). In fact these observations point to an additional conformation, possibly a γ-turn conformation around Pro, in Tetra **42** (Stradley et al., 1990; Stroup et al., 1992). A 1←3 intramolecular hydrogen bond from the amide proton of the i+2 residue to the carbonyl of the i residue is important evidence for a γ-turn conformation (Matthews, 1972; Nemethy and Printz, 1972; Madison et al., 1974; Madison et al., 1977; Pease and Watson, 1978; Stroup et al., 1987). The relatively low dδ/dT value (-3.14 ppb/K) for Gly NH is consistent with such a hydrogen bond and therefore, a γ-turn around Pro. Hence, a mixture of a type II β-turn around Pro-Gly and a γ-turn around Pro may exist in Tetra **42**.

5.4. Quantitative NOE Studies and the CPK Model Constructions

In addition to the above qualitative NOE analysis, the internuclear distances were estimated for both tetrapeptides in order to get information pertaining to the molecular conformation of these molecules. Based on the NOE distances we

constructed a 3D structure of the peptides using a Corey-Pauling-Koltun (CPK) model. By comparing the 3D structure of both tetrapeptides, we hope to extract the general structural features of these peptides and to see if they could provide insights into the biological activities of the constrained α-factor analogs.

The NOE distances can be estimated according to the equation $(r_{ij}/r_{kl})^6 = I_{kl}/I_{ij}$. Obviously a precise reference distance is needed; ideally a fixed distance such as one between a pair of methylene protons. For example the two geminal α protons of Gly (1.75 Å, Noggle and Schirmer, 1971) or the δ protons of Pro (1.77 Å, García-Echeverría et al., 1991) would be desirable for quantitative comparisons. A good reference should also have a similar correlation time to the resonances of interest because the intensity of NOE cross peaks strongly depend on the correlation time. As suggested by Saultis and Liepins, (1990) the intraresidue distance of 2.8 Å for αCH_i-NH_i can be used as reference distance for estimating internuclear distances from NOE data due to the limited values for the ϕ angle (-60° to -180°) in *L*-residues. Judged by above two criteria, the NOE cross peak between the αCH and NH of Glu also can be a suitable reference distance for the present study.

In order to reduce the possible influence of spin diffusion, ROESY spectra with three mixing times (500 ms, 200 ms and 100 ms) were acquired for Tetra **42**. The values obtained from the 500 ms ROESY spectrum are within ±0.3 of those obtained from the 100 ms ROESY spectrum except for the distance between the Gly αCH and NH which differs by 0.4 Å (Table 9). Furthermore, the distances show no correlation with the mixing time. The findings suggest that the NOE distances are not affected significantly by spin diffusion at a mixing time of 500 ms for this peptide under our experimental conditions.

Table 9
Internuclear Distances for Tetra **42** from ROESY (100 ms and 500 ms) in DMSO (25°C)

	500 ms	100 ms
αCH_{Pro}-NH_{Gly}	2.2 Å	2.4 Å
αCH_{Gly}-NH_{Gly}	2.8 Å[a]	2.6 Å[a]
	3.1 Å[a]	2.7 Å[a]
αCH_{Gly}-NH_{Glu}	2.8 Å	2.7 Å
	2.9 Å	2.8 Å
αCH_{Glu}-NH_{Glu}	2.8 Å[b]	2.8 Å[b]
βCH_{Glu}-NH_{Glu}	2.9 Å	2.8 Å
αCH_{Lys}-δCH_{Pro}	2.1 Å[a]	2.2 Å[a]
	2.2 Å[a]	2.3 Å[a]
αCH_{Glu}-γCH_{Glu}	2.0 Å	2.3 Å
εNH_{Lys}-γCH_{Glu}	2.5 Å	2.5 Å

[a] There are two αCH for Gly and two δCH for Pro. [b] This internuclear separation was assumed and was used to estimate all other internuclear separations

In the present study the distance between the δ protons of Pro was not used as a reference because a significant COSY-type cross peak, which is in same phase as the diagonal peaks in a ROESY spectrum (Bax and Davis, 1985), was found for these nonequivalent geminal protons (Figure 32). The distances were estimated based on the distance between two αCHs of Gly and on that between the αCH and NH of Glu. It was found that the distances derived from the two references

FIGURE 32: 1D slice through the Pro δCH resonance of the 200 ms ROESY spectrum of Ac-*cyclo*[Lys-Pro-Gly-Glu]-NH_2 (Tetra **42**) in DMSO

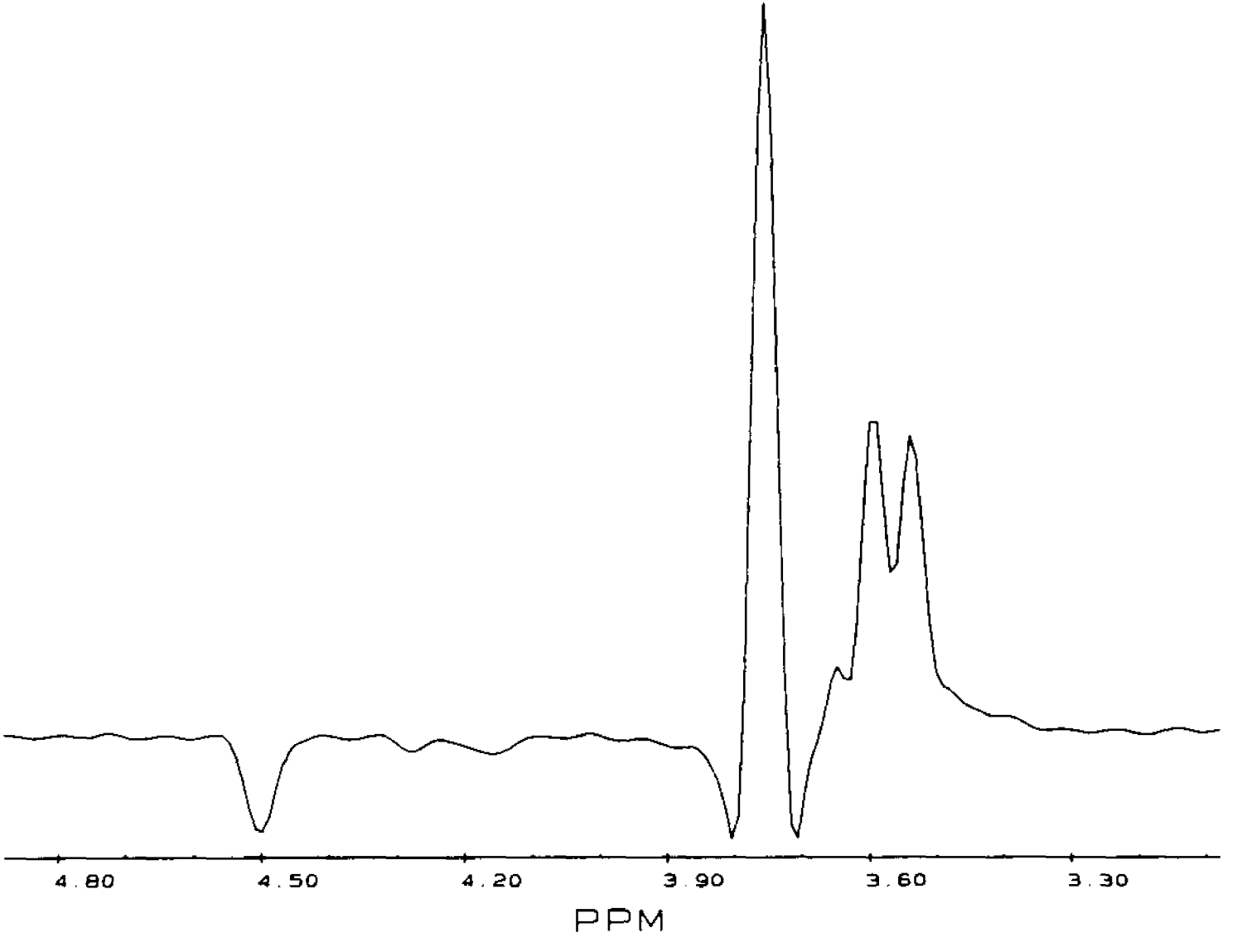
4.80
4.50
4.20
3.90
3.60
3.30
PPM

agreed with each other with a deviation of ±0.2 Å (Table 10). Therefore these two distances were used for estimating the internuclear distances in our investigation on the tetrapeptides.

Table 10
Internuclear Distances for Tetra 42 and Tetra 32 from ROESY Spectra Using the Separations between the Gly αCHs and between the Glu αCH-NH

	Tetra 42[a]			Tetra 32[b]	
αCH_{Pro}-NH_{Gly}	2.6 Å[c]	2.4 Å[d]	αCH_{Pro}-NH_{Gly}	2.1 Å[c]	2.3 Å[d]
αCH_{Gly}-NH_{Gly}	2.8 Å	2.6 Å	αCH_{Gly}-NH_{Gly}	2.5 Å	2.7 Å
	2.9 Å	2.7 Å		2.6 Å	2.8 Å
αCH_{Gly}-NH_{Glu}	2.9 Å	2.7 Å	αCH_{Gly}-NH_{Glu}	2.9 Å	3.1 Å
	3.0 Å	2.8 Å		-	-
αCH_{Glu}-NH_{Glu}	3.0 Å	2.8 Å	αCH_{Glu}-NH_{Glu}	2.6 Å	2.8 Å
αCH_{Lys}-δCH_{Pro}	2.4 Å	2.2 Å	αCH_{Orn}-δCH_{Pro}	2.0 Å	2.2 Å
	2.5 Å	2.3 Å		2.2 Å	2.4 Å

[a]Distances were measured from ROESY spectrum (100 ms). [b]Distances were measured from ROESY spectrum (500 ms). [c]Distances were estimated using the separation (1.75 Å) between the two αCHs of Gly as the reference distance. [d]Distances were estimated using the separation (2.80 Å) between the αCH_{Glu} and NH_{Glu} as the reference distance.

The internuclear distances determined for Tetra 32 are close to the reported values (Stradley et al., 1990) if a type II β-turn spans residues Orn-Pro-Gly-Glu (Table 11). However two distances have deviations larger than the experimental error range (±0.2 Å). Specifically the distance between the Gly NH and Glu NH is

longer than what would be expected for a type II β-turn (with a deviation of 0.9 Å) and the distance between the Gly αCH and NH is larger than what would be expected for a type II β-turn (with a deviation of 0.4 Å). Consistent with the results from the qualitative NOE analysis, these measured distances are not compatible with a type I β-turn. Based on the above quantitative NOE analysis we conclude that in DMSO solution Tetra **32** adopts a type II β-turn conformation with some degree of distortion.

Table 11
Measured Distances for Tetra **42** and Tetra **32** from ROESY Spectra and the Distances Expected for Standard β-turns

	Tetra **42**	Tetra **32**	type I β-turn	type II β-turn
αCH_{Pro}-NH_{Gly}	2.4 Å[a]	2.3 Å[b]	3.5 Å[c]	2.1 Å[c]
αCH_{Gly}-NH_{Gly}	2.6 Å	2.7 Å	2.9 Å	2.3 Å
αCH_{Gly}-NH_{Glu}	2.7 Å	3.1 Å	3.3 Å	3.3 Å
NH_{Gly}-NH_{Glu}	NONE	3.4 Å	2.4 Å	2.5 Å
δCH_{Pro}-NH_{Gly}	NONE	NONE	2.7 Å	5.5 Å

[a]Distances were from ROESY spectrum (100 ms) reference with the separation between the αCH and NH of Glu (2.80 Å). [b]Distances were from ROESY spectrum (500 ms) reference with the separation between the αCH and NH of Glu (2.80 Å). [c]Distances are taken from Table V (Stradley et al., 1990)

The measured distances for Tetra **42** also do not agree with those expected (Stradley et al., 1990) for a standard type I β-turn centered about Pro-Gly. For example, the distance between the Pro αCH and Gly NH is much shorter than what would be expected for a type I β-turn; the distance between the Gly αCH

and Glu NH is shorter than expected; the absence of an NOE cross peaks for NH_{Gly}-NH_{Glu} and δCH_{Pro}-NH_{Gly} means these distances must be larger than 3.0 Å but both distances would be expected shorter than 3.0 Å in a type I β-turn (Table 11). The data indicate that it is not likely that Tetra **42** adopts a type I β-turn conformation in DMSO solution.

The internuclear distances in Tetra **42** also do not fit well with those expected in a type II β-turn around the Pro-Gly sequence. Specifically the absence of an NOE cross peak between the Gly NH and Glu NH indicates that this distance must be longer than 3.0 Å. Neither this long distance nor the short distance between the Gly αCH and the Glu NH (2.7 Å) correspond to those expected for a type II β-turn (Table 11). The results raise the question of whether Tetra **42** exists in a different conformation or exists as a mixture of several conformers. No single conformation was found to fit the experimental data. However if we use αCH_{Lys}-δCH_{Pro} and δCH_{Pro}-NH_{Gly} as analogous cross-peaks to the connectivities of αCH_i-NH_{i+1} and NH_{i+1}-NH_{i+2} (Wüthrich, 1986; Dyson et al., 1988; Stradley et al., 1990; Gounariders, 1994), fairly good agreement is found between the measured distances and the expected values for a γ-turn around Pro (Table 12). The measured distances reported in Table 12 for Tetra **42** are within ±0.1 Å of the values reported for a γ-turn. Therefore the results are consistent with the qualitative conclusion that a γ-turn conformation may coexist with a type II β-turn in Tetra **42** in DMSO solution.

The NOE constraints used in construction of the Corey-Pauling-Koltun (CPK) models for Tetra **42** and Tetra **32** are reported in Table 13. Besides the distances involving the backbone resonances, those involving the side chain resonances of Glu and Lys or Orn were found to be critical for construction of the models.

Table 12
Measured Internuclear Distances of the Lys-Containing Peptides and the Distances Expected for a γ-Turn[f]

	Tetra 42	C42	γ-turn
αCH_{Lys}-δCH_{Pro}[a]	2.2 Å[c]	2.2 Å[d]	2.1 Å
αCH_{Pro}-NH_{Gly}	2.4 Å	2.3 Å	2.5 Å
αCH_{Gly}-NH_{Gly}	2.6 Å	2.5 Å[e]	2.5 Å
δCH_{Pro}-NH_{Gly}[b]	NONE	NONE	NONE

[a]This distance is analogous to αCH_i-NH_{i+1}. [b]This distance is analogous to NH_{i+1}-NH_{i+2}. [c]Distances were from the 100 ms ROESY spectrum assuming a separation between the αCH and NH of Glu (2.80 Å). [d]Distances were from NOESY spectrum (200 ms) assuming a separation between the αCH and NH of Glu (2.80 Å). [e]Distance was calculated based on half of the NOE intensity due to the assumption of overlapping Gly αCHs. [f]Distances are taken from Stroup et al. (1992)

Specifically, the distances of the Glu αCH-βCH, the Glu αCH-γCH, the Orn δCH-Glu βCH and the Pro δCH-Orn γCH were important for building the model of Tetra **32**. The distances of the Glu αCH-βCH, the Glu αCH-γCH, and the Lys εNH-Glu γCH were important for building the model of Tetra **42**. The CPK models for Tetra **42** and Tetra **32** are shown in Figure 33. In addition to the constraints shown in Table 13, the models satisfied the hydrogen bonding requirements (Table 8). Inspection of both models reveals structural features which differ as follows: (I) the γ-carbonyl of Glu has an opposite spatial orientation in Tetra **42** and Tetra **32**; (II) the direction of the pyrrolidine ring in the two models differs more than 30°; (III) if the cyclic tetra peptides are oriented so

that the *N*-acetyl terminal group is below the plane of the lactam ring then the top surface of the tetrapeptide structure has considerably higher hydrophobicity in Tetra **42** than in Tetra **32**.

Table 13
Internuclear Distances Used for Constructing the CPK Models of Tetra 42 and Tetra 32

Tetra 42		Tetra 32	
αCH_{Lys}-δCH_{Pro} (4.48 ppm-3.74 ppm)	2.2 Å[a]	αCH_{Orn}-δCH_{Pro} (4.38 ppm-3.91 ppm)	2.2 Å[b]
(4.48 ppm-3.55 ppm)	2.3 Å	(4.38 ppm-3.57 ppm)	2.4 Å
αCH_{Pro}-NH_{Gly}	2.4 Å	αCH_{Pro}-NH_{Gly}	2.3 Å
NH_{Gly}-NH_{Glu}	NONE	NH_{Gly}-NH_{Glu}	3.4 Å
βCH_{Glu}-NH_{Glu} (1.54 ppm-7.59 ppm)	2.8 Å	βCH_{Glu}-NH_{Glu} (1.64 ppm-7.24 ppm)	2.9 Å
βCH_{Glu}-αCH_{Glu}	NONE	βCH_{Glu}-αCH_{Glu} (1.85 ppm-4.27 ppm)	2.7 Å
γCH_{Glu}-αCH_{Glu} (2.04 ppm-4.15 ppm)	2.3 Å	γCH_{Glu}-αCH_{Glu} (2.19 ppm-4.27 ppm)	2.6 Å
		(2.06 ppm-4.27 ppm)	3.0 Å
εNH_{Lys}-γCH_{Glu} (7.48 ppm-2.04 ppm)	2.5 Å	δNH_{Orn}-γCH_{Glu}	NONE
εNH_{Lys}-βCH_{Glu}	NONE	δNH_{Orn}-βCH_{Glu} (6.88 ppm-1.85 ppm)	2.9 Å
		(6.88 ppm-1.64 ppm)	3.8 Å
		δCH_{Pro}-γCH_{Orn} (3.57 ppm-1.28 ppm)	3.2 Å

[a]Distances were from ROESY spectrum (100 ms) assuming a separation between αCH and NH of Glu (2.80 Å). [b]Distances were from ROESY spectrum (500 ms) assuming a separation between αCH and NH of Glu (2.80 Å).

FIGURE 33: The constructed CPK models for Ac-*cyclo*[Lys-Pro-Gly-Glu]-NH_2 (Tetra **42**, Top) and Ac-*cyclo*[Orn-Pro-Gly-Glu]-NH_2 (Tetra **32**, Bottom)

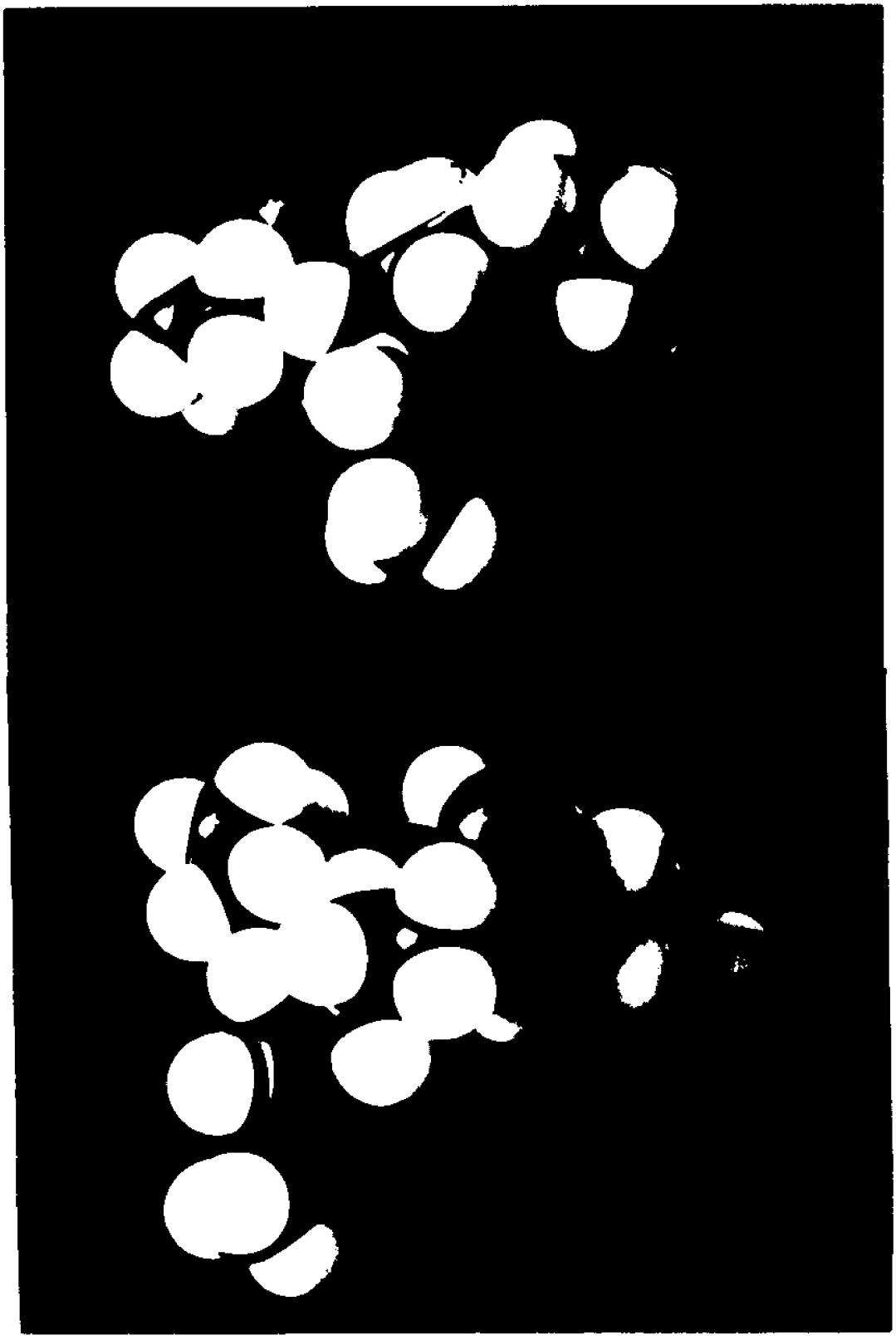

VI. Conformational Analysis of the Cyclic α-Factor Analogs

6.1. Circular Dichroism

The CD spectra of the cyclic α-factor analogs were measured in water/methanol (1:1, v/v; methanol was used to increase the solubility) (Figure 34). For comparison the CD of the corresponding linear homologs were measured in the same solvent (Figure 35). Similar CD patterns are observed for the linear analogs, which implies that changes in side chain length in either position 7 or 10 have little effect on the overall conformation of these linear peptides. All CD spectra for linear analogs show a broad minimum below 195 nm, and positive ellipticity between 217 nm and 235 nm. Such a curve would be associated with a predominantly disordered peptide. The CD patterns of the cyclic analogs differ appreciably from those of the linear analogs. Although a positive band between 217 nm and 235 nm is observed in the CD spectra of the cyclic peptides, there is a significant difference in the CD profile in the region below 217 nm between the cyclic and linear analogs. The extent of this difference varies from peptide to peptide. For example, an intense positive band at about 198 nm is observed for **C22** and **C12**, which are the most potent cyclic analogs in the series. The magnitude of the positive band below 200 nm is much less for **C32, C31, C21** and **C11**. **C(4)2** and **C41** do not show positive ellipticity below 200 nm. It should be noted that none of the linear analog gives a positive band in the same region. These comparative results indicate that constraints made between the side chains of residues 7 and 10 have significant impact on the conformation of the peptide. The CD spectra of the cyclic analogs did not resemble those for any of the regular secondary structures. However, in most cases the major difference between the CD spectrum of the linear analog and that of the cyclic analog is a positive

FIGURE 34: CD spectra of the cyclic α-factor analogs in MeOH/H_2O (1:1, v/v; 1.0 mg/mL)

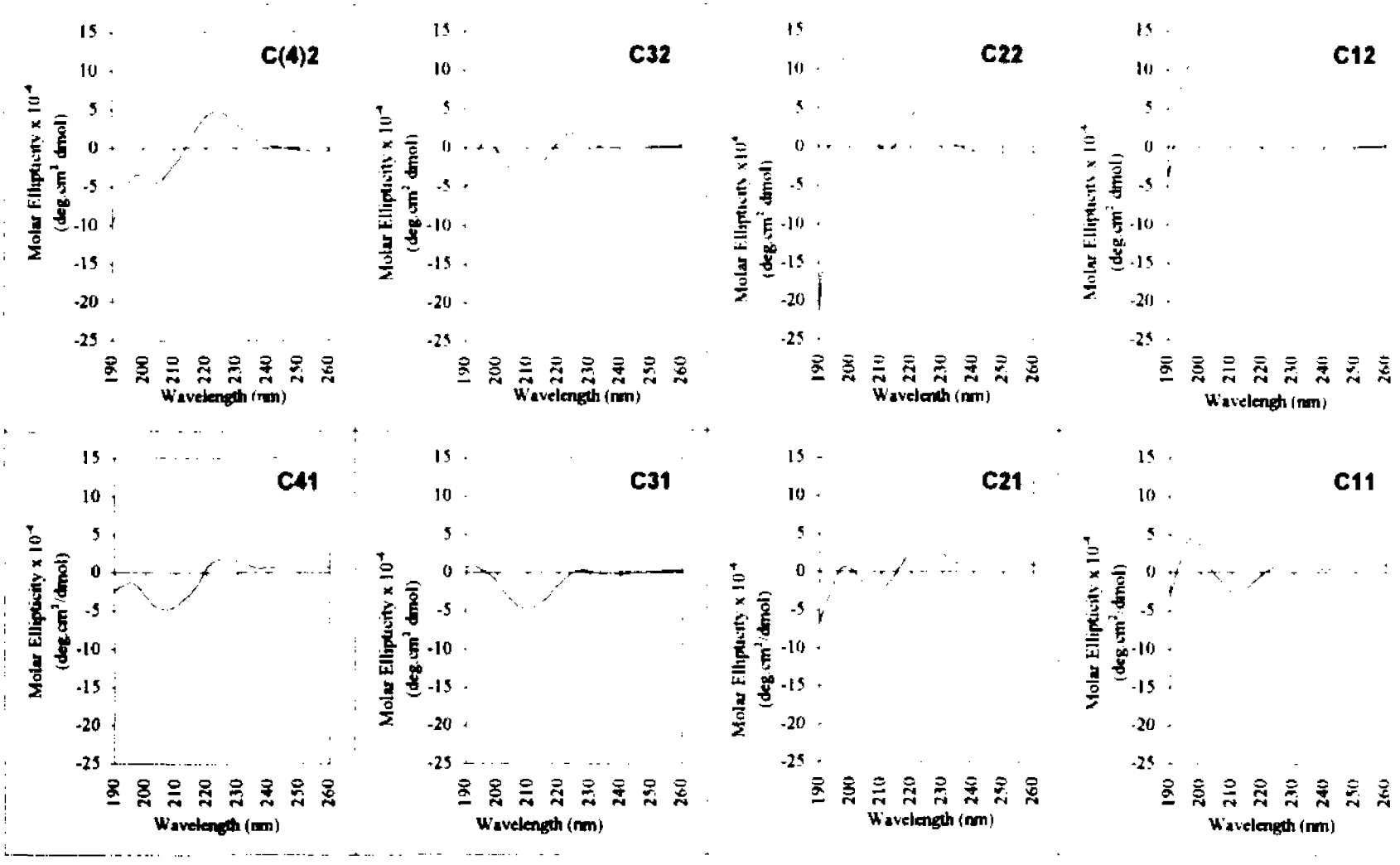
C(4)2
C32
C22
C12
C41
C31
C21
C11
Molar Ellipticity x 10⁻⁴ (deg.cm².dmol)
Wavelength (nm)
15
10
5
0
-5
-10
-15
-20
-25
190
200
210
220
230
240
250
260

FIGURE 35: CD spectra of the linear α-factor analogs in MeOH/H_2O (1:1, v/v; 1.0 mg/mL)

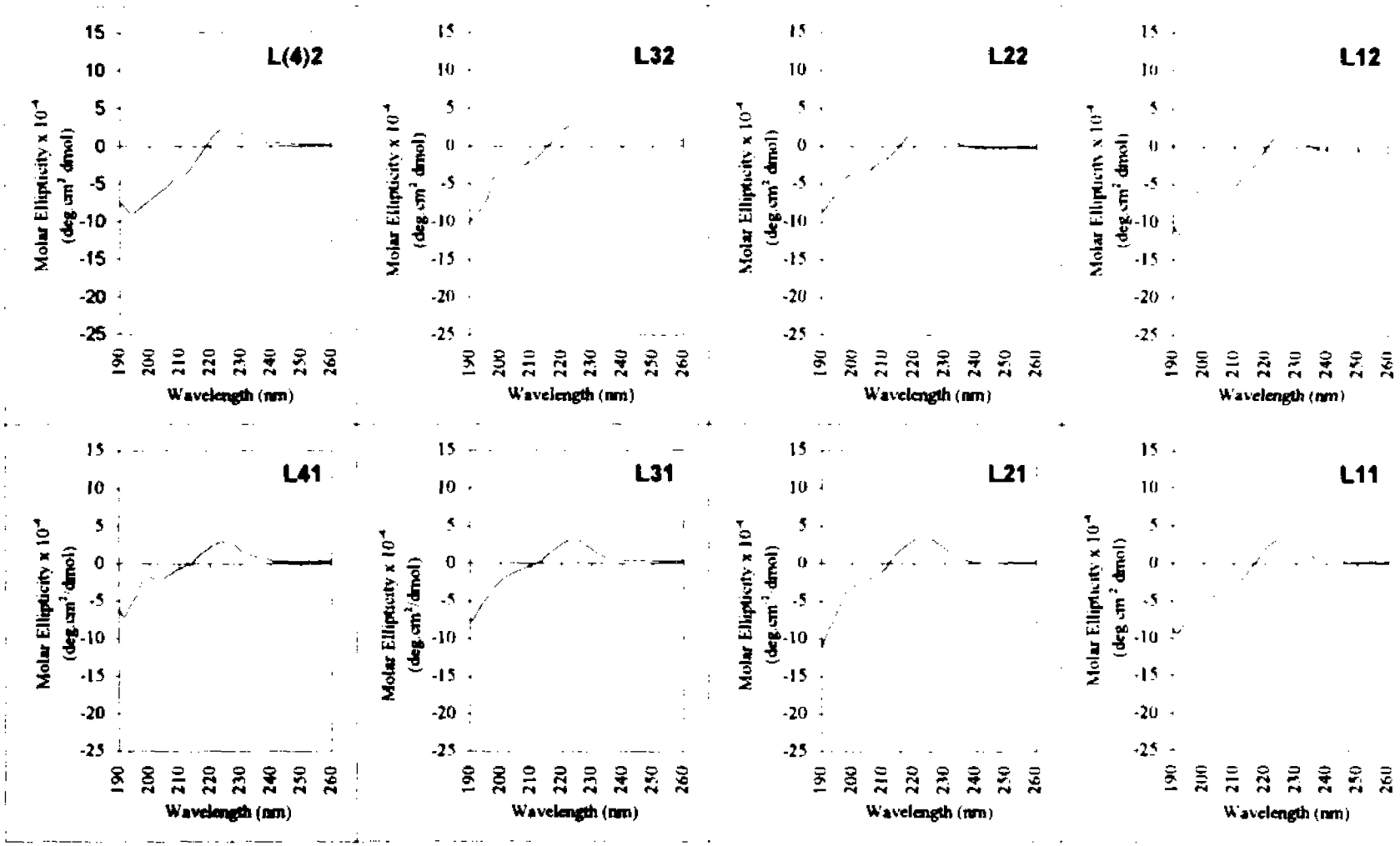
L(4)2
L32
L22
L12
L41
L31
L21
L11
Molar Ellipticity x 10⁻⁴ (deg.cm² dmol)
Wavelength (nm)
15
10
5
0
-5
-10
-15
-20
-25
190
200
210
220
230
240
250
260

contribution to the optical absorbance around 198 nm whereas their linear counterparts usually exhibited negative elipticity at this wavelength (compare Figure 34 and Figure 35).

In order to gain additional insights into the conformational preferences of the cyclic analogs we measured the CD spectra for the model compound Tetra **32** and for an equimolar mixture of **L32** and Tetra **32** in the same solvent. As stated before the model compound Tetra **32** mimics the cyclized central region of the cyclic α-factor analog **C32** and the linear analog **L32** differs from its cyclic homolog in the ionizable amine and carboxyl side chains at position 7 and 10. Like the CD spectrum in water (Figure 26), the general shape of the CD curve for Tetra **32** in water/methanol (1:1, v/v) (Figure 36, Left) is typical of those found for peptides in β-turn structures in that it was characterized by a negative nπ* band at ~225 nm and a maximum at about 200-210 nm (Woody, 1974). The CD pattern from the mixture of **L32** and Tetra **32** is qualitatively similar to that found for **C32** (Figure 36, Right). Furthermore, summation of the CD spectra from **L32** and Tetra **32** results in a curve (Figure 36, Right) which resembles the CD spectrum of **C32**. On the basis of these results it is reasonable to conclude that the central region of **C32** retains the turn structure found in Tetra **32**. This result suggests that the cyclization perturbs the conformation of the center of the pheromone and that the conformation of the cyclic lactam in the tridecapeptide is probably quite similar to that assumed by the corresponding model tetrapeptide.

FIGURE 36: CD spectra of the Orn-containing peptides in MeOH/H_2O (1:1, v/v); Tetra **32** (1.0 mg/mL), **L32** (1.0 mg/mL), **C32** (1.0 mg/mL) (Left); experimental (——) and computed (– – –) CD curves of equimolar mixtures of **L32** (2.0 mg) and Tetra **32** (0.44 mg) in 2 mL MeOH/H_2O (1:1, v/v) (Right)

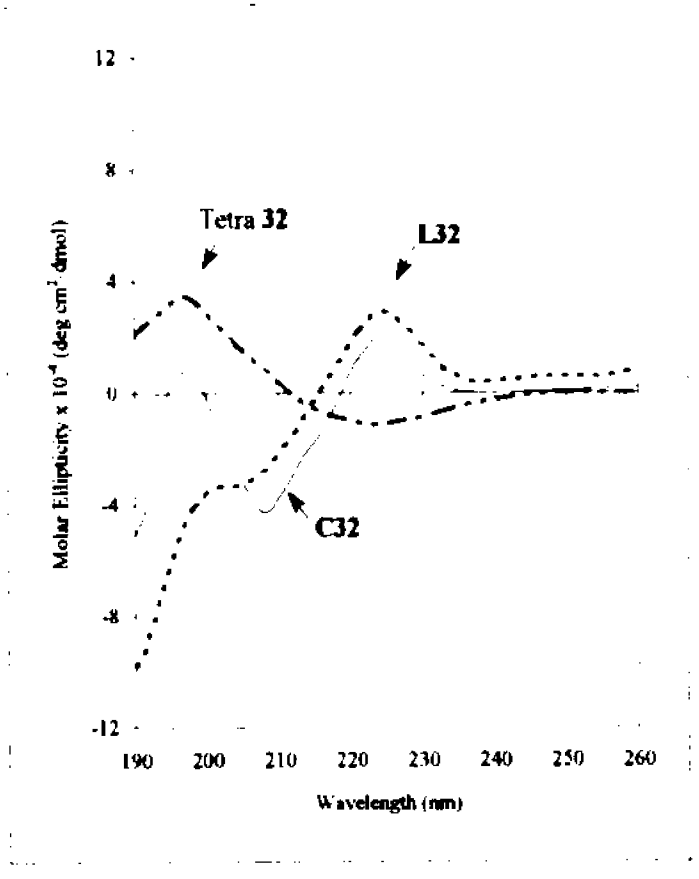
Tetra 32
L32
C32
Molar Ellipticity x 10⁻⁴ (deg cm² dmol)
Wavelength (nm)
12
8
4
0
-4
-8
-12
190
200
210
220
230
240
250
260

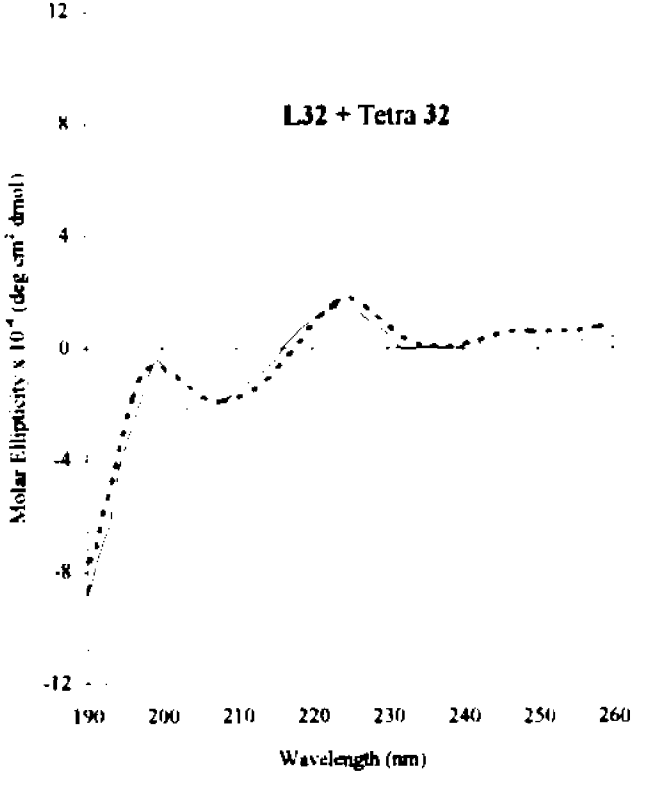
L32 + Tetra 32
Molar Ellipticity x 10⁻⁴ (deg cm² dmol)
Wavelength (nm)
12
8
4
0
-4
-8
-12
190
200
210
220
230
240
250
260

6.2. NMR Studies on Cyclic α-Factor Analogs: Resonance Assignment for Cyclo^{7,10}[Glu^{10}, Nle^{12}]α-Factor and Cyclo^{7,10}[Orn^{7}, Glu^{10}, Nle^{12}]α-Factor

The observed resonances of these analogs were assigned in the manner described previously (Section I Chapter 6). Individual amino acids were identified from their connectivity patterns in TOCSY spectra. For example, the Gly in position 9 was expected to exhibit only the αCH-NH connectivity in the TOCSY spectrum. In Figure 37 the connectivities for Nle in position 12 of **C42** is traced out. There were some difficulties in the assignments. For **C42**, the Lys^{7} NH had an identical chemical shift to the NH of Leu^{6} at 7.98 ppm and the Glu^{10} NH had an identical chemical shift to the NH of Tyr^{13} at 7.94 ppm. For **C32**, three NHs were found to have almost identical chemical shifts at about 7.9 ppm. In order to identify the type of the related residues in such a situation, we needed to rely on the side chain resonances which have characteristic chemical shifts, specifically Tyr βCHs should have chemical shifts around 3 ppm, Glu γCHs should have chemical shifts at about 2 ppm and Lys εCHs should have chemical shifts around 3 ppm. Tracing the connectivities of these resonances to other coupled resonances in the TOCSY spectrum we found that the NHs from Leu^{6}, Nle^{12} and Tyr^{13} of **C32** were overlapping near 7.9 ppm. The chemical shifts of these NHs were 7.91, 7.89 and 7.91 ppm, respectively.

The intraresidue NOE connectivities between the indole NH and the aromatic C_2H and C_7H were used to relate the indole NHs to the aromatic resonances. Based on the NOE connectivities between the βCH and the aromatic resonance C_4H, we were able to assign the side chain resonances within a given Trp residue. The side chain resonances for His in position 2 were assigned based on the NOE

FIGURE 37: TOCSY spectrum of cyclo^{7,10}[Glu^{10}, Nle^{12}]α-factor (**C42**) in DMSO (25 °C). The spin system of Nle in position 12 is shown (solid line)

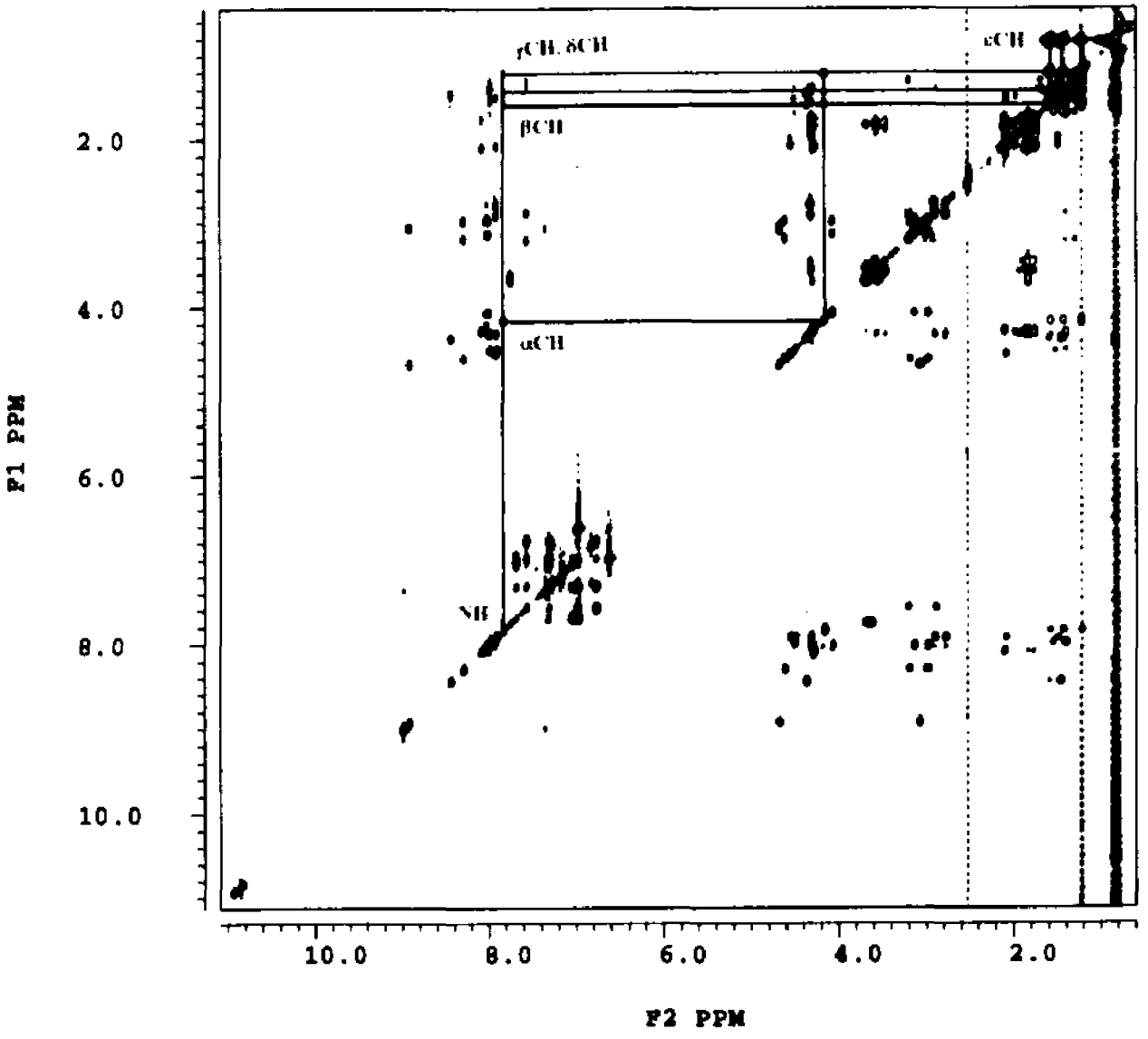
γCH, δCH
αCH
βCH
αCH
NH
2.0
4.0
6.0
8.0
10.0
F1 PPM
10.0
8.0
6.0
4.0
2.0
F2 PPM

Table 14
^{1}H Assignments for Cyclo^{7,10}[Glu^{10}, Nle^{12}]α-factor (**C42**) in DMSO (25 °C)

	αNH (ppm)	αCH (ppm)	βCH (ppm)	γCH (ppm)	δCH (ppm)	εCH (ppm)	εNH (ppm)	other (ppm)
Trp^1	8.00	4.08	3.15 2.99					N1 10.95 C2 7.15 C4 7.57 C5 6.78 C6 6.97 C7 7.31
His^2	8.93	4.69	3.08					C2 8.99 C4 7.36
Trp^3	8.31	4.62	3.22 3.00					N1 10.85 C2 7.18 C4 7.70 C5 6.99 C6 7.07 C7 7.33
Leu^4	8.45	4.38	1.47	1.59	0.84			
Gln^5	8.10	4.29	1.86 1.77	2.12				NH_2 6.83 7.28
Leu^6	7.98	4.32	1.40	1.56	0.80			
Lys^7	7.98	4.52	1.71 1.55	1.40	1.31	3.22 2.89	7.58	
Pro^8		4.30	2.00	1.85	3.69 3.56			
Gly^9	7.77	3.67						
Glu^{10}	7.94	4.55	1.52	2.09 1.98				
Pro^{11}		4.33	1.85	1.79	3.59 3.47			
Nle^{12}	7.84	4.18	1.59 1.45	1.22	1.22	0.84		
Tyr^{13}	7.94	4.31	2.91 2.78					C2,6 6.99 C3,5 6.63 OH 9.19

Table 15

^{1}H Assignments for Cyclo^{7,10}[Orn^7, Glu^{10}, Nle^{12}]α-factor (**C32**) in DMSO (25 °C)

	αNH (ppm)	αCH (ppm)	βCH (ppm)	γCH (ppm)	δCH (ppm)	εCH (ppm)	δNH (ppm)	other (ppm)
Trp^1	7.94	4.06	3.13 2.99					N1 10.92 C2 7.13 C4 7.55 C5 6.76 C6 6.98 C7 7.31
His^2	8.89	4.68	3.05					C2 8.95 C4 7.32
Trp^3	8.26	4.63	3.18 2.98					N1 10.82 C2 7.16 C4 7.67 C5 6.96 C6 7.04 C7 7.31
Leu^4	8.43	4.37	1.45	1.57	0.86 0.82			
Gln^5	8.05	4.28	1.87 1.76	2.10				NH_2 6.82 7.25
Leu^6	7.88	4.32	1.37	1.55	0.81 0.79			
Orn^7	8.23	4.41	1.76 1.50	1.32	2.96		7.04	
Pro^8		4.32	2.03	1.84	3.80 3.54			
Gly^9	7.96	3.73 3.60						
Glu^{10}	7.50	4.62	1.57 1.99	2.15				
Pro^{11}		4.34	1.96	1.81	3.51 3.49			
Nle^{12}	7.87	4.13	1.58 1.42	1.21	1.20	0.82		
Tyr^{13}	7.88	4.32	2.90 2.77					C2,6 6.96 C3,5 6.61 OH 9.19

connectivity between the βCH to the imidazole C_4H. The Gln γNH_2 were assigned based on their chemical shifts, their splitting pattern (two singlets) in 1D NMR spectra and the connectivity between these singlets in the TOCSY spectrum. The complete resonance assignments for **C42** and **C32** are given in Table 14 and Table 15, respectively. The assignments presented in this thesis support those made on **C42** by Tallon (1992) and those made on cyclo^{7,10}[Cys^7, X^9, Cys^{10}, Nle^{12}]α-factor analogs by Gounarides (1994).

6.3. Temperature Dependence and Qualitative NOE Studies

The temperature dependence of the amide proton chemical shifts (dδ/dT) were measured in DMSO-d_6 over the range 23-55 °C and are reported in Table 16. Again we found that in the Orn-containing peptide **C32**, the Glu^{10} NH has a very low temperature coefficient (-0.06 ppb/K). The lowest dδ/dT (-3.1 ppb/K) found in the Lys-containing peptide **C42** is for Gly^9 NH. These data indicate that the Glu^{10} NH is involved in a strong intramolecular hydrogen bond in **C32** and the Gly^9 NH in **C42** is participating in a weak but significant hydrogen bond.

In the 300 ms NOESY spectrum of **C32** in DMSO solution all of the expected sequential αCH_i-NH_{i+1} cross peaks are present. Strong intensities are observed for all sequential αCH_i-NH_{i+1} cross peaks except for the weak Gly$^9{}_{\alpha CH}$-Glu$^{10}{}_{NH}$ cross peak (Figure 38). Because the NH of Nle^{12} has almost the identical chemical shift to the NH of Tyr^{13}, the Nle$^{12}{}_{\alpha CH}$-Tyr$^{13}{}_{NH}$ cross peak would be weaker than it appears. Therefore this NOE cross peak is considered to be a medium one. Since the Nle$^{12}{}_{\alpha CH}$-Tyr$^{13}{}_{NH}$ residue pair is located at the terminus of the peptide, the weaker intensity is expected due to the shorter correlation time (Gounarides et al., 1993). Combined with the low dδ/dT value

(-0.06 ppb/K) for the Glu^{10} NH, the weak $Gly^{9}\alpha CH$-$Glu^{10}NH$ cross peak and the stronger $Pro^{8}\alpha CH$-$Gly^{9}NH$ cross peak suggest that residues 7-10 adopt a type II β-turn conformation. Compared with the intensity of the $Pro^{8}\alpha CH$-$Gly^{9}NH$ cross peak, the $Gly^{9}NH$-$Glu^{10}NH$ cross peak is weak (Figure 40). This distance should be 2.5 Å in an ideal type II β-turn. Therefore, it is likely that a distorted type II β-turn is present in the central region of **C32**.

Table 16
Amide Proton Temperature Coefficients (ppb/K) and $^{3}J_{\alpha NH}$ (Hz) Coupling Constants for **C42** and **C32** in DMSO

NH	**C32** dδ/dT(ppb/K)	$^{3}J_{\alpha NH}$ (Hz)	NH	**C42**[a] dδ/dT(ppb/K)	$^{3}J_{\alpha NH}$ (Hz)
His^{2}	-4.7	7.65 Hz	His^{2}	-7.2	7.75 Hz
Trp^{3}	-3.9	7.00 Hz	Trp^{3}	-6.1	6.95 Hz
Leu^{4}	-7.0	7.26 Hz	Leu^{4}	-11.4	7.85 Hz
Gln^{5}	-4.0	7.00 Hz	Gln^{5}	-6.5	7.95 Hz
Leu^{6}	---[b]	---[b]	Leu^{6}	-6.9	7.39 Hz
Orn^{7}	-6.7	5.68 Hz	Lys^{7}	-6.3	7.42 Hz
Gly^{9}	-5.9	---[c]	Gly^{9}	-3.1	3.93,5.13 Hz
Glu^{10}	-0.06	8.89 Hz	Glu^{10}	-6.3	5.91 Hz
Nle^{12}	---[b]	---[b]	Nle^{12}	-6.2	8.29 Hz
Tyr^{13}	---[b]	---[b]	Tyr^{13}	-9.6	7.71 Hz

[a]Data from Tallon (1992); [b]resonances were overlapping; [c]not resolvable.

FIGURE 38: The αCH-NH region of the 300 ms NOESY spectrum of cyclo^{7,10} [Orn^{7}, Glu^{10}, Nle^{12}]α-factor (**C32**) in DMSO (25 °C)

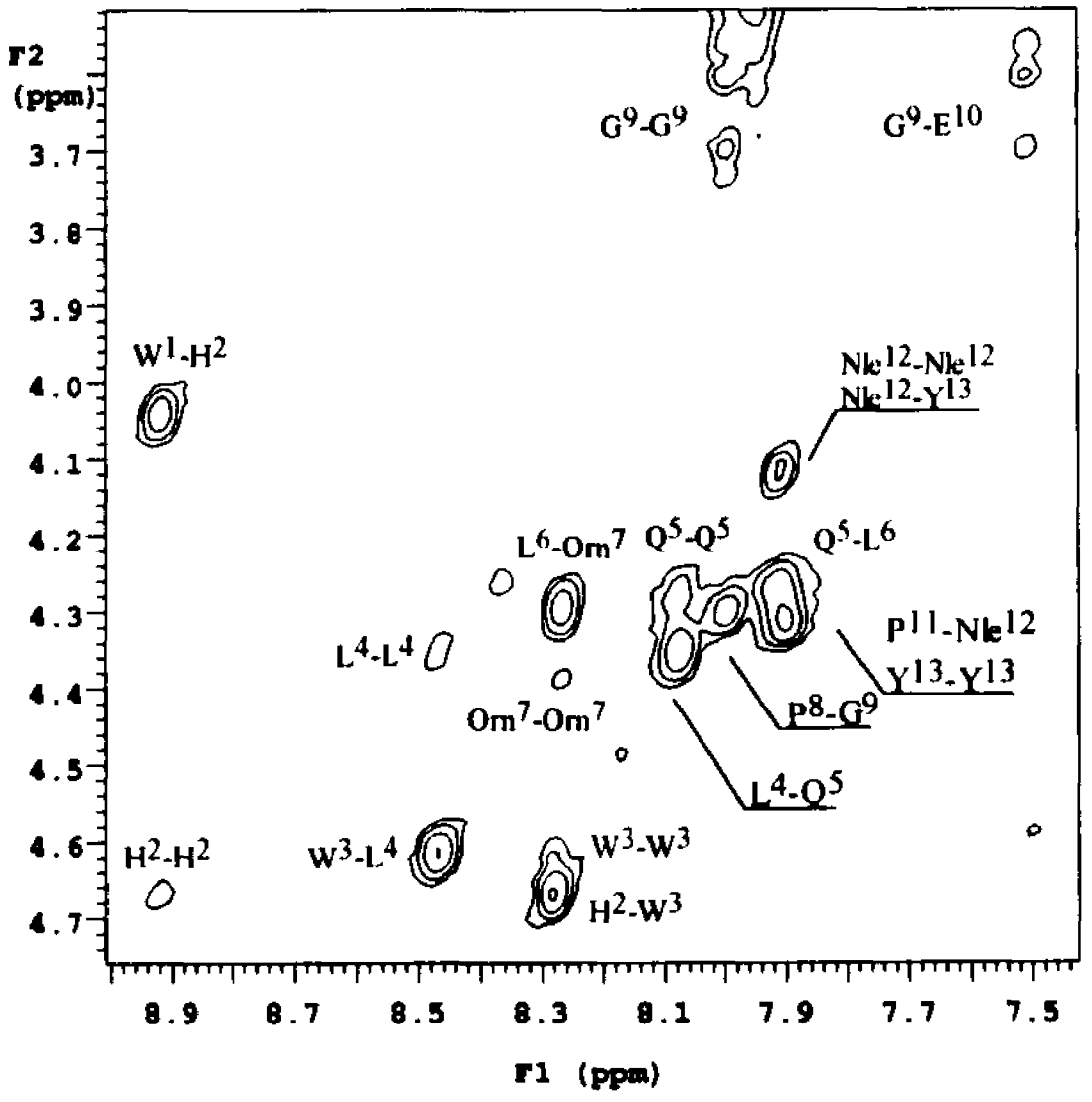
F2 (ppm)
3.7
3.8
3.9
4.0
4.1
4.2
4.3
4.4
4.5
4.6
4.7
8.9
8.7
8.5
8.3
8.1
7.9
7.7
7.5
F1 (ppm)
G9-G9
G9-E10
W1-H2
Nle12-Nle12
Nle12-Y13
L6-Om7
Q5-Q5
Q5-L6
L4-L4
P11-Nle12
Y13-Y13
Om7-Om7
P8-G9
L4-Q5
H2-H2
W3-L4
W3-W3
H2-W3

FIGURE 39: The αCH-NH region of the 400 ms NOESY spectrum of cyclo^{7,10} [Glu^{10}, Nle^{12}]α-factor (**C42**) in DMSO (25 °C)

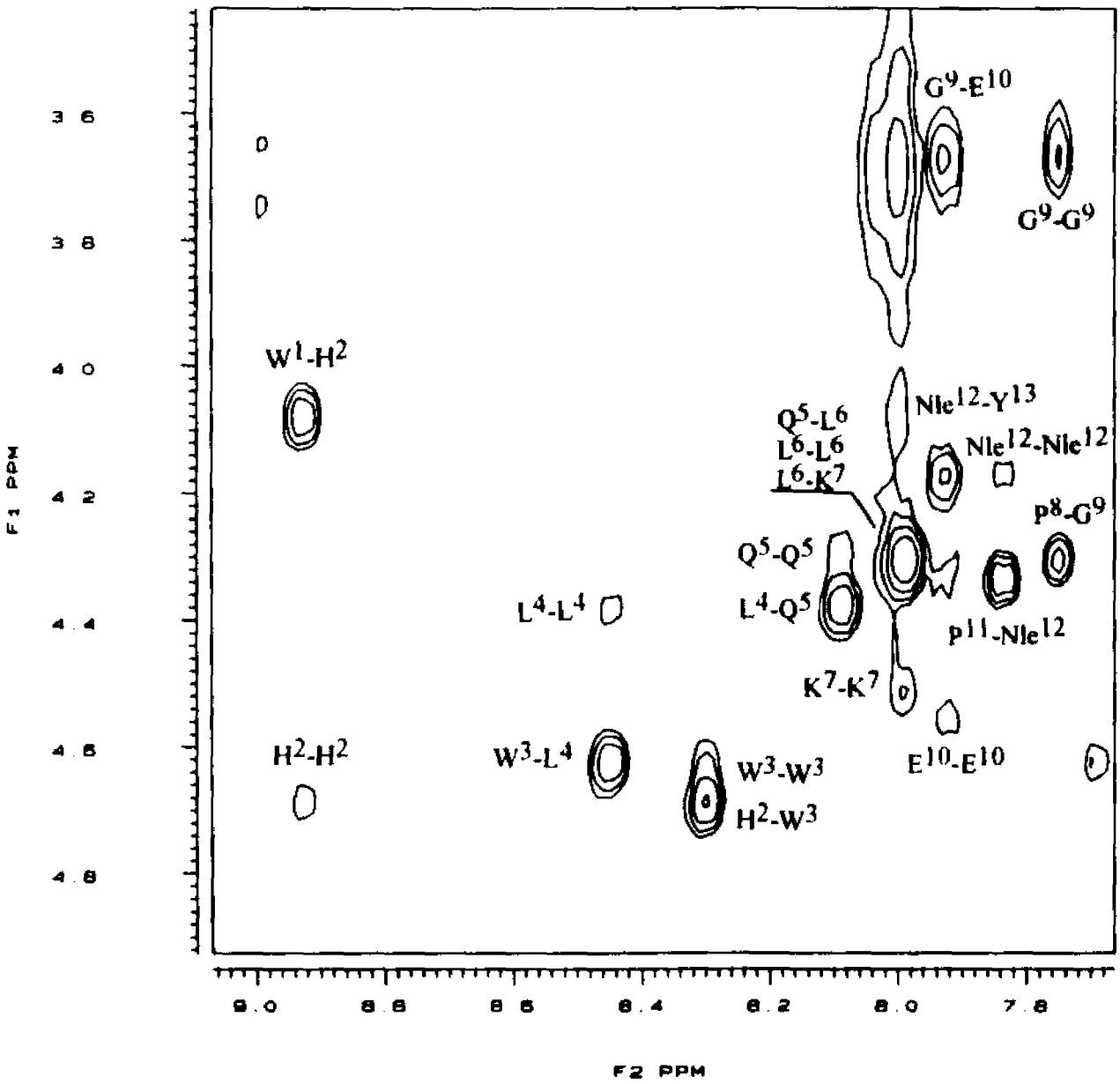
G9-E10
G9-G9
W1-H2
Nle12-Y13
Q5-L6
L6-L6
L6-K7
Nle12-Nle12
p8-G9
Q5-Q5
L4-L4
L4-Q5
p11-Nle12
K7-K7
H2-H2
W3-L4
W3-W3
H2-W3
E10-E10
3.6
3.8
4.0
4.2
4.4
4.6
4.8
F1 PPM
9.0
8.8
8.6
8.4
8.2
8.0
7.8
F2 PPM

FIGURE 40: The NH-NH region of the 300 ms NOESY spectrum of cyclo^{7,10} [Orn^{7}, Glu^{10}, Nle^{12}]α-factor (C32) in DMSO (25 °C)

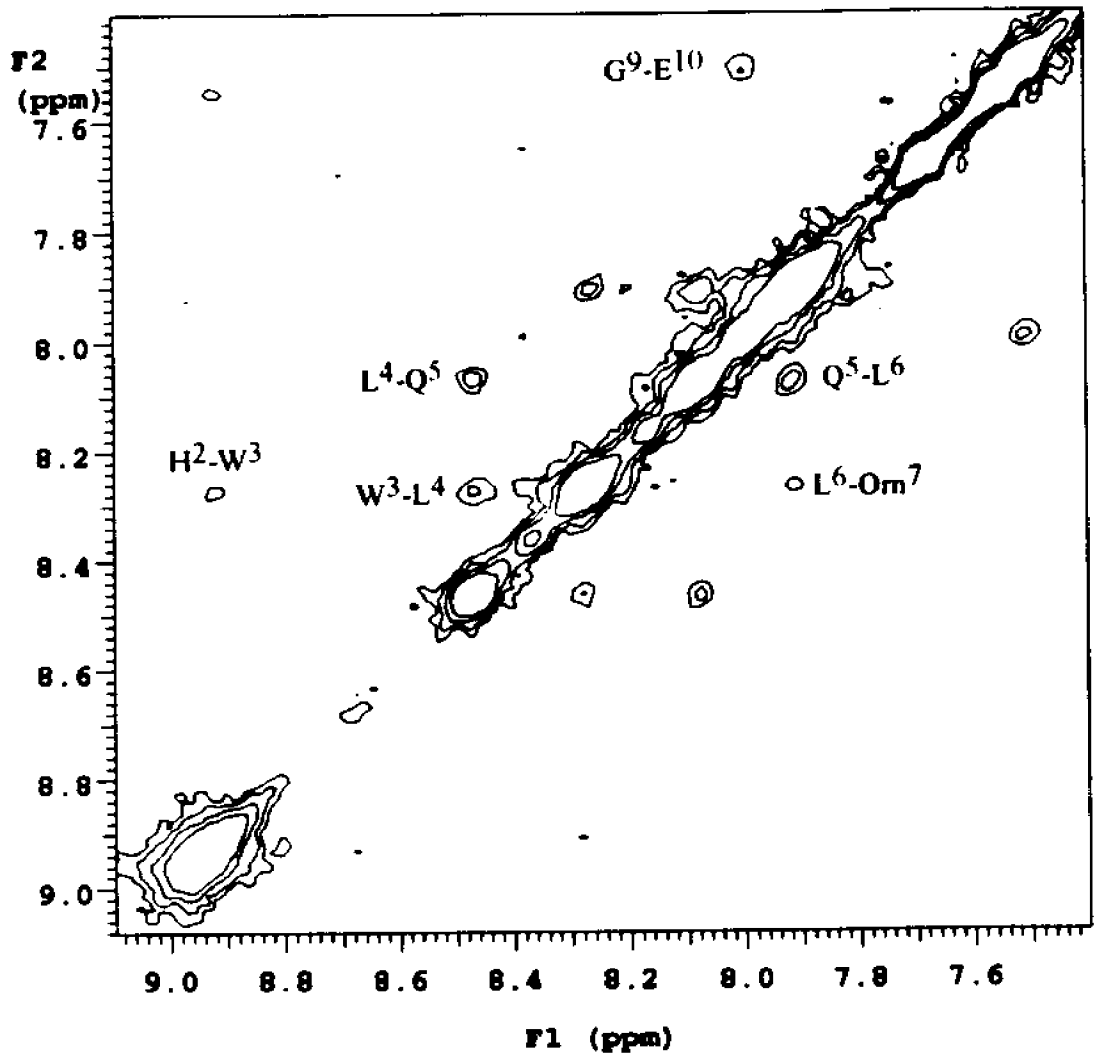
F2 (ppm)
7.6
7.8
8.0
8.2
8.4
8.6
8.8
9.0
G9-E10
L4-Q5
Q5-L6
H2-W3
W3-L4
L6-Orn7
9.0
8.8
8.6
8.4
8.2
8.0
7.8
7.6
F1 (ppm)

In the 400 ms NOESY spectrum of **C42** in DMSO all of the αCH_i-NH_{i+1} NOE connectivities were observed (Figure 39). Similar to **C32** a relatively weak cross peak is observed for the $Nle^{12}{}_{\alpha CH}$-$Tyr^{13}{}_{NH}$ residue pair which was attributed to the short correlation time of the teminal residues. The $Gly^{9}{}_{\alpha CH}$-$Glu^{10}{}_{NH}$ cross peak appears to be at medium intensity. The broadness of the peak indicates that this cross peak is likely the sum of two overlapping αCH_i-NH_{i+1} cross peaks from the Glu NH and the two closely spaced αCHs of Gly. If the overlapping cross peaks were resolved, the individual cross peaks would be weak. Given the intensity for the $Pro^{9}{}_{\alpha CH}$-$Gly^{10}{}_{NH}$ cross peak the results suggest the presence of a type II β-turn spanning through residue 7-10 in **C42**. The relatively low $^{3}J_{\alpha CH}$ coupling constants for Gly^{9} (3.93 Hz, 5.13 Hz) (Table 16) are consistent with a type II β-turn. However, the dδ/dT value (-6.3 ppb/K) for Glu^{10} NH is not supportive of this conclusion. Furthermore, the $Gly^{9}{}_{NH}$-$Glu^{10}{}_{NH}$ cross peak is absent (Figure 41), such a distance should be a short one (2.5 Å) in a type II β-turn (Stradley et al., 1990). Based on the above discussion and our conclusions on Tetra **42** it is not unreasonable that a γ-turn may be present as an additional conformation. The relatively low dδ/dT value of -3.1 ppb/K for the Gly^{9} NH is consistent with a γ-turn around Pro at position 8 in **C42** (Table 16).

For the terminal regions of both cyclic α-factor analogs, all the sequential αCH_i-NH_{i+1} connectivities observed in the NOESY spectrum have the same intensity as that of αCH_{Pro}-NH_{Gly} (Figure 38 and Figure 39). These αCH_i-NH_{i+1} cross peaks are significantly stronger than the sequential NH_i-NH_{i+1} cross peaks for the same compounds (compare Figure 38 with Figure 41 and Figure 39 with Figure 40). Furthermore, $^{3}J_{\alpha NH}$ coupling constants ranging from 7 Hz to 9 Hz are observed for the residues near the termini (Table 16). Based on above finding,

FIGURE 41: The NH-NH region of the 400 ms NOESY spectrum of cyclo^{7,10} [Glu^{10}, Nle^{12}]α-factor (**C42**) in DMSO (25 °C)

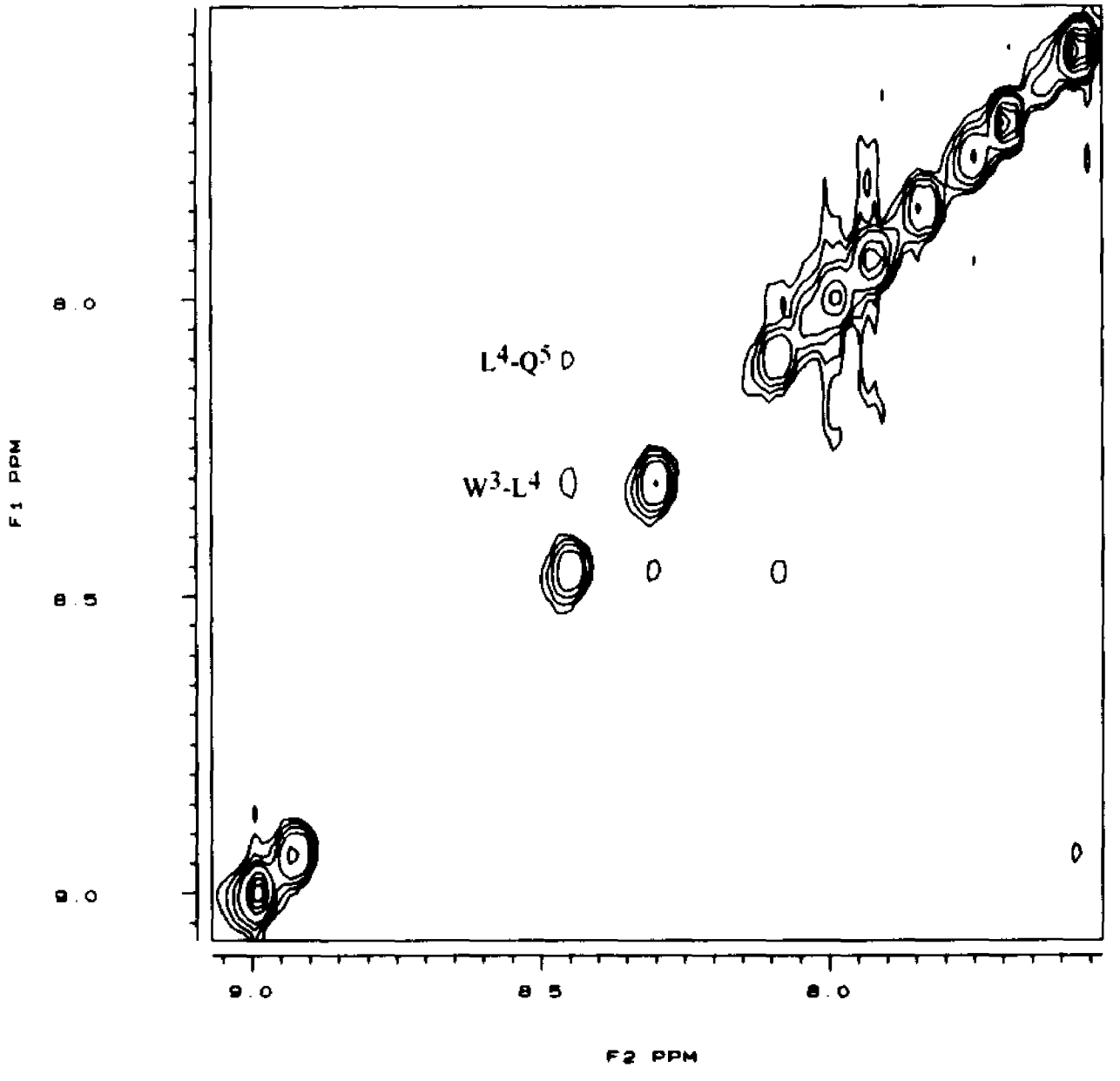
L4-Q5 D
W3-L4 O
O
O
O
9.0
8.5
8.0
F1 PPM
9.0
8.5
8.0
F2 PPM

it is possible that the termini of these cyclic analogs are present as extended peptide segments in DMSO solution (Wüthrich, 1986; Dyson et al., 1988). Since an alternating pattern of dδ/dT (one high one low etc.) is not observed for either peptide (Table 16), these extended segments are likely not part of a β-sheet conformation (Wüthrich, 1986).

6.4. Quantitative NOE Studies

In addition to the above qualitative analysis, the internuclear distances for NOE interactions involving residues 7-10 were estimated for two cyclic α-factor analogs, **C42** and **C32**, using the cross peak between the Glu αCH and NH as the reference. In order to reduce the possibility of spin-diffusion we compared the values obtained from NOESY spectra of **C42** at mixing times of 200 ms and 400 ms. The maximum deviation between the distances from the two spectra was 0.2 Å (data not shown), which indicated that spin diffusion at the longer mixing time did not affect the estimation of the internuclear distance significantly.

The measured internuclear distances from **C42** and **C32** are compared with those expected for the standard β-turns in Table 17. It appears unlikely that either peptide adopts a type I β-turn around the Pro-Gly sequence in DMSO solution. Particularly the distances of αCH_{Pro}-NH_{Gly} and δCH_{Pro}-NH_{Gly} were determined to be 2.3 Å and > 3.0 Å (no NOE observed) for **C42**; 2.0 Å and > 3.0 Å (no NOE observed) for **C32** respectively, whereas the expected distances for a type I β-turn are 3.5 Å and 2.7 Å.

Table 17
Measured Distances for **C42** and **C32** from NOESY Spectra and the Distances Expected for Standard β-Turns

	C42[a]	**C32**[b]	type I β-turn[d]	type II β-turn[d]
αCH_{Pro}-NH_{Gly}	2.3 Å	2.0 Å	3.5 Å	2.1 Å
αCH_{Gly}-NH_{Gly}	2.5 Å[c]	2.0 Å	2.9 Å	2.3 Å
αCH_{Gly}-NH_{Glu}	2.3 Å[c]	2.6 Å	3.3 Å	3.3 Å
NH_{Gly}-NH_{Glu}	NONE	2.9 Å	2.4 Å	2.5 Å
δCH_{Pro}-NH_{Gly}	NONE	NONE	2.7 Å	5.5 Å

[a]Distances were from the 200 ms NOESY spectrum using the distance between the αCH and NH of Glu (2.80 Å) as the reference distance. [b]Distances were from the 300 ms NOESY spectrum using the distance between the αCH and NH of Glu (2.80 Å) as the reference distance. [c]Calculation was based on half of the NOE intensity due to the assumption of overlapping Gly αCHs. [d]Distances are taken from Table V (Stradley et al., 1990)

The measured distances from **C32** are consistent with the distances expected for a type II β-turn except for that of αCH_{Gly}-NH_{Glu} which is shorter than expected (Table 17). Two significant deviations are observed between the measured distances and those expected for a type II β-turn around the Pro-Gly sequence for **C42**. Specifically the NOE between Gly NH and Glu NH was not observed in the NOESY spectrum of **C42** and the distance between the Gly αCH and Glu NH was determined to be 2.3 Å. Neither of above distances are consistent with those expected for a type II β-turn (Table 17). Similar to the observation for the corresponding model compound, **Tetra 42**, a fairly good agreement is found between the measured distances for **C42** and those expected for a γ-turn (Table

12). For example, no NOE is observed between the Pro δCH and Gly NH. This cross peak is analogous to the NH_{i+1}-NH_{i+2} connectivity (Wüthrich, 1986; Dyson et al., 1988; Stradley et al., 1990; Gounariders, 1994) which was not observed in the pentapeptides that were found to adopt a γ-turn (Stroup et al., 1992). The distances of αCH_{Lys}-δCH_{Pro}, αCH_{Pro}-NH_{Gly} and αCH_{Gly}-NH_{Gly} were determined to be 2.2 Å, 2.3 Å and 2.5 Å, whereas those expected for a γ-turn around Pro are 2.1 Å, 2.5 Å and 2.5 Å, respectively (Table 12). Therefore, based on the quantitative NOE analysis we conclude that in DMSO the region from residue 7 to residue 10 of **C32** adopts to a type II β-turn with some distortion and the same region in **C42** has a conformation which does not fit either a type I or a type II β-turn. Comparison of the distances from **C42** and those reported for a γ-turn (Stroup et al., 1992) suggest that a γ-turn around Pro^8 is a possible conformational feature for **C42** which perhaps coexists with a type II β-turn in this tridecapeptide.

6.5. Comparisons of the Cyclic α-Factor Analogs and the Tetrapeptides

In Section 5.4 (Chapter 6) we constructed CPK models for both Tetra **32** and Tetra **42** based on the observed NOE cross peaks and the measured amide proton temperature coefficients. The same NOE connectivities found in Tetra **32** and Tetra **42** were also found in **C32** and **C42** respectively. These NOE constraints were also estimated using the separation between the αCH and NH of Glu (2.80 Å) as a reference distance and are reported in Table 18. The distances measured from the NOESY spectrum of **C42** are very close to those from the ROESY spectrum of Tetra **42** (compare Table 13 and Table 18). Qualitative agreement is found between the distances from **C32** (Table 18) and those from Tetra **32** (Table 13). The NOE distances involving the δNH_{Orn} are found to be inconsistent

between the Orn-containing tetrapeptide Tetra **32** and the Orn-containing tridecapeptides **C32**. Specifically the distances of the δNH_{Orn}-γCH_{Glu} and the δNH_{Orn}-βCH_{Glu} for **C32** were determined to be 2.3 Å and 2.2 Å/2.6 Å, whereas for Tetra **32** the first distance was too long to be observed and the second was 2.9 Å/3.8 Å based on the NOE measurement. Because δNH of Orn has the same chemical shift as the C_6H of Trp^3, it is also possible that the cross peaks are involved with the Trp^3 C_6H instead of Orn δNH. Nevertheless, the above data suggest that conformations in the region Xxx-Pro-Gly-Glu of **C42** and **C32** are similar to that of Tetra **42** and Tetra **32**, respectively. Therefore the observations from the CPK models of Tetra **42** and Tetra **32**, are valid for the corresponding regions of **C42** and **C32**.

Table 18
Internuclear Distances Used for Constructing the CPK Models of C42 and C32

C42		C32	
αCH_{Lys}-δCH_{Pro} (4.52 ppm-3.69 ppm)	2.2 Å[a]	αCH_{Orn}-δCH_{Pro} (4.39 ppm-3.80 ppm)	2.1 Å[b]
(4.52 ppm-3.56 ppm)	2.3 Å	(4.39 ppm-3.54 ppm)	2.2 Å
αCH_{Pro}-NH_{Gly}	2.3 Å	αCH_{Pro}-NH_{Gly}	2.0 Å
NH_{Gly}-NH_{Glu}	NONE	NH_{Gly}-NH_{Glu}	2.9 Å
βCH_{Glu}-NH_{Glu} (1.52 ppm-7.94 ppm)	2.5 Å	βCH_{Glu}-NH_{Glu} (1.99 ppm-7.50 ppm)	2.7 Å
		(1.57 ppm-7.50 ppm)	2.6 Å
βCH_{Glu}-αCH_{Glu}	NONE	βCH_{Glu}-αCH_{Glu} (1.99 ppm-4.60 ppm)	2.2 Å
		(1.57 ppm-4.60 ppm)	2.7 Å
γCH_{Glu}-αCH_{Glu} (2.09 ppm-4.55 ppm)	2.5 Å	γCH_{Glu}-αCH_{Glu} (2.15 ppm-4.60 ppm)	2.8 Å
(1.98 ppm-4.55 ppm)	2.7 Å		
εNH_{Lys}-γCH_{Glu} (7.58 ppm-2.09 ppm)	2.0 Å	δNH_{Orn}-γCH_{Glu}	2.3 Å[c]
εNH_{Lys}-βCH_{Glu}	NONE	δNH_{Orn}-βCH_{Glu} (7.04 ppm-1.99 ppm)	2.2 Å[c]
		(7.04 ppm-1.57 ppm)	2.6 Å[c]
		δCH_{Pro}-γCH_{Orn} (3.54 ppm-1.32 ppm)	3.5 Å

[a]Distances were from the NOESY spectrum (200 ms) using the separation between the αCH and NH of Glu (2.80 Å) as a standard. [b]Distances were from the NOESY spectrum (300 ms) using the separation between the αCH and NH of Glu (2.80 Å) as a standard. [c]This cross peak was not unambiguously assigned because the Orn δNH was overlapped with C_6H of Trp^3.

CHAPTER 7

Discussion and Conclusions

Previous studies on a constrained congener of α-factor concluded that the pheromone was likely in a bent structure when bound to its receptor (Xue et al., 1989). Complementary biophysical analysis on linear and disulfide constrained analogs suggested that the middle of the α-factor assumes a β-turn (Jelicks et al., 1988; Naider et al., 1992; Gounarides et al., 1994). Preliminary NMR studies of the conformation of cyclo^{7,10}[Glu^{10}, Nle^{12}]α-factor (**C42**) suggested a mixture of type I and type II β-turn in this peptide (Tallon, 1992). In an extension of these studies, we synthesized a series of cyclic α-factor analogs which had lactam rings containing 18 to 14 atoms in the central region of the molecule. Biological activities of the analogs were examined by growth arrest assay (Halo assay) using strain RC629 [*sst1*] of *S. cerevisiae*. Receptor affinity of these peptides was assayed by following their competition with tritiated [Nle^{12}]α-factor. The conformations of all the synthetic peptides were assessed by circular dichroism. Conformations of two cyclic α-factor analogs, cyclo^{7,10}[Glu^{10}, Nle^{12}]α-factor (**C42**) and cyclo^{7,10}[Orn^{7}, Glu^{10}, Nle^{12}]α-factor (**C32**) were analyzed using NMR techniques and by comparison with two corresponding synthetic model compounds, Ac-cyclo[Lys-Pro-Gly-Glu]-NH_2 (**Tetra 42**) and Ac-cyclo[Orn-Pro-Gly-Glu]-NH_2 (**Tetra 32**). The structural information determined on the cyclic analogs was related to their biological activities.

During the synthesis of the peptides each synthetic step was carefully controlled for the highest possible yields and the purest possible products. For example the amino acid derivatives that were incorporated in position 7 and 10 were purified

to high homogeneity (over 99% as judged by HPLC) and were characterized by 1D NMR before use in peptide synthesis. To assure completion of the chain assembly reaction each coupling step during the solid phase peptide synthesis was examined by the Kaiser test and in all cases an additional coupling was carried out after a negative Kaiser test. As a result all crude α-factor analogs contained one major product (Figure 4-19). However the yield for the purified material is not high (no more than 20% for the cyclic α-factor analogs). Based on the fact that all peptides were made starting from the same batch of aminomethyl resin and that the yields were consistently low, we believe that the major reason for the low yield may be that the amine content (0.759 mmol/g) on the resin was lower than that stated by the manufacturer. Furthermore, in order to obtain highly homogeneous material we may have lost a certain amount of the desired product during the purification process.

It was also noticed that amide bond formation between the side chains of residues 7 and 10 became difficult when the lactam ring size decreased. For example for **C32** the cyclization required only about 12 h. But the cyclization for **C21** and **C11** required about 28 h in total and resulted in a crude product with one noticeable byproduct. Because such byproduct was not observed in the crude linear homologs we believe that the byproduct resulted from intermolecular amide bond formation (compare Figure 16 with Figure 17; and Figure 18 with Figure 19). A significant byproduct was observed in the crude tetrapeptide during the syntheses of the model compounds (Figure 21). We have isolated the byproduct from crude Tetra **42** and proved this major impurity to be the cyclic dimer resulting from interchain amide bond formation. It is worth noting that a similar phenomenon was observed in the syntheses of other corresponding model cyclic tetrapeptides in a parallel investigation (Rao et al., 1995) and in the syntheses of

cyclic analogs of enkephalin (Schiller et al., 1985). It appears that inclusion of a Xxx-Pro-Gly-Glu sequence in the center of a larger peptide (such as C42) impedes interchain reactions. This may be a consequence of a general steric effect which prevents interchain contacts or due to the fact that cyclization is favored when the Xxx-Pro-Gly-Glu sequence is present in the center of the tridecapeptide. All the peptides synthesized were purified to near homogeneity using preparative reversed-phase chromatography. The results from amino acid analysis and FABMS spectra proved that the peptides had the expected amino acid ratios and monoisotopic masses within 0.7 amu of the calculated values (Table 1 and Table 2).

Earlier investigations on the α-factor have provided important insights into residues which influence the activity of the peptide (Masui et al., 1979; Naider et al., 1986). The growth arrest analysis provided new knowledge concerning molecular groupings that influence the activity of the pheromone. Specifically, the γ-carbonyl of residue 10 was found to be a critical determinant of the potency of the pheromone. Thus, all compounds with Glu at this position were more active than those with Asp. This was true regardless of whether the pheromones were cyclic or linear. Comparison of corresponding linear and cyclic analogs showed that the linear peptides were always the most potent, which indicated that covalent linkage of the side chains of residue 7 and 10 further reduced the activity of the pheromone. The fact that the ε-amine in position 7 of the native α-factor is not essential for activity has been noted previously (Samokhin et al., 1979; Shenbagamurthi et al., 1983). An ionizable carboxylic group is not required since Gln occupies position 10 in the natural sequence of α-factor. Therefore, the observed difference in bioactivity between the cyclic analog and the corresponding linear homologs is probably the consequence of a

conformational change induced by the side chain cyclization. Similarly, the effect of the γ-carbonyl of residue 10 and the covalent constraint between the side chains of residures 7 and 10 was also observed in the binding affinity study. Interestingly, we noticed that in the Glu series the linear analogs had almost identical activities whereas the cyclic analogs exhibited virtually no change in activity except for **C32** which had very low activity. We then speculated that **C32** might possess very different structural features from the other analogs in this series.

Previous CD studies on α-factor concluded that this linear peptide is predominantly unstructured in aqueous buffer solution and becomes more ordered in organic solvents or the presence of lipid (Higashijima et al., 1983; Shenbagamurthi et al., 1985). The observed CD pattern for linear analogs in water/methanol (1:1, v/v) revealed a predominantly disordered molecule (Figure 35). The change in CD spectra from linear to cyclic α-factor analogs indicated that the covalent linkage between the side chains of residues 7 and 10 had a significant impact on the molecular conformation. In most cases the major differences observed in the spectral features of the linear and cyclic analogs were the maxima below 200 nm and the minima from ~200 to 225 nm. CD curves with such extrema would be associated with a β-turn structure (Woody, 1974). Combined with the fact that a β-turn like CD curve was observed in the model compounds, the results implied that in cyclic analogs the central region adopts a β-turn structure and the two terminal regions remain disordered structures in the solution. This hypothesis was supported by the result from the "CD additivity" experiment (Perczel et al., 1993). In such an experiment, the CD spectrum obtained from the equimolar mixture of **L32** and **Tetra 32** was almost identical to the CD curve obtained from the algebraic summation of the individually recorded

CD spectra of the above two molecules and was qualitatively similar to the CD spectrum of **C32**.

Cyclo^{7,10}[Orn^{7}, Glu^{10}, Nle^{12}]α-factor (**C32**) was found to adopt a type II β-turn spanning residues 7-10. In DMSO solution **C32** exhibited strong Pro^{8}αCH-Gly^{9}NH and weak Gly^{9}αCH-Glu^{10}NH NOE cross peaks. The Gly^{9}NH-Glu^{10}NH NOE cross peak and low amide temperature coefficient for Glu^{10} NH (-0.06 ppb/K) were consistent with a β-turn conformation in this lactam region of the peptide. This conclusion was in agreement with the result from conformational analysis on the corresponding model compound, Tetra **32**, which was found to assume a type II β-turn conformation in the same solvent.

Populations of γ-turn and type II β-turn were consistent with the NMR data on Cyclo^{7,10}[Glu^{10}, Nle^{12}]α-factor (**C42**). The type II β-turn conformation was evidenced by the strong Pro^{8}αCH-Gly^{9}NH and a weaker Gly^{9}αCH-Glu^{10}NH NOE cross peak. Absence of a Pro^{8}δCH-Gly^{9}NH NOE cross peak and low amide temperature coefficient for Gly^{9} NH (-3.1 ppb/K) were indicators for a γ-turn conformation around Pro^{8}. Evidence for the presence of more than one conformation was also revealed by the results from the conformational analysis on the corresponding model compound, Tetra **42**. We did not find any evidence for the presence of type I β-turn in **C42** as suggested by Tallon (1992). After carefully examining the NOESY spectra (200 ms and 400 ms) of **C42** we believe that the Gly^{9}αCH-Gly^{9}NH cross peak was misinterpreted as Pro^{8}δCH-Gly^{9}NH which was used as the evidence for type I β-turn. Several long-range NOE connectivities revealed by M. Tallon were either not observed in our investigations or found to be misinterpreted. For example, Glu^{10}αCH-Lys^{7}βCH and Leu^{6}αCH-Trp^{1}C7H (Trp^{3}C7H) were not observed; the Gly^{9}αCH-Glu^{10}NH

and the $Nle^{12}\alpha CH$-$Tyr^{13}NH$ were misinterpreted as the $Pro^{8}\delta CH$-$Glu^{10}NH$ and $Nle^{12}\alpha CH$-$Glu^{10}NH$ respectively. The long range NOE connectivity between Tyr^{13} OH and the NH of Lys^{7} or Leu^{6} was confirmed.

Based on the NOE constraints and the hydrogen bonding requirements, CPK models were built for Tetra **32** and Tetra **42**. These models were found to be appropriate for the corresponding Xxx-Pro-Gly-Glu regions in **C32** and **C42** because the same NOE connectivities found in tetrapeptides, Tetra **42** and Tetra **32**, were also observed in the cyclic α-factor analogs, **C42** and **C32**, respectively. The conformational consistency between the tetrapeptide and tridecapeptide was supported by the fact that the lowest dδ/dT value in Orn-containing peptides (**C32** and Tetra **32**) was found for the Glu NH and the lowest dδ/dT value in Lys-containing peptides (**C42** and Tetra **42**) was found for the Gly NH. Three significant differences in the structural features of the models were revealed: the spatial orientations of the Glu γ-carbonyl, the spatial orientations of the pyrrolidine ring of Pro, and the hydrophobicity on the outside surface of the central turn region. Since a reverse turn (a β-turn and/or a γ-turn) was observed in these peptides, such a hydrophobic surface area would face a direction opposite from that of the two terminal peptide chains. Among these the observation of different spatial orientations of the Glu γ-carbonyl group appears to be the most significant in correlation with our biological activity analysis on the cyclic and linear α-factor analogs. Specifically, from the biological activity studies we found the Glu γ-carbonyl group to be important for the α-factor activity. Compared with other analogs in the series of Glu-containing peptides, the very low activity of **C32** may reflect the fact that cyclization in this analog might force the γ-carbonyl group of residue 10 into a undesirable direction, which leads to the decrease of biological activity. Compared with **C32**, the

corresponding linear homolog, **L32**, exhibited significant increase in activity (about 100-fold improvement; one-half the activity of [Nle^{12}]α-factor). This observation might be explained by the relatively higher molecular flexibility of **L32** which allows the Glu γ-carbonyl group to be adjusted to a more desirable position.

In summary we conclude that: (I) the γ-carbonyl in residue 10 is a critical determinant for the potency of the pheromone based on the result of the biological activity study; (II) based on the amide proton temperature dependencies, NOE connectivities, quantitative NOE analysis and the comparative conformational analysis of the tetrapeptides, the active cyclic α-factor analog **C42** was found to contain mixture of a type II β-turn from residue 7 to 10 and a γ-turn around residue 8, whereas the less active cyclic α-factor analog **C32** was found to adopt a type II β-turn spanning residues 7-10; (III) CPK model building for the model compounds and the corresponding regions in cyclic α-factor analogs further revealed that the specific orientation of the Glu^{10} γ-carbonyl group may play an important role for the activity. The finding of a γ-turn as an additional conformation in the active α-factor analog clearly indicates that a type II β-turn may not be the only feature important for α-factor activity.

Future Experiments

In this investigation, none of the spectral features found for the central region of **C42** or **C32** fit any standard secondary structure perfectly. Since there was no evidence indicative of conformational averaging, we concluded, based on our present experimental data, that these peptides adopt conformations which are distorted from those of standard structures. In order to eliminate the possibility of

conformational averaging, the structures of these peptides should be examined at different temperatures and/or in different solvent systems. Use of a cryoprotective mixture, such as DMSO/water (80/20) or MeOH/water (80/20), should be a good choice for this purpose. Cryoprotective solvents not only have different solvent viscosities but also have a much lower freezing point than DMSO. For example, a mixture of DMSO/water (80/20) has a freezing point of -38 °C and a mixture of MeOH/water (80/20) has a freezing point of -100 °C (Douzou and Petsko, 1984). If the spectral features revealed in this thesis were found in studies in different solvents at various temperatures, then the conformations would be better defined. Presumably, such conformations are very useful in searching for the biologically active conformation of the peptide pheromone.

Secondly, comparison of bioactivities of the linear and cyclic α-factor analogs indicates that the conformational change induced by side chain cyclization is too drastic. The requirement for more flexibility in the central region is suggested by the decrease of the IC_{50} value with the increase of the lactam ring size among the Glu-containing cyclic analogs (Table 3). Therefore, more active cyclic analogs could be ones with a larger lactam ring size. For example, lactam analogs with 19-member or 20-member rings can be made by replacing Lys^7 with 2,7-diamino-heplanoic acid or 2,8-diamino-octanoic acid, respectively. However, it is possible that these large rings might disturb the conformations of the termini.

Thirdly, since the γ-carbonyl of residue 10 has been found to be an important determinant for the biological activity, we should further examine the topographical requirement of this group. For example, a methyl group can be added in place of the pro(*R*) or pro(*S*)-βCH of Gln^{10}, or in place of the pro(*R*) or

pro(*S*)-γCH of Gln^{10}. By introducing the methyl group in such places, the torsion angles of the side chain of residue 10 could be limited, therefore, the spatial orientation of the γ-carbonyl group of this residue could be assessed further.

REFERENCES

Anderegg, R. J., Betz, R., Carr, S. A., Crabb, J. W., Duntze, W. (1988) J. Biol. Chem., **263**, 18236-18240.

Aubry, A., Cung, M. T., Marraud, M. (1985) J. Am. Chem. Soc., **107**, 7640-7647.

Bach, A. C., II, Gierasch, L. M. (1986) Biopolymers, **25**, S175-S191.

Baffi, R., Shenbagamurthi, P., Terrance, K., Becker, J. M., Naider, F., Lipke, P. (1984) J. Bacteriol., **158**, 1152 - 1156.

Baffi, R. A., Becker, J. M., Lipke, P. N., Naider, F. (1985) Biochemistry, **24**, 3332-3337.

Ballardin, A., Fischman, A. J., Gibbons, W. A., Roy, J., Schwartz, I. L., Smith, C. W., Walter, R., Wyssbrod, H. R. (1978) Biochemistry, **17**, 4443-4454.

Barlow, A., Gounarides, J. S., Diem, M., Xue, X. B., Naider, F. (unpublished results, personal communication)

Bax, A., Davis, D. G. (1985) J. Magn. Reson., **63**, 207-213.

Bax, A., Freeman, R. (1981) J. Magn. Reson., **44**, 542-561.

Betz, R., Manney, T. R., Duntz, W. (1981) Gamete Research, **4**, 571-584.

Blumer, K. J., Reneke, J. E., Thorner, J. (1988) J. Biol. Chem., **263**, 10836-10842.

Blumer, K. J., Thorner, J. (1990) Proc. Natl. Acad. Sci. USA, **87**, 4363-4367.

Bodanszky, M., Bodanszky, A. (1984) in *The Practice of Peptide Synthesis*, pp. 24-25, Springer-Verlag, Berlin Heidelberg, New York.

Bodenhausen, G., Dobson, C. M. (1981) J. Magn. Reson., **44**, 212-216.

Bolin, D. R., Wang, C.-T., Felix, A. M. (1989) Org. Prep. Proc. Int., **21**, 67-74.

Borgias, B. A., James, T. L. (1988) J. Magn. Reson., **79**, 493-512.

Brahms, S., Brahms, J. (1980) J. Mol. Biol., **138**, 149-178.

Bruch, M. D., Noggle, J. H., Gierasch, L. M. (1985) J. Am. Chem. Soc., **107**, 1400-1407.

Burkholder, A. C., Hartwell, L. H. (1985) Nucleic Acids Res., **13**, 8463-8475.

Bussey, H. (1988) Yeast, **4**, 17-26.

Cartwright, C. P., Tipper, D. J. (1991) Mol. Cell. Biol., **11**, 2620-2628.
Chan, R. K., Otte, C. A. (1982) Mol. Cell. Biol., **2**, 11-20.

Chandrasekaran, R., Lakshminarayanan, A. V., Pandya, U. V., Ramachandran, G. N. (1973) Biochim. Biophys. Acta, **303**, 14-27.

Chou, P. Y., Fasman, G. D. (1977) J. Mol. Biol., **115**, 135-175.

Ciejek, E., Thorner, J., Geier, M. (1977) Biochem. Biophys. Res. Commun., **78**, 952-961.

Ciejek, E., Thorner, J. (1979) Cell, **18**, 623-635.

Clark, C. D., Palzkill, T., Botstein, D. (1994) J. Biol. Chem, **269**, 8831-8841.

Clark, K. L., Davis, N. G., Wiest, D. K., Hwang-Shum, J. J., Sprague, G. F., Jr. (1988) Cold Spring Harbor Symp. Quant. Biol., **53**, 611-620.

Clore, G. M., Appela, E., Yamada, M., Matsushima, K., Groeneborn, A. M. (1990) Biochemistry, **29**, 1689-1700.

Compton, L. A., Johnson, W. C., Jr., Modrich, P. (1986) Anal. Biochem., **155**, 155-167.

Crisma, M., Fasman, G. D., Balaram, H., Balaram, P. (1984) Int. J. Peptide Protein Res., **23**, 411-419.

Crawford, J. L., Lipscomb, W. N., Schellman, C. G. (1973) Proc. Natl. Acad. Sci. U. S. A., **70**, 538-542.

Deber, C. M., Madison, V., Blout, E. R. (1976) Acc. Chem Res., **9**, 106-113.

Dmochowska, A., Dignard, D., Henning, D., Thomas, D. Y., Bussey, H. (1987) Cell, **50**, 573-584.

Dohlman, H. G., Thorner, J., Caron, M. G., Lefkowitz, R. J. (1991) Annu. Rev. Biochem., **60**, 653-688.

Douzou, P., Petsko, G. A. (1984) in *Adv. in Protein Chemistry* (Anfinsen, C. B. and Edsall, J. T., Ed.), Academic Press, San Diego, **36**, 245-361.

Duntze, W., Mackay, V., Manney, T. B. (1970) Science, **168**, 1472-1473.

Dyson, H. J., Rance, M., Houghten, R. A., Lerner, R. A., Wright, P. E. (1988) J. Mol. Biol., **201**, 161-200.

Eriotou-Bargiota, E., Xue, C.-B., Naider, F., Becker, J. M. (1992) Biochemistry, **31**, 551-557.

Fejzo, J., Zolnai, Z., Macura, S., Markley, J. L. (1990) J. Magn. Reson., **88**, 93-110.
Friebolin, H. (1991) *Basic One- and Two- Dimensional NMR Spectroscopy*, VCH Publishers, New York.

García-Echeverría, C., Siligardi, G., Mascagni, P., Gibbons, W., Giralt, E., Pons, M. (1991) Biopolymers, **31**, 835-843.

Godchaux, W., Zimmerman, W. F. (1979) J. Biol. Chem, **254**, 7874-7884.

Gounarides, J. S., (1994) Ph. D. Thesis, City University of New York, New York.

Gounarides, J., Broido, M. S., Becker, J. M., Naider, F. R. (1993) Biochemistry, **32**, 908-917.

Gounarides, J. S., Xue, C.-B., Becker, J. M., Naider, F. (1994) Biopolymers, **34**, 709-720.

Greenfield, N. J., Fasman, G. D. (1969) Biochemistry, **8**, 4108-4116.

Hagen, D. C., McCaffrey, G., Sprague, G. F., Jr. (1986) Proc. Natl. Acad. Sci. USA, **83**, 1418-1422.

Hartwell, L. H. (1980) J. Cell Biol., **85**, 811-822.

Herskowitz, I. (1988) Microbiol. Rev., **52**, 536-553.

Higashijima, T., Fujumura, K., Masui, Y., Sakakibara, S., Miyazawa, T. (1983) FEBS Lett., **159**, 229-232.

Higashijima, T., Masui, Y., Chino, N., Sakakibara, S., Kito, H., Miyazawa, T. (1984) Eur. J. Biochem., **140**, 163-171.

Jelicks, L. A., Naider, F. R., Shenbagamurthi, P., Becker, J. M., Broido, M. S. (1988) Biopolymers, **27**, 431-449.

Jelicks, L. A., Broido, M. S., Becker, J. M., Naider, F. R. (1989) Biochemistry, **28**, 4233-4240.

Jiang, Y., Breslav, M., Khare, R. K., McKinney, A., Becker, J. M., Naider, F. (1995) Int. J. Peptide Protein Res., **45**, 106-115.

Jiao, D., Russell, K. C., Hruby, V. J. (1993) Tetrahedron, **49**, 3511-3520.

Johnson, W. C. (1990) Proteins: Struct., Funct., Genet., **7**, 205-214.

Julius, D., Blair, L., Brake, A., Sprague, G., Thorner, J. (1983) Cell, **32**, 839-852.

Julius, D., Schekman, R., Thorner, J. (1984) Cell, **36**, 309-318.

Kaiser, E., Colescott, R. K., Bossinger, C. D., Cook, P. I. (1970) Anal. Biochem., 34, 595-598.

Kemp, D. S., McNamara, P. (1981) Tetrahedron Lett., **22**, 4571-4574.

Kessler, H., Bermel, W., Friedrich, A., Krack, G., Hull, W. E. (1982) J. Am. Chem. Soc., **104**, 6297-6304.

Kessler, H., Griesinger, C., Kerssebaum, R., Wagner, K., Ernst, R. R. (1987) J. Am. Chem. Soc. **109**, 607-609.

Khan, S. A., Merkel, G., J. M., Naider, F. (1981) Int. J. Peptide Protein Res., **17**, 219-230.

Konopka, J. B., Jenness, D. D., Hartwell, L. H. (1988) Cell, **54**, 609-620.

Kopple, K. D., Ohnishi, M., Go, A. (1969) J. Am. Chem. Soc., **91**, 4264-4272.

Kurjan, J., Hirsch, J. P., Dietzel, C. (1991) Genes & Dev., **5**, 11-22.

Kurjan, J., Herskowitz, I. (1982) Cell, **30**, 933-943.

Levin, Y., Khare, R. K., Abel, G., Hill, D., Eriotou-Bargiota, E., Becker, J. M., Naider, F. (1993) Biochemistry, **32**, 8199-8206.

Lipke, P. N. (1976) Ph. D. Thesis, University of California, Berkeley.

MacKay, V., Manney, T. R. (1974) Genetics, **76**, 273-288.

Madison, V., Atreyl, M., Deber, C. M., Blout, E. R. (1974) J. Am. Chem. Soc., **96**, 6725-6734.

Madison, V., Deber, C. M., Blout, E. R. (1977) J. Am. Chem. Soc., **99**, 4788-4798.

Masui, Y., Chino, N., Sakakibara, S., Tanaka, T., Murakami, T., Kita, H. (1977) Biochem. Biophys. Res. Commun., **78**, 534-538.

Masui, Y., Tanaka, T., Chino, N., Kita, H., Sakakibara, S. (1979) Biochem. Biophys. Res. Commun., **86**, 982-987.

Matthews, B. W. (1972) Macromolecules, **5**, 818-819.

Moscona-Amir, E., Henis, Y. I., Yechiel, E., Barenholz, Y., Sokolovsky, M. (1986) Biochemistry, **25**, 8118-8124.

Nagayama, K., Wüthrich, K., Ernst, R. R. (1980) J. Magn. Reson., **40**, 321-334.

Naider, F., Becker, J. M. (1986) CRC Crit. Rev. Biochem., **21**, 225-248.

Naider, F., Yaron, A., Ewenson, A., Tallon, M. Xue, C., Srinivasan, J. V., Eriotou-Bargiota, E., Becker, J. M. (1990) Biopolymers, **29**, 237-245.

Naider, F., Gounarides, J., Xue, C.-B., Bargiota, E., Becker, J. M. (1992) Biopolymers, **32**, 335-339.

Nakayama, N., Miyajima, A., Arai, K. (1985) EMBO J., **4**, 2463-2468.

Nemethy, G., Printz, M. P. (1972) Macromolecules, **5**, 755-758.

Neuhaus, D., Williamson, M. P. (1989) in *The Nuclear Overhauser Effect*, VCH Publishers, Inc., New York.

Noggle, J. H., Schirmer, R. E. (1971) in *The Nuclear Overhauser Effect, Chemical Applications*, Academic Press, New York.

Ohnishi, M., Urry, D. W. (1969) Biochem. Biophys. Res. Commun., **36**, 194-202.

Olejniczak, E. T., Gampe, R. T., Fesik, S. W. (1986) J. Magn. Reson., **67**, 28-41.

Pease, L. G., Watson, C. (1978) J. Am. Chem. Soc., **100**, 1279-1286.

Perczel, A., HollÓsi, M., Foxman, B. M., Fasman, G. D. (1991) J. Am. Chem. Soc., **113**, 9772-9784.

Perczel, A., Park, K., Fasman, G. D. (1992) Anal. Biochem., **203**, 83-93.

Piantini, U., Sørensen, O. W., Ernst, R. R. (1982) J. Am. Chem. Soc., **104**, 6800-6801.

Pitner, T. P., Urry, D. W. (1972) J. Am. Chem. Soc., **94**, 1399-1400.

Provencher, S. W., Glöckner, J. (1981) Biochemistry, **20**, 33-37.

Rao, M. H., Yang, W., Joshua, H., Becker, J. M., Naider, F. (1995) Int. J. Peptide Protein Res., **45**, 418-429.

Raths, S. K., Naider, F., Becker, J. M. (1988) J. Biol. Chem., **263**, 17333-17341.

Reddy, A. P., Tallon, M. A., Becker, J. M., Naider, F. (1994) Biopolymers, **34**, 679-689.

Reneke, J. E., Blumer, K. J., Courchesne, W. E., Thorner, J. (1988) Cell, **55**, 221-234.

Rose, G. D., Gierasch, L. M., Smith, J. A. (1985) Adv. Protein Chem., **37**, 1-109.

Rose, M. D., Misra, L., Vogel, J. P. (1989) Cell, **57**, 1211-1221.

Samokhin, G. P., Lizlova, L. V., Bespalova, J. D., Titov, M. I., Smirnov, V. N. (1979) FEMS Microbiol. Letts., **5**, 435-438.

Saultis, J., Liepins, E. (1990) J. Magn. Reson., **87**, 80-91.

Schiller, P. W., Nguyen, T. M. D., Lemieux, C., Maziak, A. (1985) J. Med. Chem., **28**, 1766-1771.

Sen, M., Marsh, L. (1994) J. Biol. Chem., **269**, 968-973.

Shenbagamurthi, P., Baffi, R., Khan, S. A., Lipke, P., Pousman, C., Becker, J. M., Naider, F. (1983) Biochemistry, **22**, 1298-1304.

Shenbagamurthi, P., Steinfeld, A. S., Khan, S. A., Becker, J. M., Naider, F. (1983) Biopolymers, **22**, 815-820.

Shenbagamurthi, P., Kudu, B., Becker, J. M., Naider, F. (1985) Int. J. Peptide Protein Res., **25**, 187-196.

Sibley, D. R., Benovic, J. L., Caron, M. G., Lefkowitz, R. J. (1987) Cell, **48**, 913-922.

Singh, A., Chen, E. Y., Lugovoy, J. M., Chang, C. N., Hitzeman, R. A., Seeburg, P. H. (1983) Nucleic Acids Res., **11**, 4049-4063.

Spatola, A. F., Anwer, M. K., Rockwell, A. L., Gierasch, L. M. (1986) J. Am. Chem. Soc., **108**, 825-831.

Sprague, G. F., Jr., Blair, L. C., Thorner, J. (1983) Ann. Rev. Microbiol., **37**, 623-660.

Sprague, G. F., Jr., Thorner, J. W. (1993) in *The Molecular Biology of the Yeast Saccharomyces cerevisiae* (Broach, J. R., Pringle, J. R. and Jones, E. W., Eds.), 2nd Ed., pp. 657-744, Cold Spring Harbor Laboratory, Cold Spring Harbor, NY.

Stefan, C. J., Blumer, K. J. (1994) Mol. Cell. Biol., **14**, 3339-3349.

Stanfield, C. F., Felix, A. M., Danho, W. (1990) Org. Prep. Proc. Int., **22**, 597-603.

Stotzler, D., Kiltz, H., Duntze, W. (1976) Eur. J. Biochem., **69**, 397-400.

Stradley, S. J., Rizo, J., Bruch, M. D., Stroup, A. N., Gierasch, L. M. (1990) Biopolymers, **29**, 263-287.

Stroup, A. N., Rheingold, A. L., Rockwell, A. L., Gierasch, L. M. (1987) J. Am. Chem. Soc., **109**, 7146-7150.

Stroup, A. N., Rockwell, A. L., Gierasch, L. M. (1992) Biopolymers, **32**, 1713-1725.

Tallon, M. A., Shenbagamurthi, P., Marcus, S., Becker, J. M., Naider, F. (1987) Biochemistry, **26**, 7767-7774.

Tallon, M. A., (1992) Ph. D. Thesis, City University of New York, New York.

Tanaka, T., Kita, H. (1978) Biochem. Biophys. Res. Commun., **83**, 1319-1324.

Thorner, J. (1980) in *The Molecular Genetics of Development* (Leighton, T., Loomis, W. F., Eds.) pp. 119-179, Academic Press, New York.

Thorner, J. (1981) in *Molecular Biology of the Yeast Saccharomyces*, Part 1, (Strathern, J. N., Jones, E. W. and Broach, J. R., Eds.), pp. 143-180, Cold Spring Harbor Laboratory, Cold Spring Harbor, New York.

Torchia, D. A., Wong, S. C. K., Deber, C. M., Blout, E. R. (1972) J. Am. Chem. Soc., **94**, 616-620.

Ventkatchalam, C. M. (1968) Biopolymers, **6**, 1425-1436.

Wagner, G. (1983) J. Magn. Reson., **55**, 151-156.

Wagner, J.-C., Wolf, D. H. (1987) FEBS Letts., **221**, 423-426.

Wagner, G., Neuhaus, D., Wörgötter, E., Vasák, M., Kägi, J. H. R., Wüthrich, K. (1986) J. Mol. Biol., **187**, 131-135.

Wakamatsu, K., Okada, A., Higashijima, T., Miyazawa, T. (1986) Biopolymers, **25**, S193.

Wakamatsu, K., Okada, A., Suzuki, M., Higashijima, T., Masui, Y., Sakakibara, S., Miyazawa, T. (1986) Eur. J. Biochem., **154**, 607-615.

Wakamatsu, K., Okada, A., Miyazawa, T., Masui, Y., Sakakibara, S., Higashijima, T. (1987) Eur. J. Biochem., **163**, 331-338.

Waki, M., Kitajima, Y., Izumuya, N. (1981) Synthesis, **4**, 266-267.

Waters, M. G., Evans, E. A., Blobel, G. (1988) J. Biol. Chem., **263**, 6209-6214.

Wickner, R. B., Leibowitz, M. J. (1976) Genetics, **82**, 429-442.

Williamson, M. P., Havel, T. F., Wüthrich, K. (1985) J. Mol. Biol., **182**, 295-315.

Woody, R. W. (1974) in *Peptides, Polypeptides and Proteins*, (Blout, E. R., Bovey, F. A., Goodman, M., Lotan, L, Eds.), pp. 338-350, Wiley, New York.

Wüthrich, K. (1986) *NMR of Proteins and Nucleic Acids*, John Wiley & Sons, New York.

Xue, C.-B., Eriotou-Bargiola, E., Miller, D., Becker, J. M., Naider, F. (1989) J. Biol. Chem., **264**, 19161-19168.

Xue, C.-B., Becker, J. M., Naider, F. (unpublished results, personal communication)

Yang, W., McKinney, A., Becker, J. M., Naider, F. (1995) Biochemistry, **34**, 1308-1315.